Creep and Shrinkage in Concrete Structures

Edited by

Z. P. Bažant
Center for Concrete and Geomaterials
Northwestern University.
Evanston

and

F. H. Wittmann
Department of Materials Science
Swiss Federal Institute of Technology
Lausanne

A Wiley-Interscience Publication

JOHN WILEY & SONS
Chichester · New York · Brisbane · Toronto · Singapore

1982

Contents

Creep and Shrinkage in Concrete Structures
Edited by Z. P. Bažant and F. H. Wittmann

Chapter 7

Mathematical Models for Creep and Shrinkage of Concrete

Z. P. Bažant

7.1 INTRODUCTION

Since the advent of the computer era structural analysis capabilities have been advancing at a rapid pace. The large finite element programs to which these advances have led can however serve a useful purpose only if a good mathematical model of the material is available.

Great progress has been achieved in this direction in the field of creep and shrinkage of concrete. Within the linear range, the theory is now reasonably well understood. However, many questions and gaps of knowledge remain, despite the recent vast expansion of the literature on the subject.

This chapter attempts a state-of-art exposition, stating the principal facts, properties, and formulations, and frankly admitting the limitations, uncertainties, and questions. The reader must be warned that the survey which follows does not atempt an exhaustive coverage and is characterized by a certain degree of bias for the contributions made at my home institution with which I am most familiar.

An engineer who merely wants to get a quick information on the models he could use, and not to worry about more subtle or unanswered questions, need not study the whole of this chapter. It suffices for him to look first at Section 7.3.5 for a brief description of the simplest method of analysis, then either at Section 7.3.4 if his structural system is not large and at Sections 7.4.1, 7.4.2, and 7.4.4 if it is large, and finally at Sections 7.2.5–7.2.7, 7.7.1–7.7.4 for the characterization of material properties. Even those sections, however, are not instruction manuals and the appropriate references must be consulted for details.

7.2 CREEP AND SHRINKAGE PROPERTIES

7.2.1 Definitions

When a load is applied on a concrete specimen, the specimen first shows an instantaneous deformation which is then followed by slow further increase

of deformation. This slow increase of deformation, discovered in 1907 by Hatt,[97] is called creep. Concrete specimens slowly deform in time even in the absence of applied loads. These deformations are called shrinkage when temperature is constant.

To define creep one must consider two identical specimens subjected to exactly the same environmental histories, one specimen being loaded and the other load-free (companion specimen). The difference of the deformation of these two specimens defines the instantaneous deformation plus creep.

7.2.2 Physical nature of creep and shrinkage

Creep of concrete has its source in the hardened cement paste and, at high stresses, also in failure of the paste–aggregate bond. The paste consists of solid cement gel and contains numerous capillary pores.[72,153,152,188,194] The cement gel contains about 40 to 55% of pores in volume, has an enormous pore surface area (roughly 500 m^2/cm^3), and is made up of sheets of colloidal dimensions (of average thickness about 30 Å, with average gaps about 15 Å between the sheets). The sheets are formed mostly of calcium silicate hydrates and are strongly hydrophylic. Because the pores of cement gel are micropores of subcapillary dimensions they cannot contain liquid water or vapour; but they do contain evaporable water (water that is not chemically bound in the hydrates), which is strongly held by solid surfaces and may be regarded as (hindered) absorbed water or interlayer water. This water can exert on the pore walls a significant pressure called the disjoining pressure[25,151,194] the value of which depends on temperature and the degree of water saturation of capillary pores.

The bonds and contacts between the colloidal sheets in cement gel are highly disordered and unstable. Therefore, creep may be expected to be caused by changes in the solid structure. Although the precise creep mechanism is still debated, bonding and rebonding processes similar to movement of a dislocation may be involved, and it may also be possible that various solid particles displace or migrate (diffuse) from highly stressed zones to stress-free zones such as the surfaces of larger pores. Because of the disjoining pressure, bonds get weakened by the presence of water, and this explains why after drying the creep is less.[25,191–194]

During drying, on the other hand, the creep is higher than in sealed specimens. This effect, called drying creep or Pickett effect,[148] probably has two sources. One may be the fact that as water is diffusing out of the loaded gel micropores it creates disorder, facilitating migrations of solid particles.[16,24,25] Another cause, possibly the major one,[195] is likely to be macroscopic, namely the stresses and microcracking[52,195] produced by drying in the specimen as a whole.

As the solid particles migrate out of the loaded regions, the load on them (or the disjoining pressure) is gradually relaxed, being transferred onto more stable parts of the microstructure. This causes the creep rate to decline. At the same time hydration proceeds, which causes the volume of cement gel to increase at the expense of large (capillary) pores, and the number of bonds in the existing gel to also increase. This reduces creep, too.

Shrinkage results from the increase of solid surface tension and capillary tension due to drying, as well as from the decline of disjoining pressure in the gel.[190,194]

7.2.3 Elementary characteristics

The total strain of a uniaxially loaded concrete specimen at time t after the casting of concrete (age) may be subdivided as

$$\begin{aligned}\varepsilon(t) &= \varepsilon_E(t)+\varepsilon_C(t)+\varepsilon_S(t)+\varepsilon_T(t)=\varepsilon_E(t)+\varepsilon''(t)\\ &=\varepsilon_E(t)+\varepsilon_C(t)+\varepsilon^0(t)=\varepsilon_\sigma(t)+\varepsilon^0(t)\end{aligned} \tag{7.1}$$

in which $\varepsilon_E(t)$ is the instantaneous strain, which is elastic if the stress is small, $\varepsilon_C(t)$ is the creep strain, $\varepsilon_S(t)$ is the shrinkage strain, ε_T is the thermal dilatation, $\varepsilon^0(t)$ is the stress-independent inelastic strain, $\varepsilon''(t)$ is the inelastic strain, and $\varepsilon_\sigma(t)$ is the stress-produced strain. $\varepsilon_E(t)$ is reversible (i.e. recoverable) upon unloading right after the moment of loading but not later, due, principally, to further hydration.

The thermal strain will not interest us here beyond noting that it is calculated as $\varepsilon_T=\int_{T_0}^{T}\alpha\,dT$ where T_0 is the chosen reference temperature and α is the thermal dilatation coefficient, which roughly equals $10^{-5}\,°C^{-1}$ but actually depends on T and even more on the specific moisture content, w.

The dependence of creep on stress may be shown graphically by creep isochrones (Figure 7.1), which are the lines connecting the values of strain $(\varepsilon-\varepsilon^0)$ produced by various constant stresses α during the same time

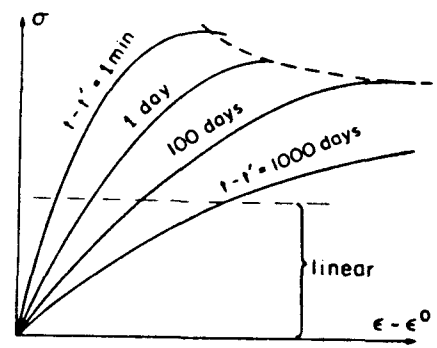

Figure 7.1 Creep isochrones

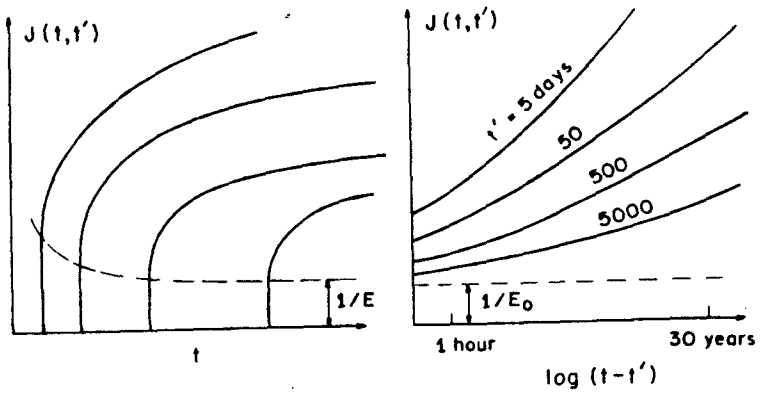

Figure 7.2 Typical creep curves for various ages t' at loading

period. Plotting creep isochrones from test results (see Figure 7.1), one finds that for stresses within the service range, or up to about 50% of the strength, the creep is approximately proportional to stress. For constant uniaxial stress σ we may then write

$$\varepsilon(t) = \sigma J(t, t') + \varepsilon^{(1)}(t) \tag{7.2}$$

in which ε is the uniaxial strain, t is the time, which we normally choose to coincide with the age of concrete, and $J(t, t')$ is the compliance function (often also called the creep function), which represents the strain at time t produced by a unit constant stress that has been acting since time t'. Due to the proportionality property, the creep is completely characterized by the function $J(t, t')$, the typical shape of which is sketched in Figure 7.2. This function may be expressed as

$$J(t, t') = \frac{1}{E(t')} + C(t, t') = \frac{1 + \phi(t, t')}{E(t')} \tag{7.3}$$

where $1/E(t')$ represents the instantaneous elastic deformation at age t', $C(t, t')$ is the creep compliance (also called the specific creep), and $\phi(t, t')$ is the ratio of the creep deformation to the elastic deformation, called the creep coefficient. The instantaneous deformation has a large inelastic (irreversible) component at high stresses but in the service stress range (below about $\frac{1}{2}$ of the strength) it is essentially elastic, i.e. reversible immediately after loading.

For long-time loading, the values of creep coefficient are usually between 1.0 and 6.0, with 2.5 as the typical value. So, realizing that creep deformations are normally larger than the elastic ones, we recognize the importance of taking creep into account in calculations of stresses, deformations, cracking, buckling, and failure of structures under sustained loads. Shrinkage

typically attains values from 200 to 800×10^{-6}. Compared to this, a typical creep strain for $E(t') = 3.5 \times 10^6$ psi (24,000 MPa), $\phi = 2.5$, and $\sigma = 2000$ psi (14 Mpa) is 1400×10^{-6}. Thus, shrinkage is normally somewhat less important than creep, except when the long-time stresses produced by load are small.

The magnitude of the part of deformation that is called instantaneous or elastic, i.e. $\varepsilon_E = \sigma/E(t')$, unfortunately suffers by ambiguity because significant creep exists even for extremely short load durations; see the typical curves at constant stress plotted in Figure 7.2 (on log-time scale) in which the left-hand side horizontal asymptote represents the true instantaneous deformation $J(t', t')$ (since $\log 0 = -\infty$). Its value is very difficult to determine experimentally and is, anyhow, not needed for static structural analysis for long-time loads. For this purpose, the deformation which coresponds to any load duration less than about 1 day (a in Figure 7.3) may serve just as well as the conventional instantaneous (or elastic) strain. The conventional elastic modulus obtained from the formulae of ACI or CEB-FIP recommendations (e.g. $57{,}000\sqrt{f'_c}$) corresponds to approximately two hours of stress duration and represents approximately half of the true instantaneous modulus.

In previous works, unfortunately, different definitions of the instantaneous (elastic) deformation have been used. Some authors imply, often tacitly, the instantaneous deformation to be that for 1 to 10 min duration (typical duration of strength tests), others that for 0.001 s. There are great differences among all the definitons of $E(t')$ used in the past. Much confusion and error has been caused by carelessly combining incompatible values of $E(t')$ and $\phi(t, t')$ or $C(t, t')$ (a with b' or b with a' in Figure 7.3).

For short-time loading, quasi-elastic structural analyses based on the effective modulus $E_{\text{eff}} = 1/J(t, t')$ normally give very good results. For loads of more than one-day duration, it makes therefore, little difference whether $E(t')$ corresponds to a duration of 1 s or 2 h, provided that $1/E(t')$ and $C(t, t')$ add up to the correct value of $J(t, t')$.

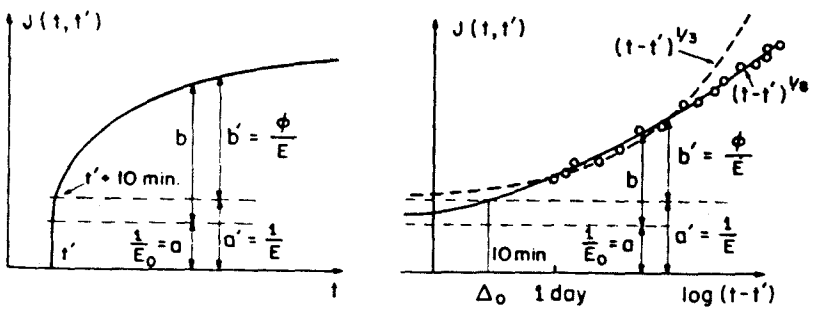

Figure 7.3 Creep curves in actual and logarithmic time scales (a = true elastic deformation, b = true creep, a' = conventional elastic deformation, b' = conventional creep)

To make these errors impossible, it is preferable to specify initially the creep properties in terms of $J(t, t')$ rather than $C(t, t')$ or $\phi(t, t')$. For the purpose of structural analysis the conventional elastic modulus may then be calculated as

$$E(t') = \frac{1}{J(t'+\Delta, t')} \tag{7.4}$$

where Δ is some chosen load duration, less than about 1 day. The creep compliance must then be evaluated as $C(t, t') = J(t, t') - J(t'+\Delta, t')$ and the creep coefficient as $\phi(t, t') = [J(t, t')/J(t'+\Delta, t')] - 1$.

7.2.4 Influencing factors

Creep and shrinkage of concrete are influenced by a large number of factors, which may be divided into intrinsic factors and extensive factors. The intrinsic factors are those material characteristics which are fixed once and for all when the concrete is cast. Extensive factors are those which can vary after the casting; they include temperature, pore water content, age at loading, etc..

The main intrinsic factors are the design strength, the elastic modulus of aggregate, the fraction of aggregate in the concrete mix, and the maximum aggregate size.[145,113] Increase of any of these factors causes a decrease of creep as well as shrinkage. This is because the aggregate does not creep appreciably and has a restraining effect on creep and shrinkage. Gap-grading of aggregate further reduces creep and shrinkage. As for shrinkage, it also increases as the water/cement ratio of the concrete mix increases.

Among the extensive factors we must distinguish the local from the external ones. The former, also called the state variables, are those which can be treated as a point property of a continuum. They are the only ones which can legitimately appear in a constitutive equation. Temperature, age, degree of hydration, relative vapour pressure (humidity) in the pores, and pore water content represent state variables affecting creep.

On the other hand, the size of specimen and the environmental humidity are not admissible as state variables in a constitutive equation even though they have a great effect on creep of a concrete specimen. Properly, the environmental humidity must be considered as the boundary condition for the partial differential equation governing pore humidity. It is the pore humidity, not the environmental one, which directly affects creep and can appear in the constitutive equation.

The effects of state variables (documented, e.g., by the text data reported by Neville and Dilger,[145] L'Hermite and Macmillan,[122] Lambotte and Mommens,[117] Hanson,[94] Harboe *et al.*,[93] Troxell *et al.*,[177] Rüsch *et al.*,[16] Wagner[182], Neville[144]) are as follows. Creep decreases as the age of concrete at the instant of loading increases (this is actually the effect of the increase in the degree of hydration). Creep also increases with increasing temperature, but this effect is offset by the fact that a temperature increase also accelerates hydration which in turn reduces creep. Creep at constant pore water content is less for a smaller pore water content or a lower relative humidity in the pores.[160,194] In most practical situations, however, this local effect is overpowered by the effect of the changes in environmental humidity (an extensive factor) upon the overall creep of a specimen or structural member. This effect is opposite—the creep of a specimen is increased, not decreased, by a decrease of environmental humidity.[160,194]

Another important non-local extensive factor which is not a state variable is the size of specimen or structural member. The drying process in a larger specimen is slower, and consequently the creep increase due to drying is less, i.e. creep is less for a larger specimen. Similarly, shrinkage is less for a larger specimen and it is also less for a higher environmental humidity.

In a sealed state, at which (due to hydration) the pore humidity is found to drop gradually to about 97–99%, concrete exhibits a small shrinkage, called the autogeneous shrinkage. It is due to volume changes in the hydration reaction and is about twenty times less than the drying shrinkage. In water immersion (100% humidity) concrete exhibits small swelling (negative shrinkage), which is about ten times less in magnitude than the drying shrinkage.

7.2.5 Constitutive properties

Among the simple formulae, the creep of concrete at constant moisture and thermal state (also called the basic creep) may be best described by power curves of load duration $(t-t')$,[194] and by inverse power curves for the effect of age t' at loading. This leads to the double power law[25,41,43,44] (Figure 7.3):

$$J(t, t') = \frac{1}{E_0} + \frac{\phi_1}{E_0}(t'^{-m} + \alpha)(t-t')^n \tag{7.5}$$

in which, roughly, $n \simeq 1/8$, $m \simeq 1/3$, $\alpha \simeq 0.05$, $\phi_1 \simeq 3$ to 6 (if t' and t are in days), and E_0 (= asymptotic modulus) $\simeq 1.5$ times the conventional elastic modulus for 28-days old concrete. These coefficients can be relatively simply determined from test data; for example, by using the foregoing estimates for E_0, and m and α and plotting $y = \log[(E_0 J - 1)/(t'^{-m} + \alpha)]$ versus $\log(t-t')$, one gets a straight-line plot whose slope is n and y-intercept is ϕ_1. Comparisions with test data are exemplified in Figure 7.4.

Temperature has a major influence on creep. To describe the creep curves at various constant temperatures, Equation (7.5) may be generalized as

$$J(t, t') = \frac{1}{E_0} + \frac{\phi_T}{E_0}(t_e'^{-m} + \alpha)(t-t')^{n_T} \tag{7.6}$$

in which $t_e' = \int \beta_T(t')\,dt'$ represents the age corrected for the effect of

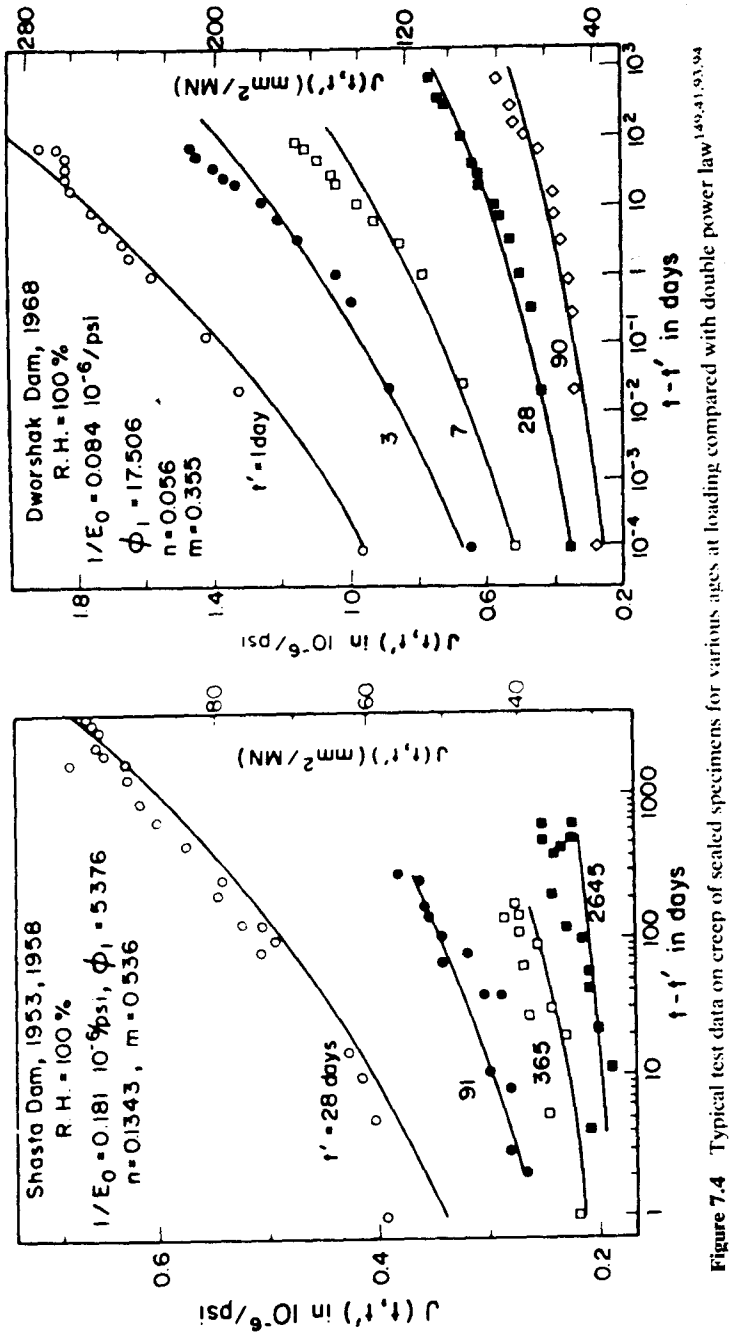

Figure 7.4 Typical test data on creep of sealed specimens for various ages at loading compared with double power law[149,41,93,94]

temperature on the rate of hydration (or aging) and is called the reduced age or the equivalent hydration period (or maturity). Coefficients ϕ_T, n_T, and β_T are empirical functions of temperature,[27] introduced such that 'at reference (room) temperature (T_0)' $\phi_T = \phi_1$, $n_T = n$, and $\beta_T = 1$. For temperature history that equals T_0 up to time t_0 and then jumps to another constant value T, we have $t'_e = t_0 + \beta_T(t - t_0)$.

Since $(t-t')^n = e^{nx}$ where $x = \ln(t-t')$, the power curves of $(t-t')$ appear on a log-time scale as curves of ever-increasing slope and with no bounded final value (Figure 7.2). The question whether there exists a bounded final value of creep (at $t \to \infty$) has been debated for some time and no consensus has been reached. It is, however, clear that if a final value exists it would be reached at times far beyond those of interest. All measurements of creep of sealed or immersed specimens indicate (except for what appears to be statistical scatter) non-decreasing slopes on a log-time scale for the entire test duration. There is no evidence of a final value. For design purposes, however, the question of existence of a bounded final value is not too important because the creep increase from 50 years to 100 years is, according to extrapolations of test data (or Equation (7.5)), anyhow insignificant. Most structures are being designed for 40- or 50-year service lives.

The power law of load duration, first proposed by Straub[173] and Shank,[170] follows theoretically from certain reasonable hypotheses about the microstructural creep mechanism, e.g. rate process theory,[192-194] or a statistical model of creep mechanism.[71] Until recently the power law had been used in conjunction with the conventional elastic modulus for the elastic term ($1/E$ instead of $1/E_0$ in Equation (7.5)). However, this definition of the elastic term greatly restricts the range of applicability. Namely, by choosing the left-hand side of the horizontal asymptote to be too high (Figure 7.3), a higher curvature of the power curve, i.e. a higher exponent (about $n \approx 1/3$), is required in order to fit the creep data for durations from 3 to 100 days. Then the large curvature due to too high an exponent (1/3 instead of 1/8) causes the curve to pass well above the creep data for longer creep durations (over 100 days); see Figure 7.3(b). It was for this reason that in the older works the power law was deemed to be inapplicable for long-time creep.

It may be of interest to add that an improvement of data fits may be achieved by the so-called log-double power law which asymptotically coincides for short load durations with the double power law and for long load durations tends to straight lines in $\log(t-t')$ which have the same slope for all t' (work in progress by J. C. Cherni, Northampton University).

To be able to fit the creep test data up to many years duration the elastic term ($1/E_0$ in Equation (7.5)) must be taken as the true instantaneous value, i.e. as the left-hand side horizontal asymptote on the log-scale, and the exponent then turns out to be around 1/8. The double power law then acquires an extraordinarily broad range of applicability. It agrees reasonably

well with the known data for creep up to 30 years' duration and at the same time it describes very well the test data for load durations under one day and as short as 1 s. It even gives approximately correct values for the dynamic modulus E_{dyn} when one substitutes load duration $t-t'=10^{-7}$ day. The conventional elastic modulus, along with its age dependence, may be considered as the value of $1/J(t,t')$ for $t-t'=0.001$ day, for which Equation (7.5) yields:

$$E(t')=\frac{E_0}{1+\phi_1'(t'^{-m}+\alpha)} \qquad \phi_1'=10^{-3n}\phi_1 \tag{7.7}$$

However, the value obtained by substituting $t-t'=0.1$ day agrees better with the ACI formula ($E=57{,}000\sqrt{f_c'}$).

Since four parameters (E_0, m, α, ϕ_1') are needed to describe the age dependence of the elastic modulus, there is only one additional parameter, namely the exponent n, which suffices to describe creep. This makes the double power law simpler than any other known formula for creep.

Many other expressions for the compliance function have been proposed.[192,193] Ross and Lorman proposed a hyperbolic expression $C(t,t')=\bar{t}/(a+b\bar{t})$, $\bar{t}=t-t'$, which is convenient for fitting of test data but is unfortunately inapplicable to long creep durations.[31] Hanson[94] proposed a logarithmic law, $C(t,t')=\phi(t')\log(1+\bar{t})$, which does not approach any final value and gives good predictions for long creep durations but for short durations is not as good as the double power law. Mörsch[137] proposed the expression $C(t,t')=\phi\{1-\exp[-(bt)^{1/2}]\}^{1/2}$ and Branson *et al.*[58–60] proposed the expression in Equation (7.13) in the sequel; these exhibit a final value. The expressions of Ross and Mörsch work better for creep at drying which we discuss in the next section. McHenry,[125] Maslov,[133] Arutyunian,[10] Bresler and Selna,[62] Selna,[168,169] and Mukaddam[138,139] used a sum of exponentials of $t-t'$ with coefficients depending on t'. Such expressions can be closely adapted to any test data and we will discuss these in Section 7.4.1.

Various expressions have been introduced with the particular purpose of enabling a certain simplified method of creep structural analysis. These include the expressions of Whitney,[185] of Glanville[85] and Dischinger,[77,78] England and Illston,[79] and Illston,[79] and Nielsen,[146,147] which lead to the rate-of-creep (Dischinger's) and rate-of-flow methods for structural analysis and will be mentioned later, and other expressions.[70,10,120]

The double power law exhibits a certain questionable property which was recently discussed in the literature.[27,33] It is the property that the creep curves for different ages t' at loading diverge after a certain creep duration, i.e. there exists a time $t-t'=t_D$ (function of t') after which the difference between these curves increases while up to this time it decreases (Figure 7.4). This property, which is shared with the ACI creep expression but not with that in the CEB-FIP Model Code, is equivalent to the condition

that $\partial^2 J(t,t')/\partial t\,\partial t'$ changes sign from positive to negative (it is non-negative if there is no divergence). One objection was that the creep recovery curves obtained by principle of superposition do not have a decreasing slope at all times if the creep curves exhibit the divergence property. This argument is however unrealistic because the principle of superposition cannot be applied to creep recovery (Section 7.3.1). Further it was thought that the divergence property might violate the second law of thermodynamics but it was proven that this is not so.[27,33] So, whether the divergence property is real depends strictly on experimental observations. The evidence from test data is ambivalent; some exhibit the divergence, many do not. It could be that the divergence property is due to some non-linear effect, in which case it would not belong to function $J(t,t')$.

Finally, we should indicate how the thermal strain is determined. Although the deformations due to changes in temperature and moisture content are in reality coupled, we may reasonably well calculate the thermal strain as

$$\varepsilon_T=\int_{T_0}^{T}\alpha(T)\,dT \tag{7.8}$$

where T_0 is the initial reference temperature, T the current temperature, and $\alpha(T)$ the coefficient of thermal expansion at temperature T. Approximately, $\alpha(T)$ may be considered to be constant (usually $\alpha=10^{-5}\,°C^{-1}$), and independent of moisture content and age. Then $\varepsilon_T=\alpha(T-T_0)$.

7.2.6 Cross-section behaviour during drying

Concrete as initially cast is wet, with pore humidity 100%. After a certain initial moist treament period, usually 7 to 14 days, most concrete structures (except for those sealed by an impervious liner) are exposed to the environment and dry gradually. The drying process is very slow. If concrete does not crack and is of good quality, it takes over 10 years for the pore humidity at mid-thicknesses of a 6-inch slab to approach that of the environment. For other thicknesses, the drying times are proportional to square of the thickness. This gives a drying time of about 1 year for a 2-inch shell, and of 360 years for a 3 ft slab (if it does not crack). In very thick uncracked structures (mass concrete) there is no significant drying except for up to about 1 foot from the surface. (These times, however, become much shorter if concrete is heated over 100%.)

Drying is the cause of most of the shrinkage and it also profoundly affects creep. Shrinkage is larger for a lower environmental humidity and for a smaller size of cross section. It also decreases as the age of concrete (or the degree of hydration) at the start of drying increases, and as the initial moist period extends. Regarding the intrinsic factors, shrinkage increases with an

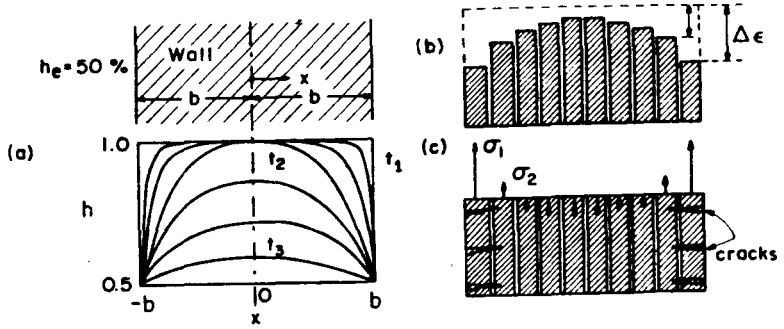

Figure 7.5 (a) Typical distributions of pore humidity at various times during drying; (b) free shrinkage and creep at various points of cross section; (c) internal stresses

increase in water/cement and cement/aggregate ratios of concrete mix and with a decrease in concrete strength. As for the effect of drying on creep, generally a strong increase of creep, compared to sealed specimens, is observed. This phenomenon is called the drying creep or Pickett effect.[148] (For test data see Neville and Dilger,[145] Ali and Kesler,[4] Troxell,[177] Keeton,[111] L'Hermite and Mamillan[122,123] Weil,[183] Rüsch,[161] Ishai,[105] Wagner,[182] Kesler,[113] Lambotte,[117] LeCamus,[119] and others.)

Certain constitutive relations that govern creep at drying have been proposed on a speculative theoretical basis (e.g. Bažant[25]). However they are considerably more complicated and, thus far, more weakly supported by experiment than those for constant pore humidity, even though the available test data have been successfully fitted.[52] The determination of constitutive relations in the presence of drying is hampered by the fact that for nearly all available creep and shrinkage tests the cross section has been in a highly non-uniform moisture state (Figure 7.5), with totally different shrinkage and creep strains at the core and the surface layer of the specimen. It is certain that this non-uniformity must lead to large internal stresses which cause non-linear triaxial behaviour and microcracking,[202] with microcracks probably so fine that they cannot be seen by the unaided eye. It was shown[52] that these phenomena have a very large effect on observed creep of drying specimens. More recently it has been proposed[195] that nearly all of the increase of creep due to drying might be due to microcracking. We will return to this question in Section 7.6.

What is presently available for long-time deformations at drying are semi-empirical formulae that indicate the overall or mean shrinkage and creep of the cross section of a test specimen. We will outline them in this section. These formulae, however, cannot be considered as a constitutive property, i.e. a point (or local) property of concrete as such. The so-called unrestrained (or free) shrinkage and creep at various points of the cross

section is no doubt rather different from the behaviour indicated by such formulae. Nevertheless, in view of the uncertainties and complexities that characterize the presently available constitutive relations at drying, the use of these formulae as constitutive relations may be justified at present for the purpose of cruder calculations aimed at determining just the internal force resultants within the cross section. The distributions of stresses due to drying, however, cannot be determined by such calculations. It should also be realized that applying the same mean creep properties to both bending and axial deformation cannot be correct since the response of concrete in the core, which dries later, has almost no effect on bending while it affects the axial deformation.

Drying is a diffusion process and, as test data confirm, the evolution of pore humidity and water content distributions in time can be reasonably well calculated from a non-linear diffusion equation.[37] Based on this equation it appears (see Section 7.6.4, Equations (7.105)–(7.107)), that the drying times are proportional to the square of the size when geometrically similar bodies are compared (Figure 7.6). The same is true of shrinkage since the free shrinkage strain appears to be a function of pore water content which, in turn, is a function of pore humidity. In practice, the size-square dependence is not exact, being spoiled by the effects of continuing hydration and microcracking, but it agrees with measurements quite well.

Using these results of the diffusion theory, we may express the mean shrinkage of the cross section as[42,43,44]

$$\bar{\varepsilon}_S(t, t_0) = \varepsilon_{sh_\infty} k_h S(\theta) \tag{7.9}$$

where

$$\theta = \frac{t - t_0}{\tau_{sh}} \qquad \tau_{sh} = c_s \frac{(k_S D)^2}{C_1} \tag{7.10}$$

Here τ_{sh} is the shrinkage square half-time (i.e. the time in which the square of shrinkage strain reaches about 1/2 of its final value); ε_{sh_∞} is the final shrinkage at humidity 0%, which depends on the mix ratios and the strength (typically 0.0005 to 0.0013); k_h is a function of environmental humidity h_e

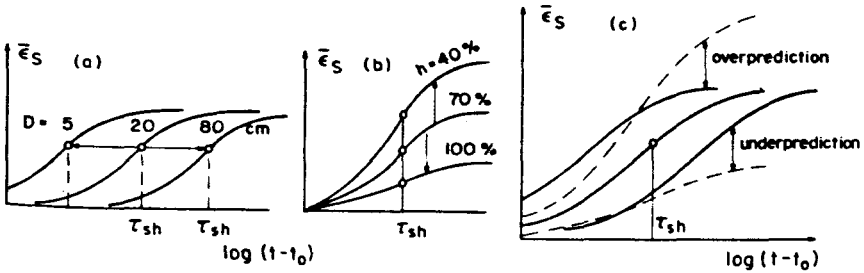

Figure 7.6 Effects of size and ambient humidity in mean shrinkage of cross section

(empirically $k_h \simeq 1-h_e^3$); $S(\theta)$ is a function giving the evolution of shrinkage in non-dimensional time θ; t_0 is the age at the start of drying; C_1 is drying diffusivity of concrete at the start of drying (10 mm^2/day in order of magnitude); k_S is the parameter of cross-section shape which can be calculated from the diffusion theory ($k_S = 1$ for slab, 1.15 cylinder, 1.25 square prism 1.30 sphere 1.55 cube); D is the effective thickness of cross section (in mm), defined as $D = 2v/s$, where v is the volume and s is the surface area exposed to drying (for a slab, D represents the actual thickness); and c_s is an empirical constant ($= 0.267$ mm^2). Because non-linear diffusion theory does not permit simple solutions, an empirical expression, namely $S(\theta) = [1 + \tau_{sh}/(t - t_0)]^{-1/2}$, is used.[43,44]

The effects of temperature T and of the age at the start of drying on shrinkage may be described by means of diffusivity and have the form $C_1 = C_0 k'_T k_t$ where C_0 is a constant, k_t is an empirical function of age t_0; and k'_T is a function of temperature which may be based on activation energy theory.

Two examples of a comparision between calculated shrinkage curves (for different cylinder diameters and different environmental humidities) and test data from the literature are given in Figure 7.7. Figure 7.5 illustrates the effect of a change in environmental humidity, h_e, which causes a vertical

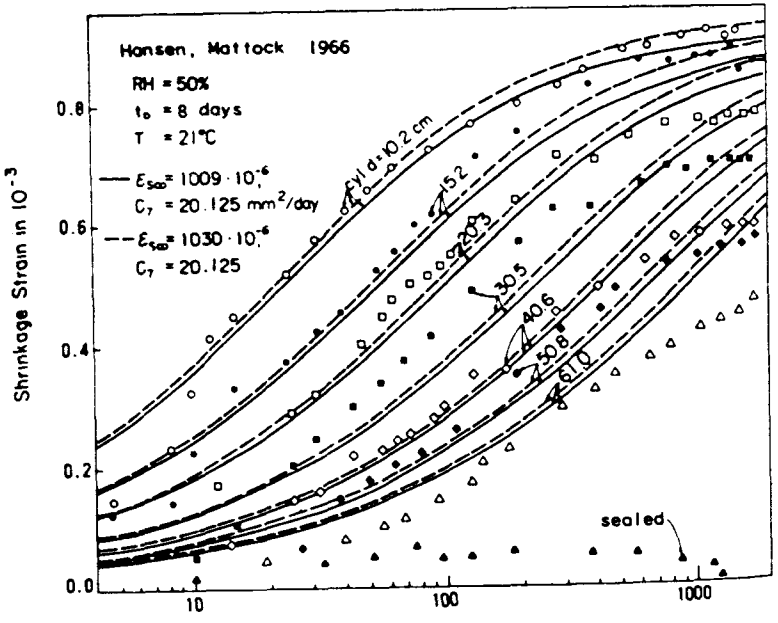

Figure 7.7 Hansen and Mattock's test data on shrinkage of cylinders of various sizes[92] compared with Equations (7.9) and (7.10) exhibiting the size-square dependence of shrinkage half-time[43]

scaling of shrinkage ordinates, and the effect of changing the size from D_0 to D, which does not cause a vertical scaling but a horizontal shift of the shrinkage curve in log-time scale (the shift is by the distance $2\log(D/D_0)$, because $\log\theta = \log(t - t_0) + 2\log D + \text{constant}$ (see Figure 7.6). In some other practical formulae,[5,60,58,59,68,161] the size effect on shrinkage is handled by scaling the ordinates. This disagrees, however, with the diffusion theory, is not supported by measurements, and leads to underprediction of long-time shrinkage for thick structural members (Figure 7.6(c)). The thickness-square dependence of shrinkage times is the simplest and most essential property of shrinkage.

It must be emphasized that the constitutive relation for the free (unrestrained) shrinkage as a local (point) property is doubtless rather different from Equations (7.9) and (7.10). The specimen size and environmental humidity are not local state variables of a continuum and are therefore inadmissible for a constitutive equation. The free shrinkage is not a function of time but of the specific water content (or pore humidity), the dependence of which on time is not a constitutive property of the material but results from the solution of a boundary value problem. The only dependence on time which is constitutive (local) in nature is that on the degree of hydration (aging).

Direct measurement of the free shrinkage requires lowering the environmental humidity gradually and so slowly that the humidity distribution within the specimen would remain almost uniform.[202] Such tests have been made for cement paste tubular specimens 1 mm thick,[200] but for large specimens the test times become impossibly long. Since microcracking, tensile non-linearity, and creep due to shrinkage-induced stresses reduce the observed shrinkage of a specimen, the free shrinkage is certain to be significantly higher than the final values observed in standard tests (Equation (7.9)).

The mean compliance function $\bar{J}(t, t')$ of the cross section in the presence of drying may be expressed approximately as:[42]

$$\bar{J}(t, t') = J(t, t') + \bar{C}_d(t, t') \tag{7.11}$$

where $J(t, t')$ is the compliance function for constant pore humidity, as given in Section 7.2 (e.g. Equation (7.5)), and $\bar{C}_d(t, t')$ is the mean additional compliance due to drying (with the indirect effect of simultaneous shrinkage) (Figure 7.8).

For a lower humidity, the drying is more severe, and thus the drying creep term increases as the environmental humidity decreases. When the size tends to infinity, there is no drying in the limit. So the drying creep term $\bar{C}_d$ must decrease with increasing size and approach zero as the size tends to infinity. Some practical models[5,58–60] disregard this condition.

Since drying follows the size-square dependence, the same should be

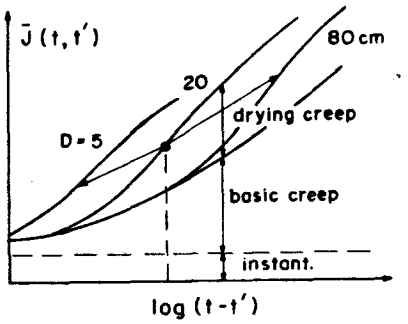

Figure 7.8 Components of mean creep of cross section at drying

expected of the drying creep term. So, we may write, in analogy to Equations (7.9) and (7.10) for shrinkage,

$$\bar{C}_d(t, t') = \frac{f_d(t')}{E_0} k_h' \bar{S}(\theta) \qquad \theta = \frac{t - t'}{\tau_{sh}} \tag{7.12}$$

where τ_{sh} is the shrinkage-square half-time (same as in Equation (7.10)) $t - t'$ = duration of load; k_h' is an empirical function of environmental humidity ($k_h' \simeq 1 - h_e^{1.5}$); $\bar{S}(\theta)$ is an empirical function of θ similar to $S(\theta)$; $f_d(t')$ is a decreasing empirical function of age at loading t'. (For detailed expressions and justification, see Bažant *et al.*[42,43].) An important property of Equation (7.12) is that the drying creep term is similar to shrinkage, thus reflecting the fact that shrinkage affects creep and is not simply additive to creep, as the experimentalists have always been emphasizing.

An essential feature is that the size-square dependence is embodied in Equation (7.12). A change in size causes a horizontal shift of the curve for the drying creep term in log-time scale, and superimposing this term on the basic creep, $J(t, t')$, we may imagine the drying term curve to slide on top of the basic creep curve as shown in Figure 7.8. A change of environmental humidity, on the other hand, causes a vertical scaling of the ordinates of this term. In this manner, many different shapes of the creep curves can be generated.

This property is not reflected in the older formulae in which both the humidity and size effects are handled by a multiplicative factor, i.e. vertical scaling of the creep curve. This then leads to underprediction of long-time creep for very thick structural members, and overprediction for very thin ones (like in Figure 7.6).

The fact that the slope of creep curves in log-time, as observed in drying environment, begins to decrease after a certain period of time (depending on the size) appears to be due solely to the drying creep term. From this we may not, however, infer that the creep curves approach a finite value since the basic creep term does not approach one.

7.2.7 Practical prediction of creep and shrinkage

To perform a finite element analysis of time-dependent behaviour, suitable analytical expressions must be selected for creep and shrinkage. Since the experimental data for the particular structure to be analysed are usually lacking and are always incomplete, functions $J(t, t')$ (or $\bar{J}(t, t')$) and $\bar{\varepsilon}_S(t)$ to be used in the analysis of a particular structure must be predicted from various influencing factors known in advance. The selection of functions should satisfy the following criteria:

(1) The functions must first of all accurately fit the available experimental data for concretes of the type considered and take into account all important factors (age, temperature and its variations, environmental humidity and its variation, size and shape of cross section, and curing conditions and their duration).

(2) The undetermined coefficients of the functions should be relatively easy to evaluate from the available experimental or empirical data.

(3) The functions should be sufficiently simple to make the numerical evaluation in the program straightforward and efficient.

The last two requirements, i.e. the requirements of simplicity, are certainly not as stringent for finite element analysis as they are for simpler hand calculations. Generally the effort spent on determination of material properties should be commensurate to that devoted to the analysis itself. Since inaccuracies in material characterization usually cause the most serious error in the results of finite element analysis, it clearly makes no sense if the analyst spends, say, only 4 hours on determining the function $J(t, t')$ and then spends one week in getting the finite element solution based on this function. He should spend an equal time on both.

Several practical models for predicting creep and shrinkage properties for a particular concrete and environmental conditions have been developed. They differ in their degree of accuracy and simplicity, and usually one of these must be traded for the other. There exist principally three comprehensive models for the analyst to choose from:

(1) Model of ACI Committee 209.[58–60]
(2) Model of CEB-FIP Model Code[68] (Rüsch *et al.*[162]).
(3) Bažant and Panula's Model (BP Model), either its complete version[43] or its simplified version.[45]

The ACI Model is the simplest one, while the BP Model is the most comprehensive one, being applicable over the broadest time range (of t, t', and t_0) and covering a number of influencing factors neglected by the other

The BP Model was obtained by computer analysis and fitting of 80 different data sets on different concretes from different laboratories (over 800 creep and shrinkage curves involving about 10 000 data points). Based on this unusually large (computerized[204]) data bank, the 90% confidence limits (i.e. the relative deviations from the mean having a 5% probability of being exceeded on the plus side, and 5% on the minus side) were found for the BP Model to be $\omega_{90} = \pm 31\%$. For the ACI Model, comparison with the same data indicated $\omega_{90} = \pm 63\%$, and for the CEB-FIP Model $\omega_{90} = \pm 76\%$.[45] This superiority of the BP Model is obtained in spite of the fact that the data set used to obtain these numbers did not include the temperature effects (which the BP Model also describes well), and that the majority of test data used for comparison pertained to small size specimens and to a limited time range (i.e. $t - t'$ from one week to one year and t' from one week to six months), which the ACI and CEB-FIP Models describe better than large specimens or long times. For very long creep durations (>10 years), for very high or very small ages at loading (>10 years, <10 days), for thick specimens (>30 cm), and for the final slopes of creep curves, which matter for extrapolation, the comparison is even more favorable to the BP Model.

However, for drying creep, the confidence limits of the BP Model ($\omega_{90} = \pm 29\%$) are not much better than those of ACI Model (±42%) and especially the CEB-FIP Model (±32%). These two models are of course intended mainly for not too massive structures in a drying environment.

The magnitude of error for all existing models is large and there is no doubt much room for improvement. The greatest part of the errors results from the effects of composition of concrete. This is documented by the fact that prediction errors are greatly reduced when the initial elastic deformation or one short-time shrinkage value is measured.[45] Finite element analysis hardly makes sense if the error in $J(t, t')$ exceeds 20%, and so availability of some short-time tests is a requirement for practical applications. Note also that preferable are creep prediction formulae which can be easily calibrated from given short-time values.[45]

At present no consensus on the proper form of the compliance function $J(t, t')$ or $\bar{J}(t, t')$ has yet been reached. Much of the disagreement is due to the great statistical scatter of available test data, and even more perhaps due to the fact that a linear theory is used for a phenomenon which is not really linear, i.e. necessitates a non-linear theory. A linear theory can be adequate only within a limited range, and specialists still disagree as to what is this range, in particular what is the type of tests to be used for determining the compliance function for a linear theory. Some include only creep or relaxation tests for all ages at loading, which alone define the compliance function completely, while others include information from creep recovery tests (without analysing them by a non-linear theory) at the expense of representing creep for high ages at loading and long times. Since a non-linear theory is not considered appropriate for building codes, the question is which form of the compliance function gives the best results in practical problems over the broadest possible range.

Since the long-time creep is of main interest, efforts have been made to compare the creep prediction models with the 'final' creep values obtained directly from creep measurements. Such comparisons suffer, however, by the error which inevitably occurs in determining such 'final' values from the test data and is just as large as the error of the creep model that is supposed to be checked. For example, it has become almost traditional for the experimentalists to use the Ross hyperbola[144,145,31]: $C = \bar{t}/(a + b\bar{t})$ where $\bar{t} = t - t'$ and $C = J(t, t') - [1/E(t')]$. This relation may be written as $1/C = b + a/\bar{t}$. So, if one plots the measured data as $1/C$ versus $1/\bar{t}$ and approximates this plot by a straight regression line, the slope of the line and its intercept with the $1/C$ axis yield coefficients a and b, and the value of b at the same time indicates the extrapolated 'final' value of creep ($\bar{t} \to \infty$). The plot looks very satisfactory if the creep data span over a limited time period, such as from $\bar{t} = 1$ week to 1 year, and one is then inclined to think that the final value obtained from this plot is good. Only such limited data were available in the early investigations in the 1930's and so the use of Ross' hyperbola appeared adequate and became standard practice. At present, however, long-range creep measurements of basic creep are available, and then gross deviations from Ross' hyperbola are found; see Bažant and Chern.[31] It is interesting to observe that even when the errors of the Ross hyperbola are not too conspicuous in the plot of $1/\bar{C}$ versus $1/\bar{t}$ they are blatant in the usual plot of $J(t, t')$ versus $\log \bar{t}$. Thus we see that the practice of showing only the plot of $1/C$ versus $1/\bar{t}$ is misleading. The inverse scales $1/C$ and $1/\bar{t}$ obscure the errors for long times by crowding together the points for large C and large $\bar{t}$. One other element of error and ambiguity was already discussed, namely the value to be used for $E(t')$ which must be decided before the plot of $1/C$ versus $1/\bar{t}$ can be constructed.

The 'final' values of creep obtained from creep test data on the basis of Ross' hyperbola were recently compared by Müller and Hilsdorf with various models for creep prediction, and it was observed that the agreement was best for the CEB-FIP 1978 Model Code. From the preceding analysis it is, however, clear that such a method of comparision of various models is fallacious.[31] The 'final' value found by extrapolating the test data strongly depends on the choice of the expression for the creep curve, in this case the Ross hyperbola, and the error of the long-time values of Ross' hyperbola compared to more realistic expressions, such as the double power law, is easily 50%. So one tacitly implies the wrong model in determining the 'final' value, and then one concludes that some other model does not agree with this 'final' value. This is a circular argument.

two models. It should be remembered that all three models are at least partially empirical (albeit to various extents) and are all based on the fitting of data obtained in certain laboratory controlled tests. Attempts at verification by measurements on structures have so far been inconclusive due to the difficulties in sorting out various influencing factors, which are much more numerous than in laboratory tests.

(I) *ACI Model.*[5] Based on the works of Branson *et al.*[60], ACI Committee 209 recommended the expressions[5]:

$$\bar{J}(t,t') = \frac{1}{E(t')}\left(1+\frac{(t-t')^{0.6}}{10+(t-t')^{0.6}}C_u\right) \qquad \bar{\varepsilon}_S(t,t_0) = \frac{t-t_0}{f_c+(t-t_0)}\varepsilon_u^s \tag{7.13}$$

in which t' is the age at loading in days, t is the current age in days, t_0 is the age of concrete in days at the completion of curing; f_c is a constant; C_u is the ultimate creep coefficient, defined as the ratio of the (assumed) creep strain at infinite time to the initial strain at loading; and ε_u^s is the ultimate shrinkage strain after infinite time. Coefficients C_u and ε_u^s are defined as functions of environmental humidity, minimum thickness of structural member, slump, cement content, percent fines, and air content; see Section 7.7.1.

(II) *CEB-FIP Model.*[68] According to the CEB-FIP Model Code, the expressions for the mean compliance function and the mean shrinkage of cross section of a structural member have the basic form

$$\bar{J}(t,t') = F_i(t') + \frac{\phi_d\beta_d(t-t')}{E_{c28}} + \frac{\phi_f[\beta_f(t)-\beta_f(t')]}{E_{c28}} \tag{7.14}$$

$$\bar{\varepsilon}_S(t,t_0) = \varepsilon_{su}[\beta_s(t)-\beta_s(t_0)] \tag{7.15}$$

in which E_{c28} is the elastic modulus of concrete at age 28 days; $\phi_d = 0.4$; ϕ_f is a coefficient depending on environmental humidity and effective thickness of member, β_f and β_s are functions of time and effective thickness, β_d is a function of load duration $t-t'$; $F_i(t')$ is a function of age at loading(= sum of instantaneous strain and initial creep strain over a period of several days). These functions are defined by graphs consisting of 16 curves. (The use of graphs is however not too convenient for computer programming.)

(III) *BP Model.* The basic form of this model utilizes Equations (7.5) and (7.9)–(7.12) which ensue from the diffusion theory and activation energy theory, as already explained. The coefficients in these equations were expressed by empirical formulae determined from test results; see Section 7.7.3. For the case of drying, these formulae are relatively complicated, which is, however, at least partly due to consideration of unusually many influencing factors and a very broad range of applicability. A program for computer evaluation of the BP Model or its fitting to given data is available (see full program listing in Ref. 199).

7.2.7.1 *Comparision of existing models*

The BP Model and the ACI Model have in common, for basic creep, the product form of the compliance function, in which a function of the age at loading multiplies a function of the stress duration. In the ACI Model, however, the multiplicative factor C_u introduces not only the effect of age at loading but also the effect of humidity and size. This is very simple but not quite realistic because the diffusion theory leads to a different form of the size effect, as mentioned before (translation in log-time rather than scaling of the ordinates). The same deficiency characterizes the ACI shrinkage formula (Equation (7.13)).

Likewise, the CEB-FIB Model does not follow the size effect of the diffusion theory. In this model, the basic form of $\bar{J}(t,t')$ is based on the idea of reversibility of deformation. The second term in Equation (7.14) is considered to represent the so-called 'reversible' (or delayed elastic) creep, and the last term the so-called 'irreversible' creep. It must be noted, however, that in the case of aging the concept of a reversible creep component lacks theoretical (thermodynamic) justification because this component cannot be defined uniquely (only reversible creep increments can).[27]

The fact that in the CEB-FIP Model the so-called 'reversible' component of $\bar{J}(t,t')$ was calibrated by fitting the creep recovery curves obtained from the superposition principle to recovery test data is also questionable[40,47,45] because linear superposition does not hold in case of unloading, as has been conclusively demonstrated by tests (cf. Section 7.3.1). The domain of approximate validity of the principle of superposition includes only non-decreasing strain histories within the service stress range. Thus, only the creep curves for various ages at loading and the relaxation curves belong to this domain and are suitable for calibrating the compliance function.

The fact that the second term in Equation (7.14) is assumed to be independent of t' and the last one independent of $t-t'$ has also been questioned, on the basis of test data.[40,27] Another aspect which was criticized on the basis of test data is that the humidity and size influences in Equation (7.14) appear only in the irreversible term,[44] and that the size effect in the shrinkage term does not correspond to diffusion theory.

The BP Model is the only one which involves the influence of temperature. It gives this influence for shrinkage, basic creep, and drying creep. It also gives the effect of the load cycling (pulsation), the effects of the delay of the start of loading after the start of drying, the time lag of loading after heating, the decrease of creep after drying, swelling in water, autogeneous shrinkage of sealed concrete,[101] etc. The price paid for this broader range of applicability is larger complexity. The BP Model differs from the ACI and CEB-FIP Models also by the absence of a final (asymptotic) value of creep. We have already commented on this aspect.

7.3 LINEAR CONSTITUTIVE RELATIONS WITH HISTORY INTEGRALS

7.3.1 Principle of superposition

Due to creep, shrinkage, and temperature changes, the stresses in structures normally vary significantly in time even if the loads are constant. Thus, the foregoing exposition of material behaviour under constant stress must be extended to formulate a constitutive equation valid for arbitrarily variable stresses or strains. This task is simplified by the fact that, within the range of service stresses (up to about 1/2 of the strength) and with the exception of decreasing strain, concrete may be approximately treated as a linear material, precisely an aging linear viscoelastic material, the theory of which rests on the principle of superposition. The linearity property simplifies structural analysis, while the aging complicates it greatly.

The principle of superposition, which is equivalent to the hypothesis of linearity, states that a response to a sum of two stress (or strain) histories is the sum of the responses to each of them taken separately. According to this principle, the strain due to any stress history $\sigma(t)$ may be obtained by regarding the history as the sum of increments $d\sigma(t')$ applied at times $t' \in (0, t)$ and summing the corresponding strains which equal $d\sigma(t')J(t, t')$ according to Equation (7.2) (Figure 7.9(a)). This yields

$$\varepsilon(t) = \int_0^t J(t, t')\, d\sigma(t') + \varepsilon^0(t) \tag{7.16}$$

in which $\varepsilon^0(t)$ is the stress-independent strain (shrinkage plus thermal strain). Equation (7.16) represents the uniaxial constitutive equation which relates general histories of uniaxial stress σ and strain ε. The integral in this equation should be understood as the Stieltjes integral, the advantage of which is that it is applicable even for discontinuous stress histories. If $\sigma(t)$ is continuous one has $d\sigma(t') = [d\sigma(t')/dt']\, dt'$, which yields the usual (Riemann)

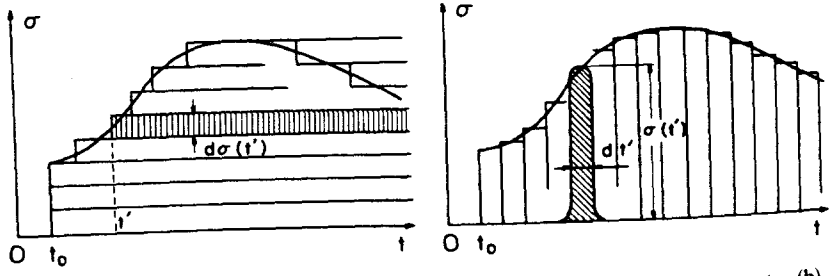

Figure 7.9 Representation of arbitrary strain history by: (a) stress increments; (b) stress impulses

integral. (The principle of superposition was stated in the works of Boltzmann[57] for non-aging materials and Volterra[181] for aging materials.)

Measurements agree with the principle of superposition very closely under the following conditions:

(1) The magnitude of stresses is below about 40% of the strength, i.e. within the service stress range.
(2) The strains do not decrease in magnitude (but the stresses can).
(3) The specimen undergoes no significant drying during creep.
(4) There is no large increase of the stress magnitude late after initial loading (cf. Section 7.5.2).

Violation of the last condition causes less error than any of the first three conditions, and so this condition may be dropped in cruder analysis. Condition (2) is very important and excludes, in particular, the creep recovery after unloading, for which the principle of superposition predicts far too much recovery (often twice the observed amount). Some investigators propsed modification of the creep function to predict recovery while keeping the assumption of linearity of creep theory. Such efforts are doomed, however, since one loses more than one gains, sacrificing close approximation of all other behaviour within the linearity range. Prediction of recovery and any response at decreasing strains requires a non-linear theory (Section 7.5.2).

Drying that is simultaneous with creep is a major cause of non-linear dependence on stress. This is probably to a large extent caused by microcracking, cracking, and tensile non-linear behaviour for internal stresses induced by shrinkage and differences in creep. Nevertheless, due to the complexity of non-linear analysis, the principle of superposition is routinely used for structures exposed to a drying environment (such as regular climate conditions) and the mean cross-section compliance $\bar{J}(t, t')$ is substituted for $J(t, t')$. We must however keep in mind that the results of such analysis can be greatly in error. The magnitude of the error is smaller for thicker members and also for prestressed members, since prestress reduces cracking. To eliminate cracking entirely, a large three-dimensional prestress (confinement) is required, which is rarely the case in practice except in spirally reinforced compressed members. However, adequate experimental data on the effects that prestress, confinement, and size have on the deviations from the principle of superposition (linearity) are not available at present.

It is interesting to observe that the proportionality property, which means that if stress history $\sigma(t)$ produces strain history $\varepsilon(t)$ then stress history $k\sigma(t)$ produces strain history $k\varepsilon(t)$, appears to have a broader applicability than the principle of superposition, being verified reasonably well for all loading that meets conditions (1) and (3) but not necessarily (2) and (4). To model

this, a non-linear integral-type constitutive relation with a singular kernel seems to work (see Section 7.5.3).

Substituting $d\sigma(t') = [d\sigma(t')/dt']\,dt'$ and integrating by parts, we may transform Equation (7.16) to the following equivalent form:

$$\varepsilon_1(t) = \frac{\sigma(t)}{E(t)} + \int_0^t L(t, t')\sigma(t')\,dt' + \varepsilon^0(t) \tag{7.17}$$

in which $L(t, t') = -\partial J(t, t')/\partial t'$. Geometrically, this equation means that we decompose the stress history into vertical strips and consider each strip as an impulse function (Figure 7.9(b)). The magnitude of each impulse is $\sigma(t')\,dt'$ (area of the strip) and its stress response is $L(t, t')\sigma(t')\,dt'$. Thus, $L(t, t')$ represents the strain at time t caused by a unit stress impulse (Dirac δ-function) at time t' ($t' \leqslant t$), and is called the stress impulse memory function.

Another useful relation is obtained by differentiating Equation (7.16):

$$\dot{\varepsilon}(t) = \frac{\dot{\sigma}(t)}{E(t)} + \int_0^t \frac{\partial J(t, t')}{\partial t}\,d\sigma(t') \tag{7.18}$$

where superimposed dots denote time derivatives. The integral gives the creep contribution to the strain rate.

7.3.2 Stress relaxation and superposition

The variation of stress at constant strain is called relaxation. It is characterized by the relaxation function, $R(t, t')$ (also called relaxation modulus), which represents the uniaxial stress σ at time t (age) caused by a unit constant strain imposed at time t'. The typical relaxation function is plotted in Figure 7.10. The response to a general strain history may then be expressed using the principle of superposition. Any strain history may be imagined to consist of small strain increments $d\varepsilon(t')$ introduced at times t', each of which can be regarded as a horizontal strip, similarly to Figure

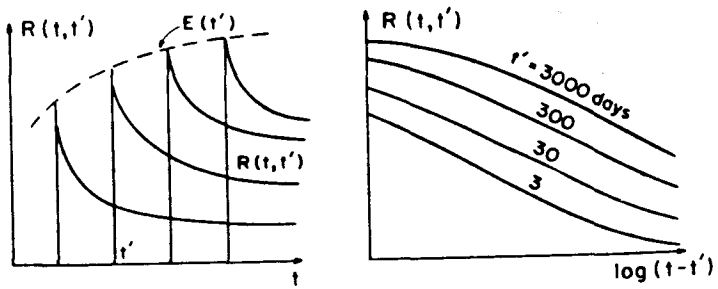

Figure 7.10 Typical relaxation curves for various ages t' at strain imposition

7.9(a)). The stress caused by each of them is $R(t, t')\,d\varepsilon(t')$. Summing all these stresses, and subtracting the shrinkage increments $d\varepsilon^0(t')$ since by definition they produce no stress, we have

$$\sigma(t) = \int_0^t R(t, t')[d\varepsilon(t') - d\varepsilon^0(t')] \tag{7.19}$$

For a given stress history, Equation (7.16) represents a Volterra integral equation for the strain history $\varepsilon(t)$. By solving Equation (7.16) for stress at given unit constant strain imposed at various ages t' one may calculate the individual relaxation curves. All these curves together define the relaxation function. Conversely, by solving Equation (7.17) (also a Volterra integral equation) for strain at given unit constant stresses applied at various ages t', one may calculate the individual creep curves, which all together define the compliance function. So, the integral equations, (7.16) and (7.17), are equivalent; one is said to be the resolvent of the other. Of the kernels, $J(t, t')$ and $R(t, t')$, only one may be specified independently and the other one follows.

In absence of drying, the relaxation function obtained by solving Equation (7.19) from the measured compliance function usually agrees with relaxation measurements quite well (Figure 7.11).

The creep function may be converted to the relaxation function by solving the integral equation (Equation (7.16)). We may use for this purpose the step-by-step algorithm given in the next section, for which a simple program was published.[22,199] There also exists a very good approximate formula[34] valid for $t - t' > 1$ day:

$$R(t, t') \simeq \frac{1 - \Delta_0}{J(t, t')} - \frac{0.115}{J(t, t-1)}\left(\frac{J(t-\Delta, t')}{J(t, t'+\Delta)} - 1\right) \tag{7.20}$$

in which $\Delta = (t - t')/2$, $\Delta_0 \simeq 0.008$, and $t - 1$ means t minus 1 day. Compared to exact solution according to the principle of superposition, the error of this formula is normally (e.g. for double power law) within 1% of the initial value, i.e. within $0.01R(28 + 0.1, 28)$.

Instead of specifying the compliance function as we did in Section 7.2, the time-dependent behaviour could, alternatively, be described in terms of the relaxation function.[91,158,93,94,115,159,76] The main reason why this is not usually done is that creep tests are somewhat easier to perform than the relaxation tests. Besides, the relaxation function can be determined from the creep function.

This is well applicable, though only for creep without moisture loss, for which the conversion is indeed very accurate. At drying the relaxation function obtained by the principle of superposition from the creep tests may deviate significantly from relaxation measurements. In such cases it might be preferable to use a directly measured relaxation (rather than compliance)

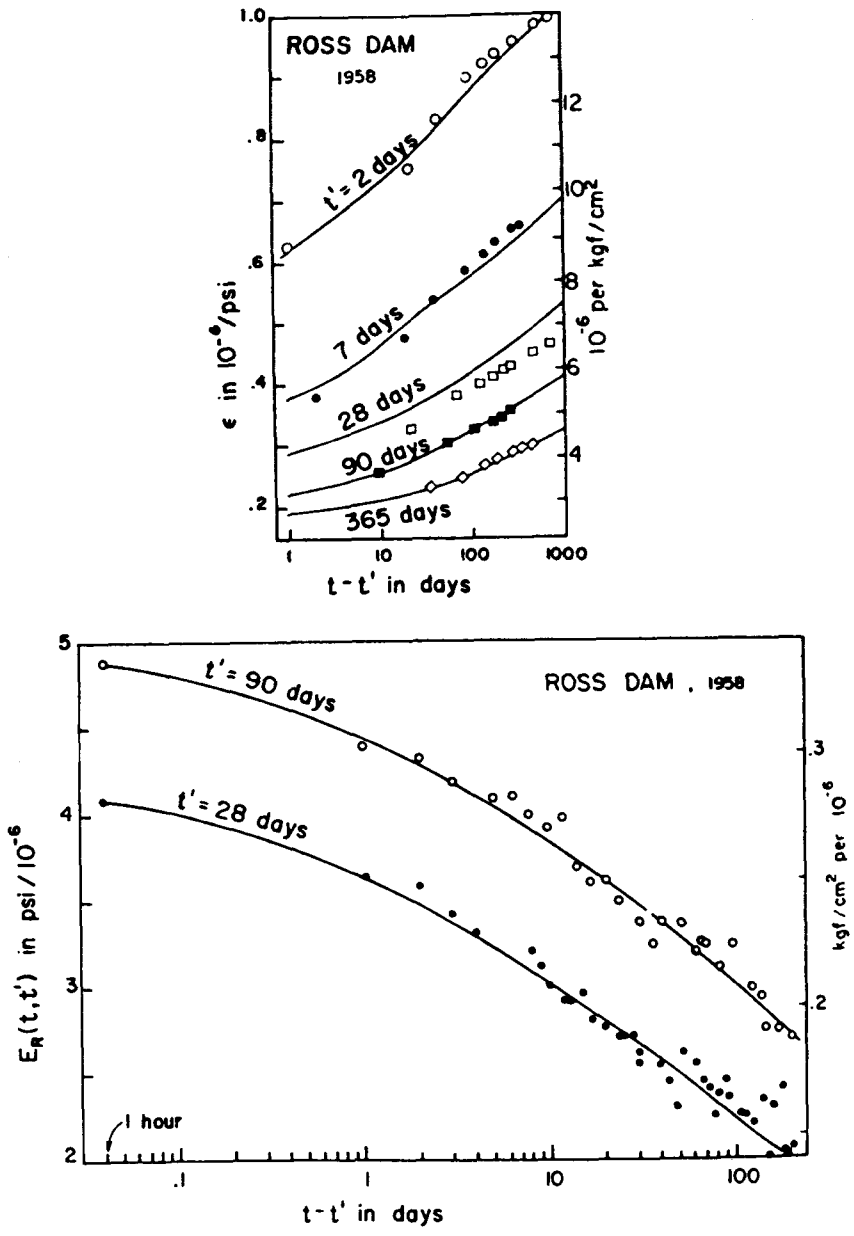

Figure 7.11 Relaxation curves calculated according to the principle of superposition from measured creep data, and their comparison with measured relaxation data. Calculations from Bažant and Wu[53]; data from Harboe *et al.*[93] and Hanson[94]

function for the analysis of certain structural problems. These are the relaxation-type problems, such as the effects of a sudden differential settlement or certain types of stress redistribution in the structure for which stresses generally decline and strains are nearly constant.

7.3.3 Multiaxial generalization and operator form

The multiaxial generalization of all preceding relations can be easily determined assuming isotropy. It suffices to write stress–strain relations of the same form as the uniaxial ones separately for the volumetric and the deviatoric components of stress and strains. Thus, analogy to Equation (7.16) provides

$$\left.\begin{aligned} 3\varepsilon^{V}(t) &= \int_0^t J^{V}(t,t')\,d\sigma^{V}(t') + 3\varepsilon^{0}(t) \\ 2\varepsilon_{ij}^{D}(t) &= \int_0^t J^{D}(t,t')\,d\sigma_{ij}^{D}(t') \end{aligned}\right\} \tag{7.21}$$

in which $\varepsilon_{ij}^{D} = \varepsilon_{ij} - \delta_{ij}\varepsilon^{V}$ is the deviator of the strain tensor ε_{ij}, $\sigma_{ij}^{D} = \sigma_{ij} - \delta_{ij}\sigma^{V}$ is the deviator of the stress tensor σ_{ij}; δ_{ij} is the Kronecker delta, $\varepsilon^{V} = \varepsilon_{kk}/3$, $\sigma^{V} = \sigma_{kk}/3$ (volumetric strain and stress). The subscripts refer to Cartesian coordinates $x_1 \equiv x$, $x_2 \equiv y$, $x_3 \equiv z$ $(i, j = 1, 2, 3)$ (and the summation rule is assumed). Functions $J^{V}(t,t')$ and $J^{D}(t,t')$ are the volumetric and deviatoric compliance functions which are related to $J(t,t')$ as follows:

$$J^{V}(t,t') = 6(\tfrac{1}{2} - \nu)J(t,t') \qquad J^{D}(t,t') = 2(1+\nu)J(t,t') \tag{7.22}$$

Here ν is the Poisson ratio, which is in general also a function of t and t', but can be considered as approximately constant ($\nu \approx 0.18$). When, however, drying creep is considered and is described by means of cross-section mean compliance $\bar{J}(t,t')$, then the corresponding mean Poisson ratio is quite variable and can drop to almost zero. Moreover, drying should also cause anisotropy, as a result of microcracking. (For test data on multiaxial creep see McDonald,[124] York,[196] Arthanari and Yu,[9] Neville and Dilger,[145] Meyer,[135] Illston and Jordaan.[103]).

Equation (7.17), based on the relaxation function, and the impulse memory formulations such as Equation (7.21), may be generalized for multiaxial stress similarly.

The linear viscoelastic stress–strain relations of aging material can be also expressed in the form of differential rather than integral equations. This will be outlined in Section 7.4.2.

The constitutive relations may be written in the form $3\varepsilon^{V} = \mathbf{K}^{-1}\sigma^{V} + \varepsilon^{0}$, $2\varepsilon_{ij}^{D} = \mathbf{G}^{-1}\sigma_{ij}^{D}$ where $\mathbf{K}^{-1}$ and $\mathbf{G}^{-1}$ are Volterra integral operators which are of non-convolution type and can be manipulated according to the rules of

linear algebra. This is exploited in the extension of elastic-viscoelastic analogy to aging materials,[129] which permits converting all equations of linear elasticity to analagous equations for creep.[129,11-14]

7.3.4 Application of principle of superposition

A numerical step-by-step solution may be based on the principle of superposition. For this purpose time t is subdivided by discrete times t_r ($r = 0, 1, 2, \ldots$) into time steps $\Delta t_r = t_r - t_{r-1}$. Time t_0 coincides with the instant of first loading t_0. If there is a sudden change of load at time t_s, it is convenient for programming to use a time step of zero duration, i.e. set $t_{s+1} = t_s$ or $t_{s+1} = t_s + 1$ second (Figure 7.12). Often such a sudden load change occurs at the start, i.e. at $t_s = t_0$, and then we choose $t_1 = t_0$ and assume the load to be applied during the first interval (t_0, t_1).

Under constant loads, the strains and stresses vary at a rate which decreases roughly as the inverse of time, and for this reason it must be possible to use increasing time steps Δt_r (Figure 7.12). This is also necessary if long times (say $t - t_0 = 50$ years) should be reached in computation, and if the initial time step should be small. Computation is most efficient if we use time steps that are constant in the log $(t - t')$ scale, i.e. $(t_r - t_0)/(t_{r-1} - t_0) =$ constant. Normally about 4 steps per decade in log-time suffice. The first step may usually be chosen as 0.1 day. If there is a sudden change of loading at some later time, one must begin again with small time steps and then increase the steps gradually as long as the load remains constant.

Using the trapezoidal rule, the error of which is proportional to $\Delta\sigma^2$, Equations (7.21) may be approximated[22,38] as

$$3\varepsilon_r^{\mathrm{V}} = \sum_{s=1}^{r} J_{r,s-1/2}^{\mathrm{V}}\,\Delta\sigma_s^{\mathrm{V}} + 3\Delta\varepsilon_r^0 \qquad 2\varepsilon_{ij,}^{\mathrm{D}} = \sum_{s=1}^{r} J_{r,s-1/2}^{\mathrm{D}}\,\Delta\sigma_{ij,}^{\mathrm{D}} \tag{7.23}$$

where $\Delta\sigma_s^{\mathrm{V}} = \sigma_s^{\mathrm{V}} - \sigma_{s-1}^{\mathrm{V}}$, $\Delta\sigma_{ij,}^{\mathrm{D}} = \sigma_{ij,}^{\mathrm{D}} - \sigma_{ij,}^{\mathrm{D}}{}_{,}$, $\sigma_s^{\mathrm{V}} = \sigma^{\mathrm{V}}(t_s)$, etc.; subscripts r, s refer to the discrete times t_r, t_s. For $J_{r,s-1/2}^{\mathrm{V}}$ one has two options; either one may take it as $(J_{r,s}^{\mathrm{V}} + J_{r,s-1}^{\mathrm{V}})/2$ where $J_{r,s}^{\mathrm{V}}$ is a notation for $J^{\mathrm{V}}(t_r, t_s)$, or one may take it as $J^{\mathrm{V}}(t_r, t_{s-1/2})$ where $t_{s-1/2}$ denotes the middle of time interval

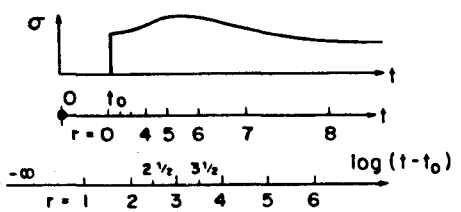

Figure 7.12 Discrete subdivision of time

(t_{s-1}, t_s) in the log $(t - t_0)$ scale, i.e. $t_{s-1/2} = t_0 + [(t_s - t_0)(t_{s-1} - t_0)]^{1/2}$. A similar notation applies to $J_{r,s-1/2}^{\mathrm{D}}$.

Writing Equation (7.23) also for $\varepsilon_{r-1}^{\mathrm{V}}$ and $\varepsilon_{ij,r-1}^{\mathrm{D}}$ and subtracting it then from Equation (7.23), one obtains[22] for volumetric and deviatoric increments:

$$\Delta\sigma_r^{\mathrm{V}} = 3K_r''(\Delta\varepsilon_r^{\mathrm{V}} - \Delta\varepsilon_r''^{\mathrm{V}}) \qquad \Delta\sigma_{ij,}^{\mathrm{D}} = 2G_r''(\Delta\varepsilon_{ij,}^{\mathrm{D}} - \Delta\varepsilon_{ij,}''^{\mathrm{D}}) \tag{7.24}$$

in which

$$K_r'' = \frac{1}{J_{r,r-1/2}^{\mathrm{V}}} \qquad G_r'' = \frac{1}{J_{r,r-1/2}^{\mathrm{D}}} \quad \text{for } r \geq 1 \tag{7.25}$$

$$3\Delta\varepsilon_r''^{\mathrm{V}} = \sum_{s=1}^{r-1} \Delta J_{r,s}^{\mathrm{V}}\,\Delta\sigma_s^{\mathrm{V}} - 3\Delta\varepsilon_r^0 \qquad 2\Delta\varepsilon_{ij,}''^{\mathrm{D}} = \sum_{s=1}^{r-1} \Delta J_{r,s}^{\mathrm{D}}\,\Delta\sigma_{ij,}^{\mathrm{D}} \quad \text{for } r \geq 2 \tag{7.26}$$

$$\Delta\varepsilon_r''^{\mathrm{V}} = \Delta\varepsilon_1^0 \qquad \Delta\varepsilon_{ij,}''^{\mathrm{D}} = 0 \quad \text{for } r = 1$$

$$\Delta J_{r,s}^{\mathrm{V}} = J_{r,s-1/2}^{\mathrm{V}} - J_{r-1,s-1/2}^{\mathrm{V}} \qquad \Delta J_{r,s}^{\mathrm{D}} = J_{r,s-1/2}^{\mathrm{D}} - J_{r-1,s-1/2}^{\mathrm{D}} \tag{7.27}$$

Since $\Delta\varepsilon_r''^{\mathrm{V}}$, $\Delta\varepsilon_{ij,}''^{\mathrm{D}}$ and K_r'', G_r'' can be evaluated from the values of the stresses before the current time t_r, their values are known before solving σ_r and ε_r. Therefore, Equation (7.24) may be regarded as an incremental elastic stress–strain relation,[22,38] with bulk modulus K_r'', shear modulus G_r'', and inelastic (initial) strains of volumetric and deviatoric components $\Delta\varepsilon_r''^{\mathrm{V}}$, $\Delta\varepsilon_{ij,}''^{\mathrm{D}}$. The incremental elastic stiffness matrix can be set up using K_r'' and G_r''. The creep analysis is thus reduced to a sequence of elastic analyses for the individual time steps. Each of them can be carried out by finite elements. Within each time step, the prescribed increments of loads and displacements must be considered.

Analogous equations may be written for uniaxial behaviour, e.g. for frame analysis.

Algorithms in which the integral from Equation (7.16) is approximated by the rectangle rule, yielding the sum $\sum J_{r,s-1}\,\Delta\sigma_s$ instead of that in Equation (7.23), have been used in practice. However, they are not any simpler. Their error, being of first rather than second order in $\Delta\sigma$, is larger and so more time steps (and more computer storage for the stress history) are required.

To gain an idea of accuracy, the convergence is illustrated in Table 7.1 which gives the values of $R(t, t_0)$ calculated from $J(t, t')$ by the above second-order algorithm (Equations (7.24)–(7.27)) as well as by the first-order algorithm mentioned before. Table 7.1 also gives the values of $J(t, t_0)$ calculated from $R(t, t')$ using a similar second-order algorithm based on Equation (7.19). The calculation of $R(t, t_0)$ was made[22] for ACI compliance function, $t = 1035$ days, $t_0 = 35$ days, and discrete times $t_r = t_0 + [10^{r/m}(0.1$ day)]; $r = 1, 2, 3, \ldots$; $m =$ number of steps per decade. The calculation of $J(t, t_0)$ was made for $R(t, t')$ obtained by the formula in Equation (7.20)

Table 7.1 Convergence of step-by-step method based on superposition

Number m of steps per decade	$R(t, t_0)$ from $J(t, t')$ 2nd-order method		$R(t, t_0)$ from $J(t, t')$ 1st-order method		$J(t, t_0)$ from $R(t, t')$ 2nd-order method	
1					2.3429	424
2	0.3532	60	0.3311	157	2.3845	235
4	0.3592	26	0.3468	88	2.4070	113
8	0.3618	12	0.3556	43	2.4183	54
16	0.3630	5	0.3599	20	2.4237	27
32	0.3635	2	0.3619	10	2.4264	
64	0.3637		0.3629		—	

from double power law with $n=0.14$, $m=0.3$, $\alpha=0.04$, $\phi_1=1$, and for $t_0=28$ days, $t=10{,}028$ days, and discrete times $t_r=t_0+[10^{r/m}(0.0001\text{ day})]$. From the table we see that algorithms based on $J(t,t')$ or $R(t,t')$ are about equally accurate and that in order to keep the error below 1%, about 4 steps per decade suffice for the second-order method and 16 steps per decade for the first-order method.

It is interesting to note that the simple replacement of the impulse memory integral in Equation (7.17) with a sum is computationally less efficient and does not always produce a convergent step-by-step solution. It is partly for this reason that Equation (7.16) has recently been favoured over Equation (7.17) used in earlier works.[1,10,18-20,129]

The foregoing type of algorithm based on the principle of superposition is effective and works well for small to medium size structural systems.[102,201] For large systems with many unknowns, however, the demands for computer storage as well as time become excessive. For each finite element one must store all the preceding values of all stress components, and at each time step one must evaluate long sums from these values. This requires a very large storage capacity, which must normally be met by peripheral storage. Numerous transfers to and from the peripheral storage at each time step then greatly prolong the running time. A decade ago these demands were forbidding and only medium-size structural systems could be solved (and at great expense) by the step-by-step methods based directly on the compliance function.[154,69,164] Today even large systems could be solved in this manner on the largest computers in existence. However, that would be wasteful. Far more effective methods have recently been developed, and we will discuss these in Section 7.4.

7.3.5 Age-adjusted effective modulus method

In case the structure is suddenly loaded at time t_0 and afterwards the loads are steady, the simplest method is to use a certain quasi-elastic stress–strain relation for the total increment from t_0, the time of first loading, to current time t. For uniaxial stress σ_{11} this relation may be written as:

$$\Delta\varepsilon_{11}=\frac{\Delta\sigma_{11}}{E_{11}}+\Delta\varepsilon''_{11}\qquad \Delta\varepsilon''_{11}=\frac{\sigma_{11}(t_0)}{E(t_0)}\,\phi(t,t_0)+\Delta\varepsilon^0 \tag{7.28}$$

where $\Delta\sigma_{11}=\sigma_{11}(t)-\sigma_{11}(t_0)$, $\Delta\varepsilon_{11}=\varepsilon_{11}(t)-\varepsilon_{11}(t_0)$, $\varepsilon_{11}(t_0)=\sigma_{11}(t_0)/E(t_0)$; and E'' serves as the apparent elastic modulus for the increment, $\Delta\varepsilon''_{11}$ is the inelastic strain increment, $\Delta\varepsilon^0$ is the shrinkage strain increment. One might think at first that a good estimate would be $\Delta\varepsilon_{11}=\Delta\sigma_{11}/E(t_0)+\frac{1}{2}[\sigma(t_0)+\sigma(t)]\,\phi(t,t_0)/E(t_0)$, which is equivalent to Equation (7.28) if we set $E''=E(t_0)/[1+\phi(t,t_0)/2]$. However, comparisons with the exact solution of the integral equation shows that this value of E'' is usually too high, and far too high when t_0 is great. A better estimate, actually far better in case of high t_0, is $\varepsilon_{11}(t)=\sigma_{11}(t)/E_{\text{eff}}$ with $E_{\text{eff}}=E(t_0)/[1+\phi(t,t_0)]=$ effective (sustained) modulus;[126,80] this relation is obtained from Equation (7.28) when $E''=E_{\text{eff}}$. The best estimate thus seems to be $E''=E(t_0)/[1+\chi\phi(t,t_0)]$ where χ is some coefficient between 0.5 and 1.0.

Calibrating the value of χ according to approximate but good results for $\Delta\sigma$ for the relaxation test (and neglecting the age dependence of $E(t)$), Trost[176] obtained suitable approximate values of χ, typically $\chi=0.8$ to 0.9. Subsequently, an exact statement (a theorem) which underlies the effectiveness of this approach and applies also for age-dependent $E(t)$, was found.[23] Namely, if the strain history is linear in $J(t,t')$, i.e. of the form $\varepsilon(t)=\varepsilon_0+c_1J(t,t_0)$ (Figure 7.13), then the stress history is linear in $R(t,t_0)$, i.e. of the form $\sigma(t)=\sigma_0+c_2R(t,t_0)$, and Equation (7.28) is exact if

$$E''=\frac{E(t_0)-R(t,t_0)}{\phi(t,t_0)} \tag{7.29}$$

as proven by Bažant[23] (see Section 7.7.5). The method is effective because the actual histories of stress and strain in structures under a steady load or a load which changes gradually at a decaying rate (shrinkage) are rather close to linear functions of $J(t,t_0)$ and $R(t,t_0)$.

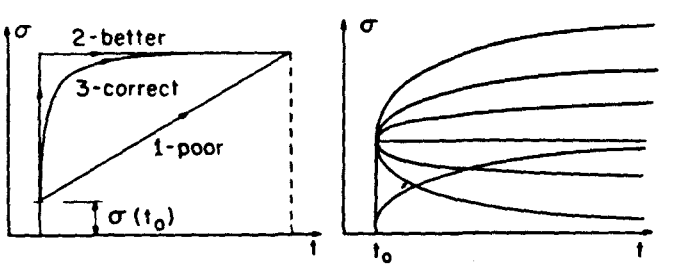

Figure 7.13 Strain histories expressed as a linear combination of the relaxation function

E'' is called the age-adjusted effective modulus. The term comes from the fact that in the absence of aging (or when t_0 is high) E'' is nearly exactly equal to E_{eff}, which reveals that the difference between E'' and E_{eff} is almost entirely due to aging. For practical calculations of E'', it suffices to use in Equation (7.29) the approximate expression for $R(t, t_0)$ according to Equation (7.20).

In case of multiaxial stress, Equation (7.28) may be generalized as

$$\Delta\varepsilon^{V}=\frac{\Delta\sigma^{V}}{3K''}+\Delta\varepsilon''^{V} \qquad \Delta\varepsilon_{ij}^{D}=\frac{\Delta\sigma_{ij}^{D}}{2G''}+\Delta\varepsilon_{ij}''^{D} \tag{7.30}$$

with

$$\Delta\varepsilon''^{V}=\frac{\sigma^{V}(t_0)}{3K(t_0)}\phi(t, t_0)+\Delta\varepsilon^{0} \qquad \Delta\varepsilon_{ij}''^{D}=\frac{\sigma_{ij}^{D}(t_0)}{2G(t_0)}\phi(t, t_0) \tag{7.31}$$

in which K'' and G'' are the bulk and shear moduli that correspond to Poisson's ratio ν and Young's modulus E'' given by Equation (7.29); i.e. $3K''=E''/(1-2\nu)$, $2G''=E''/(1+\nu)$.

In the case where several steady loads or imposed deformations start at different times t_0, the effect of each of them may be analysed separately according to Equations (7.28) or (7.31) and the results may then be superimposed.

For applications see, e.g. Bažant, Carreira and Walser,[30] Bažant and Najjar,[38] Bažant and Panula.[45]

7.4 LINEAR CONSTITUTIVE RELATIONS WITHOUT HISTORY INTEGRALS

7.4.1 Degenerate kernel

The need for storing and using the complete history of stresses or strains may be eliminated if the integral-type creep law (Equations (7.16) or (7.19) or (7.21)) can be converted to a rate-type creep law, i.e. a creep law given by a system of first-order differential equations. It appears that this can always be done, not exactly but with any desired accuracy. The key is to approximate the kernel of one of the integral equations for the creep law (Equations (7.16) or (7.19) or (7.21)) by the so-called degenerate kernel, the general form of which is a sum of products of functions of t and functions of t'. The form may be written as

$$J(t, t')=\sum_{\mu=1}^{N}[1/C_\mu(t')]-\sum_{\mu=1}^{N}[B_\mu(t)/(B_\mu(t')C_\mu(t'))]$$

where C_μ and B_μ are functions of time. It is more convenient to denote

$y_\mu(t)=-\ln B_\mu(t)$, in which case $B_\mu(t)=\exp[-y_\mu(t)]$. Thus, the most general form of a degenerate kernel may always be written as

$$J(t, t')=\sum_{\mu=1}^{N}\frac{1}{C_\mu(t')}\{1-\exp[y_\mu(t')-y_\mu(t)]\} \tag{7.32}$$

In previous works only the special case when

$$y_\mu(t)=t/\tau_\mu \quad (\mu=1, 2, \ldots, N) \tag{7.33}$$

has been considered. Constants τ_μ are called the retardation times. Equation (7.32) then becomes

$$J(t, t')=\sum_{\mu=1}^{N}\frac{1}{C_\mu(t')}\{1-\exp[-(t-t')/\tau_\mu]\} \tag{7.34}$$

This is a series of real exponentials, called the Dirichlet series (sometimes also called the Prony series).† To represent the instantaneous (elastic) part of the compliance function, we choose very small first retardation time $\tau_1(\mu=1)$, e.g. $\tau_1=10^{-9}$ day, which means that the first term of the series is nearly exactly $1/C_1(t')$ and represents the instantaneous compliance; then we have $C_1(t')=E(t')$. This is more convenient for computer programming than using in Equation (7.3) a separate instantaneous term which is not a part of the sum.

When plotted in $\log(t-t')$ scale, the individual exponential terms in Equation (7.40) look like step functions with the step spread out over the period of about one decade (Figure 7.14(a)). Outside this decade on both left and right, each exponential term gives an almost horizontal curve. The point $t-t'=\tau_\mu$ is located roughly at the centre of the rise. The approximation of a creep curve by a sum of exponential curves (Equation (7.34)) may be imagined as shown in Figure 7.14(b). By passing horizontal strips and picking as τ_μ the times at the centre of the rise for each strip, it is possible to obtain graphically a crude Dirichlet series approximation (i.e. the values of $\hat{E}_\mu(t')$ for each chosen t'). From this graphical construction several salient properties become evident.

(1) The approximation is not unique, since various divisions in horizontal strips in Figure 7.14 can be used to approximate the same creep curve. In particular, various choices of τ_μ must yield equally good results. Therefore, the values of τ_μ must be chosen in advance. Attempting to calculate them, e.g. from a least-square condition, leads to an unstable problem characterized by an ill-conditioned equation system and a non-unique solution.[118]

(2) For the sake of simplicity, one can choose the same τ_μ values for the

† Hardy and Riesz,[96] Lanczos,[118] Cost,[73] Schapery,[166] Williams.[187]

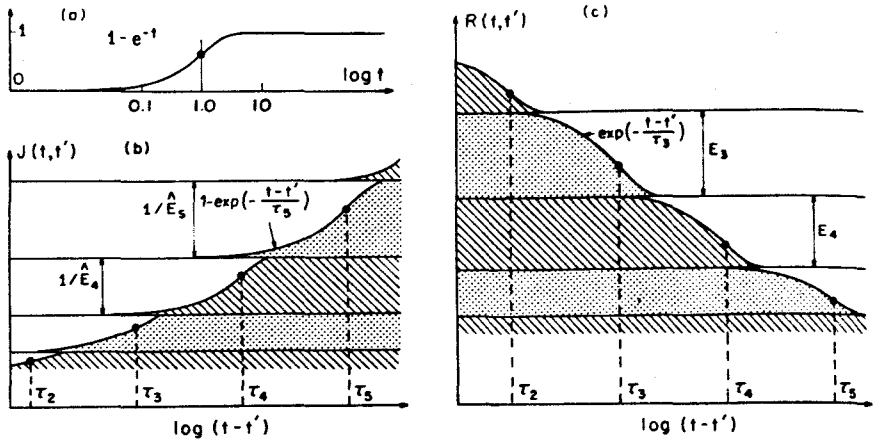

Figure 7.14 Representation by Dirichlet series

creep curves for all ages t' at loading, i.e. τ_μ can be considered to be constant without any loss in the capability to fit test data.

(3) The choice of τ_μ is however not entirely arbitrary. Since the rise of each exponential term spreads roughly over one decade, τ_μ values cannot be spaced more than a decade apart in log $(t-t')$ scale. So, the smallest possible number of exponential terms is obtained with the choice

$$\tau_\mu = 10^{\mu-2}\tau_2 \quad (\mu = 2, 3, \ldots, N) \tag{7.35}$$

although the choice $\tau_\mu = a^{\mu-2}\tau_2$ with $a < 10$ gives a somewhat better accuracy and smoother response curves.

(4) The values of τ_μ must cover the entire time range of interest. If we want to calculate the response from time $\tau_{\min}$ until $\tau_{\max}$ after load application, the smallest τ_μ (i.e. τ_2) must be such that $\tau_2 \leqslant 3\tau_{\min}$ and the last one such that $\tau_N \geqslant 0.5\tau_{\max}$.

(5) To take aging into account accurately, the smallest τ_μ must be much less than the age of concrete, t_0, when the structure is first loaded, i.e. $\tau_2 \leqslant 0.1t_0$.

The functions $C_\mu(t')$ may in general be identified from any given $J(t, t')$ by a computer subroutine based on minimizing a sum of square-deviations from given $J(t, t')$. This subroutine is listed in Ref. 28. (However, do not take from Ref. 28 the subroutine that converts $J(t, t')$ into $R(t, t')$ since it contains two misprints; use the one from Ref. 22 or 199.) When the creep curves are given by $J(t, t')$ as power curves, i.e.

$$J(t, t') = [1 + \Psi(t')(t-t')^n]/E_0, \tag{7.36}$$

there exists explicit formulae[26]

$$\frac{1}{\hat{E}_\mu(t')} = \begin{cases} \dfrac{1}{E_0} + a(n)\left(\dfrac{\tau_1}{0.002}\right)^n \Psi(t') & \text{for } \mu = 1 \\ b(n)\left(\dfrac{\tau_1}{0.002}\right)^n 10^{n(\mu-1)}\Psi(t') & \text{for } 1 < \mu < N \\ 1.2b(n)\left(\dfrac{\tau_1}{0.002}\right)^n 10^{n(N-1)}\Psi(t') & \text{for } \mu = N \end{cases} \tag{7.37}$$

in which the coefficients may be determined from Table 7.2. An explicit formula also exists when $J(t, t') = \Psi(t') \log (t - t' + \text{constant})$; see Bažant and Wu;[51] or Bažant.[26,25]

Although the use of degenerate kernel permits conversion to a rate-type creep law, it does not eliminate all numerical difficulties. The reason is that the smallest retardation time τ_μ must be rather short, say three days, in order to represent the initial rapid creep adequately. With the usual step-by-step integration methods, however, the time step Δt must not exceed the smallest τ_μ for reasons of numerical stability and must be kept much less than this, say $\Delta t = 0.1$ day, to assure sufficient accuracy. Then, however, an enormous number of time steps would be needed to reach the long-time solution for, say, 50 years of load duration. Yet small time steps Δt after 10 years of loading should not be required because all variables in case of steady loading vary so slowly that even with a one-year interval their change is small. So, it should be possible to increase the time step gradually from a small initial value, such as 0.1 day, to a large value, such as one year. There exists algorithms which enable this without causing numerical instability and loss of accuracy. These are the recursive exponential algorithms, and we will explain them later.

The choice of reduced times $y_\mu(t)$ for the general degenerate kernel (Equation (7.32)) is still under investigation (J. C. Chern at Northwestern University). It appears that a suitable expression is

$$y_\mu(t) = (t/\tau_\mu)^{q_\mu} \quad (\mu = 1, 2, \ldots, N) \tag{7.38}$$

where q_μ = constants ($q_\mu > 0$). Choosing $q_\mu < 1$ obviously helps in representing the decline of the creep rate due to aging. Regarding the choice of

Table 7.2 Coefficients for Dirichlet series expansion of power function of exponent n

n	0.05	0.10	0.15	0.20	0.25	0.30	0.35
$a(n)$	0.6700	0.4465	0.2929	0.1885	0.1154	0.0611	0.0156
$b(n)$	0.0819	0.1161	0.1229	0.1152	0.1007	0.8042	0.0681

retardation times, we should observe that function $1-\exp[-y_\mu(t)]$ (Equation (7.32)) gives a step that spreads over a width of about one decade in $\log t^{q_\mu}$ rather than in $\log t$. So it is appropriate to require that the ratio of $\tau_\mu^{q_\mu}$ to $\tau_{\mu-1}^{q_{\mu-1}}$ would not exceed 10, $\bar{q}_\mu$ being the larger of q_μ and $q_{\mu-1}$. This suggests the rule

$$\tau_\mu = 10^{1/\bar{q}_\mu}\tau_{\mu-1} \quad (\mu = 3, 4, \ldots, N) \tag{7.39}$$

Now we see that having exponents $q_\mu < 1$ has the advantage that times τ_μ can be spread farther apart in $\log t$ scale, the farther apart the smaller is q_μ. It appears that q_μ can be as small as 2/3 without impairing the representation of typical test data (as found by J. C. Chern). In that case we would need about 33% fewer τ_μ to cover the same time range, which brings about a substantial reduction in storage requirements for internal variables ε_μ as well as a reduction in computer time.

Similarly to Equation (7.34), the most general degenerate form of the relaxation function is

$$R(t, t') = \sum_{\mu=1}^{N} E_\mu(t') \exp[y_\mu(t') - y_\mu(t)] \tag{7.40}$$

where $y_\mu(t)$ are reduced times defined again by Equation (7.33), except that τ_μ are here called the relaxation times (rather than retardation times). So far, the reduced times have been always considered proportional to actual time τ_μ, as in Equation (7.33). Then we have the Dirichlet series expansion

$$R(t, t') = \sum_{\mu=1}^{N} E_\mu(t') \exp[-(t-t')/\tau_\mu] \tag{7.41}$$

For the choice of τ_μ the same rules hold as before, except that τ_1 need not be very small, while $\tau_N = 10^9$ days, if the final creep value should be bounded. So we may set

$$\tau_\mu = 10^{\mu-1}\tau_1 \quad (\mu = 1, 2, \ldots, N-1) \tag{7.42}$$

Functions $E_\mu(t')$ may be crudely determined by a graphical procedure based on splitting the individual relaxation curves in horizontal strips (see Figure 7.14(c)). For accurate results, functions $E_\mu(t)$ may be identified by the method of least squares, for which an efficient subroutine is listed by Bažant and Asghari[28] and a refined one is given in the program described by Bažant, Rossow and Horrigmoe[46] and fully listed in Ref. 199. At first, however, the function $R(t, t')$ must be obtained from $J(t, t')$, as described in Section 7.3.4.

The plot of $E_\mu(t)$ versus $\log \tau_\mu$ is called the relaxation spectrum; its example is shown in Figure 7.15.

All that has been said of the uniaxial compliance or relaxation function also applies separately to volumetric and deviatoric compliance functions and relaxation functions.

A compliance function in the form of Dirichlet series was used by McHenry[125] and by Maslov[133] and Arutyunyan,[10] although for the purpose of converting the structural problem from integral to differential equations in time rather than for the purpose of avoiding the storage of history in a step-by-step solution. The latter advantage of degenerate kernel was first utilized by Selna[168,169] and Bresler and Selna;[62] but their algorithm did not allow increasing the time step beyond a fraction of the smallest retardation time. The exponential algorithm which admits arbitrary time step was first developed for non-aging materials; see Zienkiewicz and Watson,[198] Taylor, Pister and Goudreau[175] and Mukaddam.[138] The exponential algorithms for aging materials, based on degenerate forms of compliance as well as relaxation functions, were developed by Bažant[21] and were applied in a small finite element program by Bažant and Wu.[51,53] Other forms of exponential algorithms which differ in various details were developed by Kabir and Scordelis,[108] Argyris *et al.*,[7,8] Pister *et al.*,[150] and Willam.[186] They used their algorithms in large finite element programs. Smith, Cook and Anderson,[171] Smith and Anderson,[172] and Anderson,[6] implemented Bazant's algorithm[21,51] based on a degenerate form of the compliance function in the general purpose finite element program NONSAP. The same, but for a degenerate form of the relaxation function, was implemented in NONSAP by Bažant, Rossow, and Horrigmoe.[46]

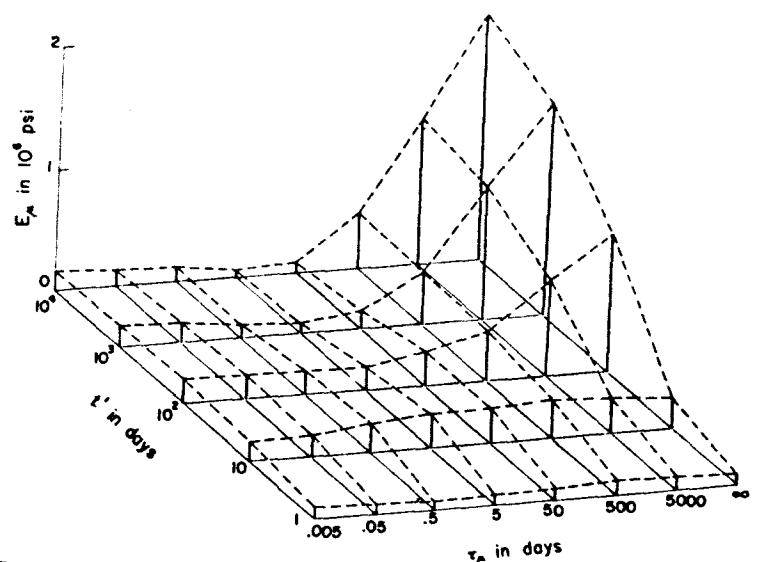

Figure 7.15 Example of relaxation spectra for Dworshak Dam concrete (Corresponding to Figure 7.17(a))

In concluding the subject of Dirichlet series compliance or relaxation functions we should emphasize that they represent merely an approximation to the real creep law (e.g. power law), justified by computational convenience. The Dirichlet series involves too many empirical coefficients to accept it as the creep law *per se*. In organizing a versatile program, the creep properties should be input either in the form of the parameters of some of the creep laws explained in Section 7.2 or as numerical measured values of $J(t, t')$ (and $\varepsilon_S(t, t_0)$). The former involves much fewer parameters for the input than the Dirichlet series. For example, for the double power law only five parameters need to be read on input to characterize all uniaxial creep, instantaneous deformation, and aging. The program should then automatically generate the parameters of the Dirichlet series (or of the rate-type formulation to be described next). The input of the finite element program by Bazant, Rossow, and Horrigmoe,[46] fully listed in Ref. 199, is organized in this manner, with various options (see Section 7.7.4).

7.4.2 Rate-type constitutive relations

As already mentioned, the degenerate compliance function (Equation (7.32)) can be exploited to convert the integral-type creep law to a differential equation. Substituting Equation (7.32) into Equation (7.16), we may write the resulting expression for $\varepsilon(t)$ in the form

$$\varepsilon(t) = \sum_{\mu=1}^{N} \varepsilon_\mu(t) + \varepsilon^0(t) \tag{7.43}$$

in which

$$\varepsilon_\mu(t) = \int_0^t \frac{d\sigma(t')}{C_\mu(t')} - \gamma_\mu(t) \qquad \gamma_\mu(t) = \exp[-y_\mu(t)] \int_0^t \exp[y_\mu(t')] \frac{d\sigma(t')}{dy_\mu(t')} \frac{dy_\mu(t')}{C(t')} \tag{7.44a,b}$$

Now, expressing the derivatives $d\varepsilon_\mu/dy_\mu$ and $d^2\varepsilon_\mu/dy_\mu^2$, we may check by substitution that the ε_μ always satisfy the following linear differential equations:

$$\frac{d^2\varepsilon_\mu}{dy_\mu^2} + \frac{d\varepsilon_\mu}{dy_\mu} = \frac{1}{C_\mu(t)} \frac{d\sigma}{dy_\mu} \quad (\mu = 1, 2, \ldots, n) \tag{7.45}$$

Furthermore, expressing the derivative $d\gamma_\mu/dy_\mu$ from Equation (7.44), we may check that the γ_μ always satisfy the differential equations:

$$\frac{d\gamma_\mu}{dy_\mu} + \gamma_\mu = \frac{1}{C_\mu(t)} \frac{d\sigma}{dy_\mu} \quad (\mu = 1, 2, \ldots, n) \tag{7.46}$$

ε_μ and γ_μ are related to ε by the differential equations

$$\dot{\varepsilon} = \sum_\mu \dot{\varepsilon}_\mu + \dot{\varepsilon}^0 \qquad \dot{\varepsilon}_\mu = \frac{\dot{\sigma}}{C_\mu(t)} - \dot{\gamma}_\mu \tag{7.47}$$

One can further check that integration of Equation (7.45) yields Equation (7.44) for ε_μ, and integration of Equation (7.46) yields Equation (7.44b) for γ_μ. Thus the rate-type creep law given either by Equations (7.45) and (7.47) or by Equations (7.46) and (7.47) is equivalent to the integral-type creep law in Equation (7.16) with $J(t, t')$ given by Equation (7.32). In Equations (7.45) or (7.46), functions $y_\mu(t)$ are treated as independent variables, analogous to time; so we may call $y_\mu(t)$ the reduced times. Obviously, $y_\mu(t)$ must be monotonically increasing functions of actual time t.

The derivatives with respect to y_μ may be expressed in terms of time derivatives, substituting $d\varepsilon_\mu/dy_\mu = \dot{\varepsilon}_\mu/\dot{y}_\mu$, $d^2\varepsilon_\mu/dy_\mu^2 = (\ddot{\varepsilon}_\mu \dot{y}_\mu - \dot{\varepsilon}_\mu \ddot{y}_\mu)/\dot{y}_\mu^3$. Thus, Equation (7.45) becomes

$$\ddot{\varepsilon}_\mu + \left(\dot{y}_\mu - \frac{\ddot{y}_\mu}{\dot{y}_\mu}\right)\dot{\varepsilon}_\mu = \frac{\dot{y}_\mu}{C_\mu(t)} \dot{\sigma} \tag{7.48}$$

The form of a rate-type constitutive relation may be interpreted in terms of a rheologic model consisting of springs and dashpots. For an aging material, the spring moduli E_μ and dashpot viscosities are functions of age t. Consider the Kelvin chain model in Figure 7.16(a), in which ε_μ denotes the strain of the μth Kelvin unit. Now, for an aging elastic response, we must realize that we cannot say that the stress in the spring is $E_\mu(t)\varepsilon_\mu$; but we can say[27,14] that the rate of the stress is $E_\mu(t)\dot{\varepsilon}_\mu$ (see Section 7.5.1). The stress in the dashpot is $\eta_\mu(t)\dot{\varepsilon}_\mu$ and its rate is $[\eta_\mu(t)\dot{\varepsilon}_\mu]^\cdot$. So the rate of total stress in the μth Kelvin unit is $[\eta_\mu(t)\dot{\varepsilon}_\mu] + E_\mu(t)\dot{\varepsilon}_\mu$, which yields:[21]

$$\ddot{\varepsilon}_\mu + \frac{E_\mu(t) + \dot{\eta}_\mu(t)}{\eta_\mu(t)} \dot{\varepsilon}_\mu = \frac{\dot{\sigma}}{\eta_\mu(t)} \tag{7.49}$$

Note that this differential equation for $\varepsilon_\mu(t)$ is of second order, while for a non-aging material it is of first order. To obtain $J(t, t')$ for the Kelvin chain model, we need to integrate Equation (7.49) for the stress history $\sigma = 1$ for $t \geq t'$ and $\sigma = 0$ for $t < t'$, and using initial conditions $\varepsilon_\mu(t') = 0$

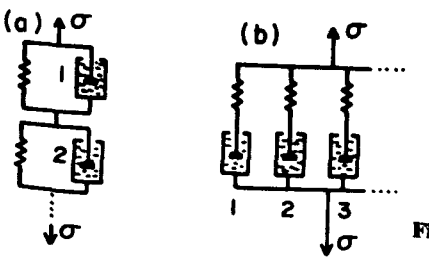

Figure 7.16 Kelvin and Maxwell chain models

and $\dot{\varepsilon}_\mu(t') = 1/\eta_\mu(t')$, we obtain[14]

$$J(t,t') = \sum_{\mu=1}^{N} \int_0^{t'} \frac{1}{\eta_\mu(\tau)} \exp\left[f_\mu(\tau) - f_\mu(t)\right] d\tau \qquad f_\mu(\xi) = \int_0^{\xi} \frac{E_\mu(\theta)}{\eta_\mu(\theta)} d\theta \tag{7.49a}$$

Equating the coefficients of Equations (7.49) and (7.48) we conclude that[14]

$$\eta_\mu(t) = \frac{C_\mu(t)}{\dot{y}_\mu(t)} \qquad E_\mu(t) = C_\mu(t) - \frac{C_\mu(t)}{\dot{y}_\mu(t)} \tag{7.50}$$

In particular, for $y_\mu = (t/\tau_\mu)^q$ (Equation (7.38)), we have

$$\eta_\mu(t) = \tau_\mu^q C_\mu(t) \frac{t^{1-q}}{q} \qquad E_\mu(t) = C_\mu(t) - \tau_\mu^q \dot{C}_\mu(t) \frac{t^{1-q}}{q} \tag{7.51}$$

So we can always find a Kelvin chain model which is equivalent to the most general degenerate kernel.[13,14] A more difficult question is whether the values of η_μ obtained from Equation (7.50) are thermodynamically admissible. For example, the minus sign in Equation (7.50) makes us worry lest E_μ become negative. These questions will be discussed in Section 7.5.1.

An analogous formulation is possible for the degenerate form of the relaxation function (Equations (7.40), (7.41)). Substituting Equation (7.40) into the superposition integral in Equation (7.19) we obtain

$$\sigma(t) = \sum_{\mu=1}^{N} \sigma_\mu(t) \tag{7.52}$$

$$\sigma_\mu(t) = \exp\left[-y_\mu(t)\right] \int_0^t \exp\left[y_\mu(t')\right] E_\mu(t) \left[d\varepsilon(t') - d\varepsilon^0(t')\right] \tag{7.53}$$

Now expressing the derivative $d\varepsilon_\mu/dy_\mu$, we may check that the σ_μ, called the partial stresses, satisfy the differential equations

$$\frac{d\sigma_\mu}{dy_\mu} + \sigma_\mu = E_\mu(t) \frac{d(\varepsilon - \varepsilon^0)}{dy_\mu} \tag{7.54}$$

Conversely, integration of Equation (7.54) with Equation (7.52) yields Equation (7.53), which implies Equation (7.40). Thus, the rate-type creep law given by Equations (7.52) and (7.54) is equivalent to the integral-type creep law with the degenerate kernel (Equation (7.40)).

Noting that $(d/dy_\mu) = (d/dt)/\dot{y}_\mu$, we may rewrite Equation (7.54) as

$$\dot{\sigma}_\mu + \dot{y}_\mu(t)\sigma_\mu = E_\mu(t)(\dot{\varepsilon} - \dot{\varepsilon}^0) \tag{7.55}$$

Observe that, in contrast to the aging Kelvin chain (Equation (7.49)), the differential equation for the aging Maxwell chain is of the first order rather than the second order.

Consider now the Maxwell chain model (Figure 7.16b), in which σ_μ denotes the stress in the μth Maxwell unit. The strain rate in the spring is $\sigma_\mu/E_\mu(t)$ and that in the dashpot is $\sigma_\mu/\eta_\mu(t)$. Summing them, we get the total strain rate $\dot{\varepsilon} - \dot{\varepsilon}^0 = (\dot{\sigma}_\mu/E_\mu) + (\sigma_\mu/\eta_\mu)$, which may be written as

$$\dot{\sigma}_\mu + \frac{E_\mu(t)}{\dot{y}_\mu(t)} \sigma_\mu = E_\mu(t)(\dot{\varepsilon} - \dot{\varepsilon}^0) \tag{7.56}$$

Comparing the coefficients of this equation and Equation (7.55), we see that $E_\mu(t)$ is indeed the spring modulus, as we may have anticipated, and that the viscosity of the μth dashpot is

$$\eta_\mu(t) = E_\mu(t)/\dot{y}_\mu(t) \tag{7.57}$$

In particular, for $y_\mu = (t/\tau_\mu)^q$ (Equation (7.38)) we have

$$\eta_\mu(t) = \tau_\mu^q E_\mu(t) \frac{t^{q-1}}{q} \tag{7.57a}$$

Variables σ_μ or ε_μ (or γ_μ) represent what is known in continuum thermodynamics as internal variables (i.e. state variables that cannot be directly measured). The current values of these variables characterize the effect of the past history of the material. Thus, we need to store only the current values of, say, about four internal variables ($\mu = 1, \ldots, 4$) to characterize the stress history from, say, $t - t' = 0.1$ day until 10^4 days. This makes the computations much more efficient. Another term for σ_μ is the hidden stresses or partial stresses, and for ε_μ the hidden strains or partial strains.

A comparison of Maxwell chain model predictions with some test data from the literature is shown in Figure 7.17.

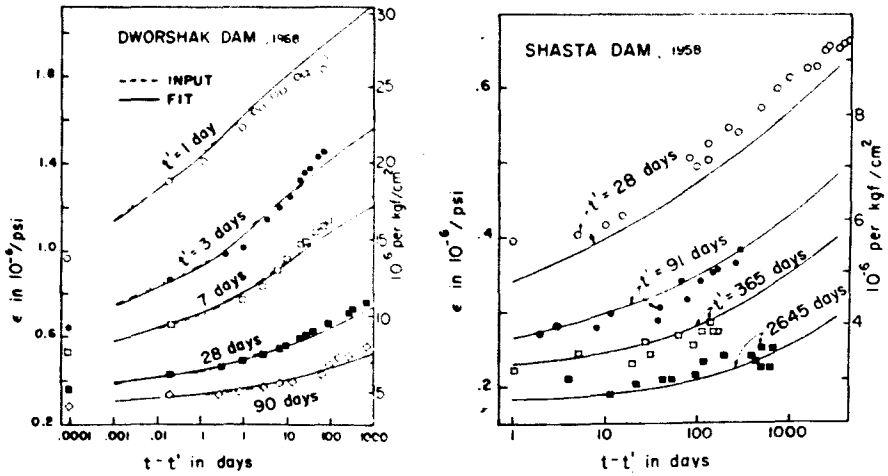

Figure 7.17 Creep curves for various ages at loading according to the Maxwell chain model, compared with test data[53,149,93,94]

By writing analogous equations for the deviatoric and volumetric components, the foregoing rate-type stress–strain relations are easily generalized to three dimensions.

Since both Maxwell and Kelvin chains can approximate the integral-type creep law with any desired accuracy, these two models must be mutually equivalent, and equivalent also to any other possible spring–dashpot model. For non-aging materials this was rigorously demonstrated long ago by Roscoe.[157] However, certain subtle questions remain in the case of aging material. It appears that not every $J(t, t')$ can be represented by each model unless we relax certain thermodynamic restrictions on the aging process (Section 7.5.1). Thus, the complete mutual equivalence of various spring–dashpot (linear) rheologic models and their equivalence to a general linear integral-type creep law apparently do not hold true in case of aging.

7.4.3 Temperature effect

To include the temperature influence, the compliance function of the form of Dirichlet series was generalized by Mukaddam and Bresler,[139] with further refinements by Mukaddam[138] and Kabir and Scordelis.[108] Although a temperature increase always intensifies creep, the use of the integral-type formulation however presents a difficult question: What is the difference between the effects of the current temperature and the past temperatures on the present creep rate? It seems that this question cannot be approached with the integral-type formulation in other than a totally empirical manner.

For the rate-type formulation this difficult question does not arise, since the formulation is history-independent, and so only current temperature matters. Thus, the creep rate must be adjusted only according to the current temperature T, and so must be the rate of aging and the rate of change of internal variables such as γ_μ or σ_μ. The chief advantage of the rate-type formulation is that a well-founded physical theory, namely the rate-process theory,[86,74] lends itself naturally for describing the rate changes due to temperature.

A temperature increase has two mutually competing effects. Firstly, it accelerates creep, i.e. increases the creep rate. This indicates that the retardation or relaxation times should be reduced as temperature increases. Secondly, a temperature increase further causes an acceleration of hydration or aging, thereby indirectly also reducing creep.

The competition of these two effects explains why rather different temperature influences have been observed in various tests. The creep acceleration (or increase) always prevails. In an old concrete, the creep reduction due to faster aging is small since most of the cement has already been hydrated. However, in a young concrete, in which much hydration still remains to occur, the effect of the acceleration of aging can largely offset the acceleration of creep.

The effect of temperature on the rate of aging may be described by replacing concrete age with a certain equivalent age t_e (also called maturity) representing the hydration period for which at temperature T the same degree of hydration is reached as that reached during actual time period t at reference temperature T. Like for all chemical reactions, the rate of hydration depends only on the current temperature and not on the past temperatures. Therefore, for variable temperature we have (cf. Equation (7.6)):

$$t_e = \int \beta_T \, dt \tag{7.58}$$

where β_T is a function of current temperature. Again, like for all chemical reactions, the rate of hydration should follow the activation energy concept[86,74] (Arrhenius's equation), and so

$$\beta_T = \exp\left[\frac{U_h}{R}\left(\frac{1}{T_0} - \frac{1}{T}\right)\right] \tag{7.59}$$

Here T is the current temperature (in K), T_0 is a reference temperature (in K) (normally 296 K), R is the gas constant, and U_h is the activation energy of hydration; $U_h/R \simeq 2700$ K.

The change of creep rate due to temperature may be modelled by accelerating the rate of growth of the reduced times $y_\mu(t)$ as if the retardation or relaxation times τ_μ increased. This may be expressed by replacing the previous relation $y_\mu(t) = (t/\tau_\mu)^{q_\mu}$ (Equation (7.38)) by

$$y_\mu(t) = \left(\varphi_T \frac{t}{\tau_\mu}\right)^{q_\mu} \quad (\mu = 1, 2, \ldots, N) \tag{7.60}$$

where φ_T is a function of current temperature $T(t)$. Since the creep mechanism no doubt consists in breakage and reformation of bonds, which represent thermally activated processes on the molecular scale, coefficient φ_T should also follow the activation energy concept. This indicates that[54]

$$\varphi_T = \exp\left[\frac{U_a}{R}\left(\frac{1}{T_0} - \frac{1}{T}\right)\right] \tag{7.61}$$

where U_a is the activation energy of creep; $U_a/R \simeq 5000$ K. Note also that it makes no difference whether or not the rate coefficient φ_T is applied for $\mu = 1$, since the corresponding deformation is almost instantaneous.

It is possible that the activation energies U_a differ for various $\mu = 2, 3, \ldots, N$ but analysis of existing test data[54] did not indicate a need for introducing such a complication. Moreover, it is also possible that more than one activation energy is associated with each τ_μ, as well as with the aging

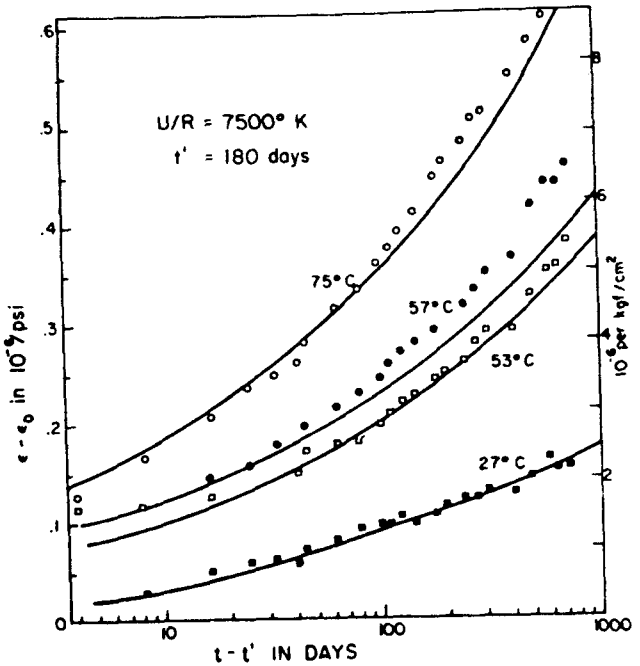

(a)

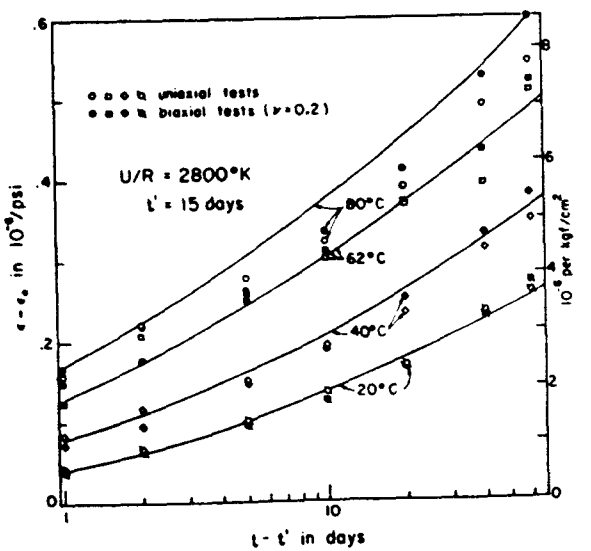

(b)

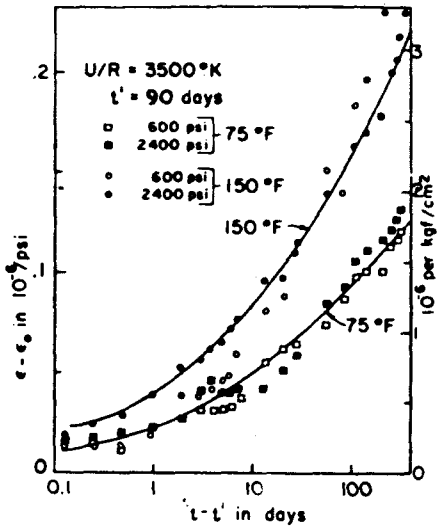

(c)

Figure 7.18 Creep curves for various temperatures according to Maxwell chain and activation energy models[24], compared with unaxial and biaxial creep measurements[88,89,9,196]

rate (Equation (7.59)); this would make Equations (7.59) and (7.61) inapplicable; but these equations seem to approximate the existing test results reasonably well, as well as can be desired in view of the usual statistical scatter. Fits of some test data from the literature obtained with the use of Equations (7.49)–(7.61) are illustrated in Figure 7.18.

It should be noted that when physical concepts such as activation energy are used, Maxwell chain is often preferable over Kelvin chain (cf. Section 7.5.1). Further, it shoud be noted that since the effective retardation or relaxation times change from τ_μ to τ_μ/φ_T, the time range covered by the rate-type model shifts to the left when the temperature increases. Thus, a broader spectrum of relaxation times is necessary to cover the same time range at various temperatures. Denoting as $\tau_{min} \leq t - t_0 \leq \tau_{max}$ the range of load durations for which the creep effects should be accurately calculated, and considering that temperatures vary between T_{min} and T_{max}, we must use a sufficient number of τ_μ (spaced according to Equation (7.34)) such that

$$\tau_2 \leq 3\tau_{min}\varphi_{T_{min}} \qquad \tau_N \geq 0.5\tau_{max}\varphi_{T_{max}} \tag{7.62}$$

This is for Kelvin chain. For Maxwell chain, replace τ_2 and τ_N with τ_1 and τ_{N-1}.

The compliance function at arbitrarily variable temperature $T(t)$ may be obtained by evaluating the integral in Equations (7.43) and (7.44) for stress history $\sigma = 1$ for $t \geq t'$ and $\sigma = 0$ for $t < t'$. Replacing $C_\mu(t')$ with $C_\mu(t'_e)$, we thus obtain

$$J(t,t') = \sum_{\mu=1}^{N} \frac{1}{C_\mu(t'_e)} \{1 - \exp[-y_\mu(t') - y_\mu(t)]\} \qquad t'_e = \int_0^{t'} \beta_T \, dt$$

$$y_\mu(t) = \frac{1}{\tau_\mu} \int_0^t \varphi_T(t') \, dt' \qquad (7.63)$$

as the Dirichlet series expansion of the compliance function at variable $T(t)$. If temperature is constant after t', we have $y_\mu(t') - y(t) = (t - t')\tau_\mu \varphi_T$, and if T is constant since time $t = 0$, we further have $t'_e = \beta_T t'$. For generally variable stress, the principle of superposition (Equation (7.16)) based on $J(t, t')$ from Equation (7.63) fully defines the stress–strain relation and is equivalent to the rate-type form (Equations (7.46), (7.47), (7.58)–(7.61)).

Equation (7.63) shows that the compliance function $J(t, t')$ at any temperature kept constant after time t' may be obtained from $J(t, t')$ at reference temperature T_0 by the following replacements

$$t' \to t'_e \qquad t - t' \to (t - t')\varphi_T \qquad (7.64)$$

We see that the modification of the double power law which we introduced in Equation (7.6)[26,43] conforms to this rule (which may also be derived from a model of visoelastic porous material in which the volume of the solid grows).[43] Also note that if β_T were 1, Equation (7.63) would conform to the time-shift principle for thermorheologically simple materials (unless φ_T would depend also on μ). However, β_T spoils that.

The formulations of Mukaddam[138] and Mukaddam and Bresler[139] and Kabir[107] are similar to Equation (7.63) but differ in two respects. First, $\varphi_T(t')(t - t')/\tau_\mu$ is used instead of $y_\mu(t) - y_\mu(t')$, which is equivalent only at constant temperature; and, second, t' is used instead of t'_e, which means that the acceleration of aging due to temperature increase is neglected. Furthermore, Mukaddam and Bresler[139] consider C_μ as constants and instead they introduce an empirical 'age-shift' function $\bar{\varphi}(t')$, which is analogous to the formulation used for polymers ('thermorheologically simple' materials).[82,163,187] This approach is convenient for graphical fitting of test data by the time-shift method but does not yield a degenerate form of the compliance function, thus making inapplicable the rate-type formulation. This makes it impossible to find a numerical algorithm that does not need storage of the history, and also precludes the use of the activation energy concept.

The use of $\varphi_T(t')(t - t')/\tau_\mu$ instead of $y(t) - y(t')$ leads in case of variable temperature to certain self-contradictions and non-uniqueness of results. To illustrate it, consider two temperature histories: one for example such that $T = 20\,°C$ all the time, and the other one such that $T = 20\,°C$ all the time

except for a rapid rise from 20 °C to 50 °C between 99.99 days and 100 days and rapid drop from 50 °C to 20 °C between 100 days and 100.01 days. Then, for a constant stress applied at $t' = 100$ days, the resulting strains at, say, $t = 1000$ days are rather different for the two temperature histories, while they should be nearly exactly the same. Thus, the response is obtained as a discontinuous functional of the loading history while it obviously should be a continuous functional. As another example, consider two other temperature histories, one such that $T = 20\,°C$ all the time, and the other one such that $T = 50\,°C$ all the time except for a drop from 50 °C to 20 °C between 99.9 days and 100 days and a rise from 20 °C to 50 °C between 100 days and 100.1 days. Then one gets the same strains for $t = 1000$ days while the strains should obviously be very different.

Another recently studied effect of temperature is the apparent acceleration of creep shortly after any sudden temperature change, positive or negative. This effect, sometimes called transitional thermal creep,[104] probably has the same physical mechanism as the increase of creep due to a humidity change, and is doubtless also strongly influenced by microcracking.[25,52] Thus it probably does not arise only from the constitutive equation but is influenced by the stress field in the whole specimen. These effects will be more clearly discussed in Section 7.6.3.

Above 100 °C the creep properties are rather different. At constant moisture content, creep continues to increase according to the activation energy.[131,3] Moisture loss however reduces creep significantly,[130–132] even when it happens during creep.[36] The creep in pressurized water over 100 °C is much less than the creep of sealed specimens.[36] The creep Poisson ratio[36] at 200 °C reaches about 0.46. The elastic modulus steadily decreases with increasing temperature.[55,75]

Important experimental data on creep at high temperatures were reported by Browne,[64] Browne and Bamforth,[66] Browne and Blundell,[65] Hannant,[88] Fahmi *et al.*,[81] Komendant *et al.*,[116] Maréchal,[131–3] York *et al.*,[196] Hickey,[99] Nasser and Neville,[142,143] Seki,[167] etc.

7.4.4 Application in numerical structural analysis

Although the degenerate form of the kernel allows conversion to differential equations, the usual step-by-step methods for ordinary differential equations cannot be applied. This is either because numerical stability requirements prevent an increase of Δt beyond a certain unacceptably small limit or because accuracy requirements do not allow this when the usual unconditionally stable algorithms, such as the central or backward difference methods are used.

Very large time steps, orders of magnitude larger than the shortest retardation or relaxation time, are necessary to reach long times such as 50

years after load application. Such large steps are possible only if we use integration formulae that are exact under certain characteristic conditions, namely for the case when the stress or strain rates and all material stiffness and viscosity prameters are considered constant within each time step although they are allowed to vary by jumps between the steps. Such algorithms were proposed by Bažant.[21] For non-aging materials, a similar algorithm was formulated by Taylor, Pister, and Goudreau,[175] and by Zienkiewicz, Watson, and King.[197]

Let time t be subdivided by discrete times t_r ($r = 1, 2, 3, \ldots$), and let Δ refer to the increments from t_r to t_{r+1}, e.g. $\Delta y_\mu = y_{\mu_{r+1}} - y_{\mu_r}$, $\Delta\sigma = \sigma_{r+1} - \sigma_r$. Assuming $C_\mu(t)$ and $d\sigma/dy_\mu$ to be constant from t_r to t_{r+1}, and setting $C_\mu = C_{\mu_{r+1/2}}$, $d\sigma/dy_\mu = \Delta\sigma/\Delta y_\mu$, the integral of Equation (7.46) then yields exactly,[21] for uniaxial stress,

$$\gamma_{\mu_{r+1}} = \gamma_{\mu_r} \exp(-\Delta y_\mu) + \frac{\lambda_\mu}{C_{\mu_{r+1/2}}} \Delta\sigma \tag{7.65}$$

in which $C_{\mu_{r+1/2}} = C_\mu(t_{r+1/2})$ and

$$\lambda_\mu = [1 - \exp(-\Delta y_\mu)]/\Delta y_\mu \tag{7.66}$$

Substituting Equation (7.65) into Equation (7.44b), Equations (7.43)–(7.44a) may be brought to the form.[21]

$$\Delta\varepsilon = \frac{\Delta\sigma}{E''} + \Delta\varepsilon'' + \Delta\varepsilon^0 \tag{7.67}$$

in which

$$\frac{1}{E''} = \sum_{\mu=1}^{N} \frac{1-\lambda_\mu}{C_{\mu_{r+1/2}}} \qquad \Delta\varepsilon'' = \sum_{\mu=1}^{N} [1 - \exp(-\Delta y_\mu)]\gamma_{\mu_r} \tag{7.68}$$

We may now observe that E'' and $\Delta\varepsilon''$ can be evaluated if all γ_{μ_r} are known up to the beginning of the current time step, t_r. Thus Equation (7.67) may be treated as an elastic stress–strain relation with elastic modulus E'' and inelastic strain increment $\Delta\varepsilon''$. Using this relation, the structural problems with prescribed load changes or displacement increments during the step (t_r, t_{r+1}) may be solved, yielding the value of $\Delta\sigma$. The internal variables γ_μ at the end of the step, $\gamma_{\mu_{r+1}}$, may then be evaluated[21] from Equation (7.65). Then one can proceed to the next step.

As for the choice of time steps, it is most effective to keep them constant in the scale $\log(t - t_1)$ where t_1 is the instant when the first load is applied on the structure or first deformations are imposed. Thus, after choosing the first step (t_1, t_2) we generate subsequent t_r as $t_{r+1} - t_1 = 10^{1/m}(t_r - t_1)$ where m is the chosen number of steps per decade ($m = 2$ to 4 suffices for good accuracy). The load and imposed deformations must either be constant after t_1 or vary gradually at a rate which declines with $t - t_0$ (as, e.g. the shrinkage

deformations do). If there is a sudden load (or enforced deformation change) at time t_s, one must start again with a small time step (t_s, t_{s+1}) and then increase the steps so as to keep them constant in $\log(t - t_s)$, i.e. use $t_{r+1} - t_s = 10^{1/m}(t_r - t_s)$.

It is instructive to explain the role of coefficients λ_μ in Equations (7.68) or (7.69). Among all τ_μ there may be one, say τ_m, which is of the same order of magnitude as the current time step Δt. Then for all $\tau_\mu < \tau_m$ we have $\Delta y_\mu \gg 1$, $\exp(-\Delta y_\mu) \simeq 0$, $1 - \exp(-\Delta y_\mu) \simeq 1$ and $\lambda_\mu \simeq 0$, whereas for all $\tau_\mu > \tau_m$ we have $\Delta y_\mu \ll 1$, $\exp(-\Delta y_\mu) \simeq 1$, $1 - \exp(-\Delta y_\mu) \simeq 0$, and $\lambda_\mu \simeq 1$. Thus, we see from Equation (7.68) that the partial compliances $1/C_\mu$ which contribute to the instantaneous incremental compliance $1/E''$ are only those for which $\tau_\mu < \tau_m$ (or $\tau_\mu \ll \Delta t$). This is intuitively obvious because the stress in the dashpots of Kelvin units for which $\tau_\mu \ll \Delta t$ must almost completely relax within a time less than the step duration. So, the effect of λ_μ as the time step is increased in the step-by-step computation is to gradually 'uncouple' the dashpots as their relaxation time becomes too small compared to Δt. Furthermore, from the values of λ_μ we see that the inelastic strain increments are negligible and the behaviour becomes elastic for all $\tau_\mu > \tau_m$, i.e. $\tau_\mu \ll \Delta t$.

Equations analogous to Equations (7.65)–(7.68) hold for the volumetric and deviatoric components. When the spatial problem is solved by finite elements, the computational algorithm may be described as follows:

(1) Initiate stresses σ_{ij}, strains ε_{ij}, and internal variables $\gamma_{ij_{\mu_r}}$ at starting time t_1 as zero for all finite elements; set r as 1.

(2) For each finite element (and each integration point of finite element) calculate the volumetric and deviatoric inelastic strain increments and bulk and shear moduli for the step[21]

$$\Delta\varepsilon''^{\mathrm{V}} = \sum_{\mu=1}^{N} (1 - e^{-\Delta y_{\mu_r}})\gamma_{\mu_r}^{\mathrm{V}} \qquad \Delta\varepsilon_{ij}''^{\mathrm{D}} = \sum_{\mu=1}^{N} (1 - e^{-\Delta y_{\mu_r}})\gamma_{ij_{\mu_r}}^{\mathrm{D}} \tag{7.69a}$$

$$K'' = \left(\sum_{\mu=1}^{N} (1-\lambda_\mu)\hat{K}_{\mu_{r+1/2}}^{-1}\right)^{-1} \qquad G'' = \left(\sum_{\mu=1}^{N} (1-\lambda_\mu)\hat{G}_{\mu_{r+1/2}}\right)^{-1} \tag{7.69b}$$

Here γ_μ^{D}, $\gamma_{ij_\mu}^{\mathrm{D}}$ are the volumetric and deviatoric components of internal variable tensor γ_{ij_μ} (corresponding to γ_μ in uniaxial formulation, Equation (7.44)); $K_{r+1/2}$ and $G_{r+1/2}$ are the bulk modulus and shear modulus corresponding to equivalent age $t_{e_{r+1/2}}$ at the time when the actual age is $t_{r+1/2}$; $\hat{K}_{\mu_{r+1/2}}$ and $\hat{G}_{\mu_{r+1/2}}$ are the bulk and shear moduli for individual terms of Dirichlet series expansion, corresponding to moduli for $t' = t_{e_{r+1/2}}$ in the uniaxial formulation (7.36).

(3) The incremental stress–strain relation for each finite element and each integration point has then the form

$$\Delta\sigma^{\mathrm{V}} = 3K''(\Delta\varepsilon^{\mathrm{V}} - \Delta\varepsilon''^{\mathrm{V}} - \Delta\varepsilon^0) \qquad \Delta\sigma_{ij}^{\mathrm{D}} = 2G''(\Delta\varepsilon_{ij}^{\mathrm{D}} - \Delta\varepsilon_{ij}''^{\mathrm{D}}) \tag{7.70}$$

Since moduli K'' and G'' and inelastic strain increments $\Delta\varepsilon''^{V}$ and $\Delta\varepsilon_{ij}''^{D}$, as well as $\Delta\varepsilon^0$, can be determined in advance, we may treat Equation (7.70) as an elastic stress–strain relation. So we have an elastic problem with general inelastic (or initial) strains, which may be solved by a finite element program in the usual manner. In this elastic analysis we also apply all load increments as prescribed for the current time step (t_r, t_{r+1}), if any, and all displacement increments if any are prescribed. The solution yields displacement increments Δu_i for all nodes and strain increments $\Delta\varepsilon_{ij}$ for all elements and all integration points in the elements. We then split $\Delta\varepsilon_{ij}$ into the volumetric and deviatoric components $\Delta\varepsilon^V$ znd $\Delta\varepsilon_{ij}^D$, calculate the volumetric and deviatoric stress increments $\Delta\sigma^V$ and $\Delta\sigma_{ij}^D$ from Equation (7.70), and superimpose them to get $\Delta\sigma_{ij}$ for all finite elements and all integration points in the elements.

(4) Then we evaluate the volumetric and deviatoric parts of the internal variables γ_{ij_μ} at the end of the step, t_{r+1}, from the recurrent relations:

$$\gamma_{\mu_{r+1}}^V = \gamma_{\mu_r}^V e^{-\Delta y_\mu} + \frac{\lambda_\mu}{3K_\mu''}\Delta\sigma^V \qquad \gamma_{ij_{\mu,r+1}}^D = \gamma_{ij_\mu r}^D e^{-\Delta y_\mu} + \frac{\lambda_\mu}{2G_\mu''}\Delta\sigma_{ij}^D \quad (\mu = 1, 2, \ldots, n) \tag{7.71}$$

for all μ, all elements and all integration points.

(5) If $t_r <$ final time, go back to step 2 and start the next time step resetting r $(r \leftarrow r+1)$.

The most efficient way for programming is to take an existing elastic finite element program (which can handle arbitrary inelastic strains), place it in a DO loop over discrete times and attach separate subroutines for steps 2 and 4 described above. The foregoing algorithm,[21] along with a model for cracking, has been put in this manner on general purpose finite element program NONSAP by Anderson *et al.*[6,171,172,207]

To illustrate accuracy, Table 7.3 gives the stress $\sigma(t)$ at 29031 days due to strain 10^{-6} enforced at $t_0 = 35$ days, as computed according to Equations (7.65)–(7.71) with Dirichlet series approximation of ACI compliance function for various numbers of steps up to terminal time t. The first time step was always $\Delta t = 0.1$ day. We see that this algorithm is even more accurate

Table 7.3 Numerical results for stress relaxation obtained with Bažant's[21] exponential algorithm based on Dirichlet series expansion of compliance function

No. of time steps	Approx. no. of steps per decade	$\sigma(t)$
13	2	1.5320
25	4	1.5411
49	9	1.5438
97	18	1.5443
193	35	1.5445

than the second-order step-by-step method based on superposition (Table 7.1).

The Maxwell chain model offers certain theoretical advantages over the Kelvin chain model (Section 7.5.1), and therefore a similar algorithm was developed[21] for the relaxation function. We assume $E_\mu(t)$, $d\varepsilon^0/dy_\mu$ and $d\varepsilon/dy_\mu$ in (7.54) to be constant from t_r to t_{r+1}, setting $E_\mu = E_{\mu_{r+1/2}}$ and $d\varepsilon^0/dy_\mu = \Delta\varepsilon^0/\Delta y_\mu$. Equation (7.54) is then a linear first-order differential equation with constant coefficients and the initial conditions $\sigma_\mu(t) = \sigma_{\mu_r}$. Integration then yields (exactly), for uniaxial stress,

$$\sigma_{\mu_{r+1}} = \sigma_{\mu_r} e^{-\Delta y_\mu} + E_{\mu_{r+1/2}}\lambda_\mu(\Delta\varepsilon - \Delta\varepsilon^0) \tag{7.72}$$

where λ_μ is given again by Equation (7.66). Substituting this in Equation (7.52), we obtain $\Delta\sigma = E''(\Delta\varepsilon - \Delta\varepsilon'' - \Delta\varepsilon^0)$ where

$$E'' = \sum_{\mu=1}^{N} \lambda_\mu E_{\mu_{r+1/2}} \qquad \Delta\varepsilon'' = E'' \sum_{\mu=1}^{N} (1 - e^{-\Delta y_\mu})\sigma_{\mu_r} \tag{7.73}$$

Since E'' and $\Delta\varepsilon$ can be evaluated before σ_{r+1} and ε_{r+1} are known, we may determine $\Delta\sigma$ and $\Delta\varepsilon$ by an elastic structural analysis based on elastic moduli E'' and inelastic strain increments $(\Delta\varepsilon'' + \Delta\varepsilon^0)$. This algorithm is based on the relations:[21]

$$K'' = \sum_{\mu=1}^{N} \lambda_\mu K_{\mu_{r+1/2}} \qquad G'' = \sum_{\mu=1}^{N} \lambda_\mu G_{\mu_{r+1/2}} \tag{7.74}$$

$$3K''\Delta\varepsilon''^{V} = \sum_{\mu=1}^{N} (1 - e^{-\Delta y_\mu})\sigma_{\mu_r}^V, \qquad 2G''\Delta\varepsilon_{ij}''^{D} = \sum_{\mu=1}^{N} (1 - e^{-\Delta y_\mu})\sigma_{ij_{\mu_r}}^D \tag{7.75}$$

where σ_{ij_μ} are the partial stresses coresponding to σ_μ from Equation (7.54); and K_μ, G_μ are coefficients of Dirichlet series expansions of $J^V(t, t')$ and $J^D(t, t')$, corresponding to $E_\mu(t')$ from Equation (7.41). The volumetric and deviatoric internal variables (partial stresses) at the end of time step Δt_r are determined from the recursive relations:[21]

$$\sigma_{\mu_{r+1}}^V = \sigma_{\mu_r}^V e^{-\Delta y_\mu} + 3K_{\mu_{r+1/2}}(\Delta\varepsilon^V - \Delta\varepsilon^0) \qquad \sigma_{ij_{\mu_{r+1}}}^D = \sigma_{ij_{\mu_r}}^D e^{-\Delta y_\mu} + 2G_{\mu_{r+1/2}}\Delta\varepsilon_{ij}^D \tag{7.76}$$

The computational algorithm is essentially the same as that described before, except that Equations (7.68)–(7.69) are replaced by Equations (7.74)–(7.75), Equations (7.71) are replaced by (7.76) and σ_μ are used instead of γ_μ. Bažant and Wu[52] used this algorithm in a small finite element program, and recently Bažant, Rossow and Horrigmoe[46] put this algorithm on the general purpose finite element program NONSAP.

Figures 7.17 and 7.18 give examples of comparison with tests.

It is again instructive to explain the role of coefficients γ_μ in Equations (7.73) or (7.74). Let τ_m be that τ_μ which is of the same order of magnitude

as the correct Δt. Then for all $\tau_\mu < \tau_m$ we have $\Delta y_\mu \gg 1$, $e^{-\Delta y_\mu} \simeq 0$, $1 - e^{-\Delta y_\mu} \simeq 1$, and $\lambda_\mu \simeq 0$, whereas for all $\tau_\mu > \tau_m$ we have $\Delta y_\mu \ll 1$, $e^{-\Delta y_\mu} \simeq 1$, $1 - e^{-\Delta y_\mu} \simeq 0$ and $\lambda_\mu \simeq 1$. The stiffness of Maxwell chain model for the given step is given by Equation (7.74) and we see that the partial stiffnesses K_μ or G_μ which contribute to the overall stiffness are only those for which $\tau_\mu > \tau_m$, i.e. $\tau_\mu \ll \Delta t$. This is intuitively obvious, because the stress in Maxwell units for which $\tau_\mu \ll \Delta t$ must completely relax within a time less than the step duration. Thus the effect of τ_μ as the time step increases during the computation is to gradually 'uncouple' the Maxwell units whose relaxation time is too short with regard to the current Δt. Further, we see that the inelastic strain increments are negligible and the behaviour is elastic for all $\tau_\mu < \tau_m$, i.e. $\tau_\mu \ll \Delta t$.

Another useful temporal step-by-step algorithm which avoids the storage of the previous history by exploiting the Dirichlet series expansion of the compliance function was developed by Kabir and Scordelis[108] and further applied by Van Zyl and Scordelis,[180,179] Van Greunen[178] and Kang.[110,109] This algorithm is similar to Zienkiewicz, Watson and King's[197] algorithm for non-aging materials; it consists of similar formulae involving exponentials $e^{-\Delta y_\mu}$, but it is of lower-order accuracy than the preceding algorithms. Its approximation error is of the first order $O(\Delta t)$ or $O(\Delta\sigma)$ rather than the second order, $O(\Delta t^2)$ or $O(\Delta\sigma^2)$, since the integral in Equation (7.16) is approximated with a rectangle rule. This less accurate approximation has the advantage that the same incremental elastic stiffness matrix of the structure may be used in all time steps if the age of concrete is the same in all finite elements, while in the preceding algorithms the changes in E'' (or G'', K'') cause that this matrix is different in each time step. This advantage is, however, lost if the structure is of non-uniform age or if changes of stiffness due to cracking or other effects are to be considered.

Finally it should be mentioned that, for the analysis of creep effects of composite beams during construction stages, Schade and Haas[165] produced a general finite element program using Euler–Cauchy and Runge–Kutta methods in conjunction with an aging Kelvin chain, and dealt successfully with the stability problems due to the shortest retardation time.

7.5 NON-LINEAR EFFECTS

7.5.1 Difficulties with aging in linear viscoelasticity

In every constitutive theory it is necessary to check that no thermodynamic restriction is violated. For non-aging materials this is relatively easy and well understood,[56,155] but not so for aging. Obviously, not every function of t and t' is acceptable as a compliance function $J(t, t')$. Certain thermodynamic

restrictions, such as $\partial J(t, t')/\partial t \geq 0$, $\partial^2 J(t, t')/\partial t^2 \leq 0$ and $[\partial J(t, t')/\partial t']_{t=t'} \leq 0$ are intuitively obvious and we will not discuss them. However, some further restrictions are necessary to express certain aspects of the physical mechanism of aging, particularly the thermodynamic restrictions due to the fact that any new bonds produced by a chemical reaction must be without stress when formed.

At present we know how to guarantee fulfillment of these thermodynamic restrictions only if we first convert the constitutive relation to a rate-type form and then make the hypothesis that these restrictions should be applied to internal variables such as the partial strains or partial stresses in the same way they would be applied to strains and stresses. If we did not accept this hypothesis we could not say anything about thermodynamic restrictions. It might be possible that no thermodynamic restrictions are violated by stresses and strains when they are violated by partial stresses or partial strains. But we cannot guarantee it. It is certainly a matter of concern if we have such violations. It has been found[27] that this actually happens for certain existing creep laws used in the past and we will outline the nature of the problem briefly.

If we reduce the compliance function to a rate-type form corresponding to a spring–dashpot model, fulfillment of the second law of thermodynamics can be guaranteed by certain conditions on spring moduli E_μ and viscosities η_μ. (The second law might be satisfied by the compliance function even when some of these condition are violated, but we cannot be certain of it.) Two obvious conditions are $E_\mu \geq 0$ and $\eta_\mu \geq 0$. However, the second law leads to a further condition when the spring moduli are age-dependent:[27]

$$\dot{\sigma}_\mu = E_\mu(t)\dot{\varepsilon}_\mu \quad \text{for } \dot{E}_\mu \geq 0 \tag{7.77}$$

$$\sigma_\mu = E_\mu(t)\varepsilon_\mu \quad \text{for } \dot{E}_\mu \leq 0 \tag{7.78}$$

where σ_μ and ε_μ are the stress and the strain in the μth spring. The first relation pertains to a solidifying material, such as an aging concrete, while the second relation pertains to a disintegrating (or melting) material, such as concrete at high temperatures (over 150 °C) which cause dehydration. If Equation (7.78) is used, it can be shown that the expression $\dot{D}_{ch} = -\sigma_\mu^2 \dot{E}_\mu / 2E_\mu^2$ represents the rate of dissipation of strain energy due to the chemical process, particularly due to disappearance of bonds while the material is in a strained state (i.e. a state in which elastic energy exists in addition to the bond energy). Thus, to assure that $\dot{D}_{ch} \geq 0$ we must have $\dot{E}_\mu \leq 0$ if Equation (7.78) is used. So the dissipation inequality is violated if Equation (7.78) is used (or if its use is implied) for an aging (solidifying, hardening) material.

Many different rate-type forms of the creep law are possible. One form, which differs from the one that we already analysed, can be obtained by

expanding the memory function $L(t, t')$ from Equation (7.17) into Dirichlet series:

$$L(t, t') = \sum_{\mu=1}^{N} \frac{1}{\eta_\mu(t')} e^{-(t-t')/\tau_\mu} \tag{7.79}$$

Substituting this into Equation (7.17) we obtain

$$\varepsilon = \sum_{\mu=1}^{N} \varepsilon_\mu + \varepsilon^0 \qquad \varepsilon_\mu(t) = \int_0^t \frac{\sigma(t')}{\eta_\mu(t')} e^{-(t-t')/\tau_\mu} \, dt' \tag{7.80}$$

By differentiating $\varepsilon_\mu(t)$ and denoting $E_\mu(t) = \eta_\mu(t)/\tau_\mu$, one can readily verify that $\varepsilon_\mu(t)$ satisfies the differential equation

$$\sigma = E_\mu(t)\varepsilon_\mu + \eta_\mu(t)\dot{\varepsilon}_\mu \tag{7.81}$$

From this, the non-viscous part of stress σ is $\sigma_\mu = E_\mu(t)\varepsilon_\mu$, and we see that this represents an elastic relation that is admissible only for a disintegrating (melting, dehydrating) material. Thus Equation (7.79), which has been used as the basis of one large finite element program for creep of reactor vessels, implies violation of the dissipation inequality.[27] This puts the practical applicability in question, as the critics think. The proponents of the models that imply Equation (7.81) believe however that the problem is not serious since the solidifying process may be counteracted by drying or temperature decrease, and that a separate application of the thermodynamic restrictions to the solidfying behaviour is not required. Maybe, but what about the special case of constant humidity and temperature?

We may note that Equation (7.81) along with $\varepsilon = \sum_\mu \varepsilon_\mu$ corresponds to a Kelvin chain model[27] the springs of which are, however, governed by an incorrect equation (Equation (7.78)). If the correct equations for the springs are used ($\dot{\sigma}_\mu = E_\mu \dot{\varepsilon}_\mu$), then the Kelvin chain is characterized by second-order rather than first-order differential equations (Equation (7.49)). The violation of the dissipation inequality by Equations (7.79) or (7.80) is actually due to the fact that the equation for partial strains (Equation (7.81)) is of the first order. One can show[27] that even if a non-linear rate-type creep law is considered such that $\varepsilon = \sum_\mu \varepsilon_\mu$ and $\dot{\varepsilon}_\mu = f_\mu(\sigma, \varepsilon_\mu)$, Equation (7.78) which violates the dissipation inequality is implied as long as these are first-order equations. This is one inherent difficulty of using Kelvin chain type models (i.e. decomposing ε into partial strains ε_μ). By contrast, the differential equations for the aging Maxwell chain must be of the first order for an aging (solidifying) material, which is one advantageous property of Maxwell chains.

Kelvin chain models (which are implied by making a strain summation assumption $\varepsilon = \sum \varepsilon_\mu$) have another limitation. Consider the degenerate creep compliance in Equation (7.32). We calculate $\partial^2 J/\partial t \, \partial t'$ and substitute

$\dot{C}_\mu(t') = [(C(t') - E_\mu(t'))]\dot{y}_\mu(t')$ and $C_\mu(t') = \eta_\mu(t')y_\mu(t')$ according to Equation (7.50) for the Kelvin chain. This yields

$$\frac{\partial^2 J(t, t')}{\partial t \, \partial t'} = \sum_{\mu=1}^{N} \frac{\dot{y}_\mu(t)}{\dot{y}_\mu(t')} \frac{E_\mu(t')}{[\eta_\mu(t')]^2} \exp[y_\mu(t') - y_\mu(t)] \tag{7.82}$$

Here we must always have $\dot{y}_\mu > 0$ and $E_\mu \geq 0$. Consequently, thermodynamically admissible Kelvin chain models always yield a compliance function such that

$$\frac{\partial^2 J(t, t')}{\partial t \, \partial t'} \geq 0 \tag{7.83}$$

The same conclusion may be reached from Equation (7.49a).

Now, what is the meaning of this inequality? Geometrically, it means that the slope of a unit creep curve would get greater as t' increases, which means that two creep curves for different t', plotted versus time t (not $t - t'$, see Figure 7.7(a)) would never diverge as t increases. Is this property borne out by experiment? Due to the large scatter of creep data we cannot answer this with complete certainty, but quite a few test data, although not the majority of them, indicate a divergence of adjacent creep curves beginning with a certain creep duration $t - t'$.[33,27] As for the creep formulae, the double power law (Equation (7.5)) as well as the ACI formulation always exhibit divergence after a certain value of $t - t'$, whereas the CEB-FIP formulation does not. Thus, aging Kelvin chain models cannot closely approximate this behaviour without violating the thermodynamic restrictions $E_\mu \geq 0$, $\nu_\mu \geq 0$, $\dot{E}_\mu \geq 0$. Indeed, the previously described algorithms for determining $E_\mu(t)$ yield negative E_μ for some μ and some t whenever $J(t, t')$ with divergent creep curves is fitted.

For aging Maxwell chain models, by contrast, it is possible to violate inequality (7.83) without violating any of the thermodynamic restrictions.[27] Therefore, the aging Maxwell chain models are more general and seem theoretically preferable for describing concrete creep. The equivalence of Maxwell and Kelvin chains to each other as well as to any other rheologic model[157] does not quite apply in the case of aging.

The Maxwell chain model is, however, not entirely trouble-free either. When long-time creep data are fitted, the condition $E_\mu \geq 0$ can be satisfied but the condition that $\dot{E}_\mu \geq 0$ for all μ and all t cannot (Figure 7.16), as numerical experience reveals. (Thus far, however, this question has been studied only for $y_\mu = t/\tau_\mu$; for a general $y_\mu(t)$ a definite answer must await further results.)

Note that we merely evade answering the question if we restrict ourselves to an integral-type creep law, for without its conversion to a rate-type form we cannot know whether our formulation of aging is thermodynamically admissible. We also evade the answer by introducing a rate-type model

without recourse to a rheologic spring–dashpot model, since every rate-type model can be visualized by some such rheologic model.

We must admit, however, that the question of uniqueness of representation by a rheologic model remains unsettled. If we find that a certain creep function $J(t, t')$ leads to one unsatisfactory rate-type model, we are not sure that the same creep function might also be represented by some other rate-type model that is satisfactory.

To summarize, we have two kinds of rate-type models: (a) those whose form is fundamentally objectionable (Equation (7.78)) because it always violates the dissipation inequality; and (b) those which are of correct form (Equation (7.77)) and can represent the aging creep curves for various t' over a limited time range but cannot do so for a broad time range without violating the thermodynamic restrictions ($E_\mu \geq 0$ or $\dot{E}_\mu \geq 0$) for some period of time. Although for the second kind of models the problems are less severe, none of the presently known linear rate-type models is entirely satisfactory.

After a long effort it now seems as if the typical shape of concrete creep curves for various t' cannot be completely satisfactorily described with a linear rate-type model. Hence, the difficulties are likely caused by our use of a linear theory for what is actually a non-linear phenomenon. And measurements relative to the principle of superposition suggest that this may indeed be so. On the other hand, the magnitude of the error caused by the shortcomings outlined in this section is not known well and might not be too serious in many cases. Thus, we will continue to use linear rate-type models in the foreseeable future.

To understand the nature of the aging effect in creep, it was attempted to deduce the constitutive relation from an idealized micromechanics model of the solidification process in a porous material.[26] This approach yielded a certain form of creep function (giving in particular support to the double power law); it did not however answer the questions we just discussed.

7.5.2 Adaptation and flow

There are basically two kinds of deviations from the principle of superposition:

(1) High-stress non-linearity or flow, which represents an increased creep compared to the principle of superposition;[83,87,114]
(2) Low stress non-linearity or adaptation, which represents a diminished creep compared to the principle of superposition.

The high-stress non-linearity is significant for basic creep only beyond the service stress range, i.e. above approximately 0.5 of the strength. On the other hand, the adaptation non-linearity is quite significant within the service stress range. It is mainly observed when, after a long period of sustained stress (within the allowable stress range), a further sudden load, positive or negative, is superimposed.

A mathematical model for both these types of non-linearity was recently developed.[35] For certain reasons it is appropriate to introduce the non-linearities in an expression for the creep rate $\dot{\varepsilon}$ rather than for total strain ε. Thus, starting with Equation (7.18) for the creep rate, one makes this equation non-linear in the following manner:

$$\dot{\varepsilon}(t) = \frac{\dot{\sigma}(t)}{E(t_e)} + g[\sigma(t)] \int_0^t \frac{\partial J(t, t'_e)}{\partial t} \frac{\mathrm{d}\sigma(t')}{1 + a(t')} + \dot{\varepsilon}_f(t) \tag{7.84}$$

The integral term describes what is called the adaptation, which is brought about in two ways. First, the age effect in creep function and elastic modulus is introduced by replacing age t with a more general expression for the equivalent hydration period;

$$t_e = \int \beta_T \beta_\sigma \, \mathrm{d}t \tag{7.85}$$

where coefficient β_σ, for which a formula is given by Bažant and Kim,[35] is added to account for the gradual increase of bonding (or adaptation) caused in cement paste by sustained compressive stress.[98] Second, an additional stiffening of response (adaptation) is obtained through function $a(t')$ which is defined by an evolution equation of the type $\dot{a}(t) = F_1(t)F_2(\sigma)$. In the limit for very rapid loading these non-linear effects vanish.

Functions $g[\sigma(t)]$ and $\dot{\varepsilon}_f(t)$ describe the high-stress non-linearity. The function $\dot{\varepsilon}_f(t)$, called flow, has the form:

$$\dot{\varepsilon}_f(t) = \frac{\sigma(t) - \alpha(t)}{E_0} f[\sigma(t)] \dot{\phi}(t) \tag{7.86}$$

where $f[\sigma(t)]$ gives an increased creep rate at high stress, and $\alpha(t)$ may be regarded as the location of the centre of a loading surface that gradually moves toward the sustained stress value (similar to kinematic hardening in plasticity). The evolution equation for $\alpha(t)$ is of the type $\dot{\alpha}(t) = f_1[\sigma(t), \alpha(t)]f_2(t)$.

The adaptation and flow non-linearities are illustrated by test data in Figure 7.19, 7.20, and 7.21. For further data see Aleksandrovskii *et al.*,[2,3] Roll,[156] Freudenthal and Roll,[83] Komendant,[116] Brettle,[63] Meyers and Slate,[136] and others.

7.5.3 Singular history integral for non-linear creep

In the foregoing model, the non-linearities at the working stress level are modelled by adjustments to the superposition principle. These non-

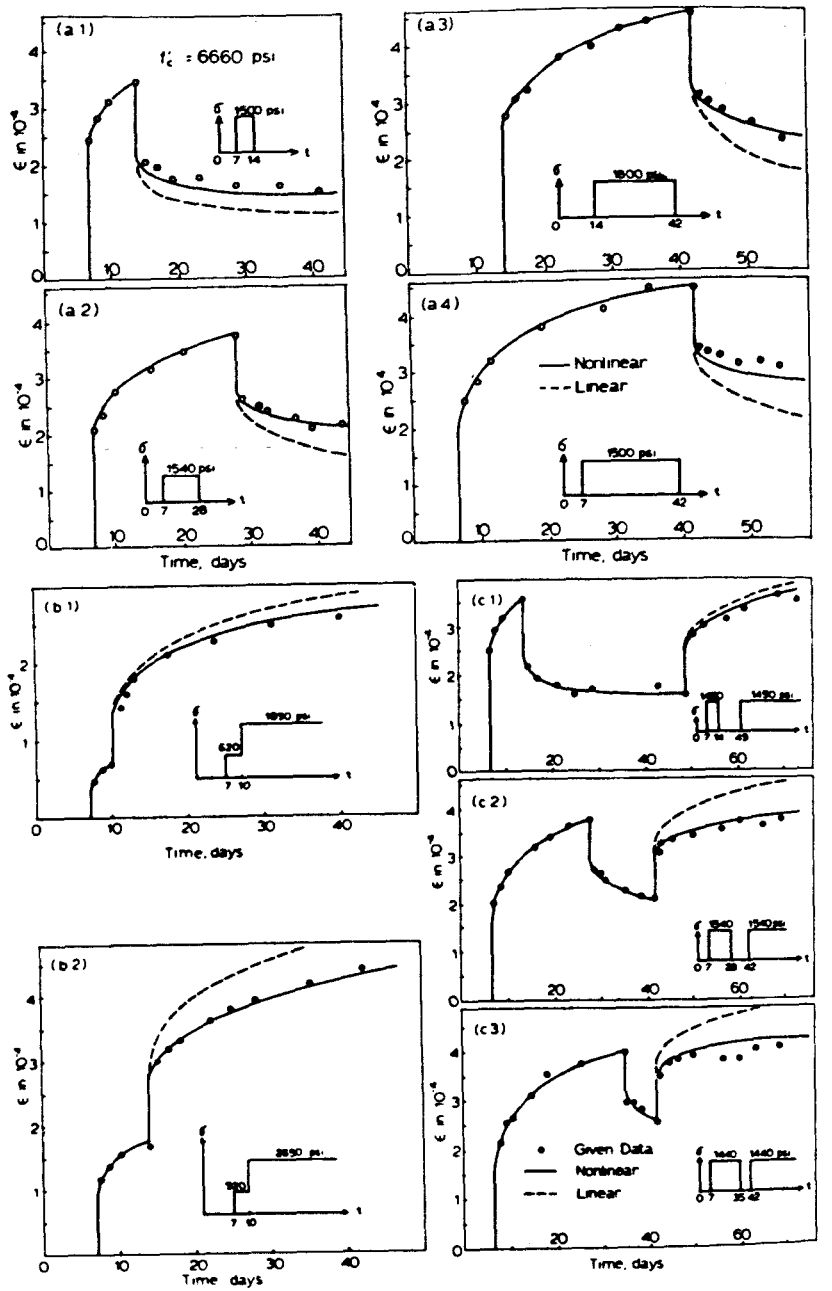

Figure 7.19 Typical test results[141] showing adaptation non-linearities: solid lines, predictions of nonlinear theory; dashed lines, predictions of linear theory[34,35]

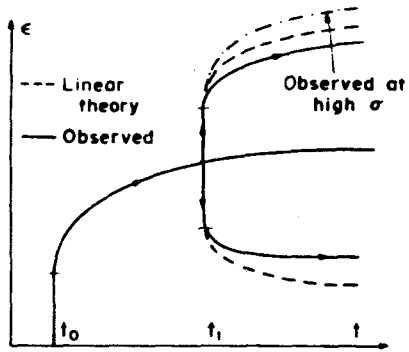

Figure 7.20 Deviation from superposition principle for unloading and for step increase of load

linearities may however have a deeper cause in the essential creep mechanism, and so it may be more realistic to abandon the underlying linear superposition principle itself. At the same time it is necessary to preserve the proportionality of the response to an arbitrary load history within the working stress range, a property which is well verified experimentally.[158,141] Such a development has been made recently[50,206] and we will outline it briefly.

We consider a uniaxial creep law of the form

$$\frac{\mathrm{d}}{\mathrm{d}t}[\gamma(t)^p] = \int_0^t Q(t,\tau)\,\mathrm{d}[\sigma(\tau)^r] \tag{7.87}$$

in which

$$Q(t,\tau) = Ft^{-k}\tau^{-m}(t-\tau)^{-u}[\kappa(t)^s - \kappa(\tau)^s]^{-v} \tag{7.88}$$

$$\kappa(t) = \int_0^t |\mathrm{d}\gamma(\tau)| \tag{7.89}$$

Here σ is uniaxial stress; γ is creep strain; t is time (= age of concrete); κ is the path length of creep strain (intrinsic time); k, m, p, r, s, u, and v are non-negative material constants ($s > 0$); $R(t,\tau)$ is the creep kernel; F is a function of $\sigma(t)$ and $\gamma(t)$ which models the creep increase beyond proportionality at high stress. Since we are not interested in this phenomenon at high stress,[116,127,105] we will consider only the case F = constant, which is sufficient for working stress levels. The integral in Equation (7.87) is a Stieltjes integral. For continuous and differentiable $\sigma(t)$ this integral may be replaced by the usual Riemann integral, substituting $\mathrm{d}[\sigma(\tau)^r] = r\sigma(\tau)^{r-1}\,\mathrm{d}\sigma(\tau)/\mathrm{d}\tau$.

If we consider a single-step load history ($\sigma = 0$ for $t < t'$, σ = constant > 0

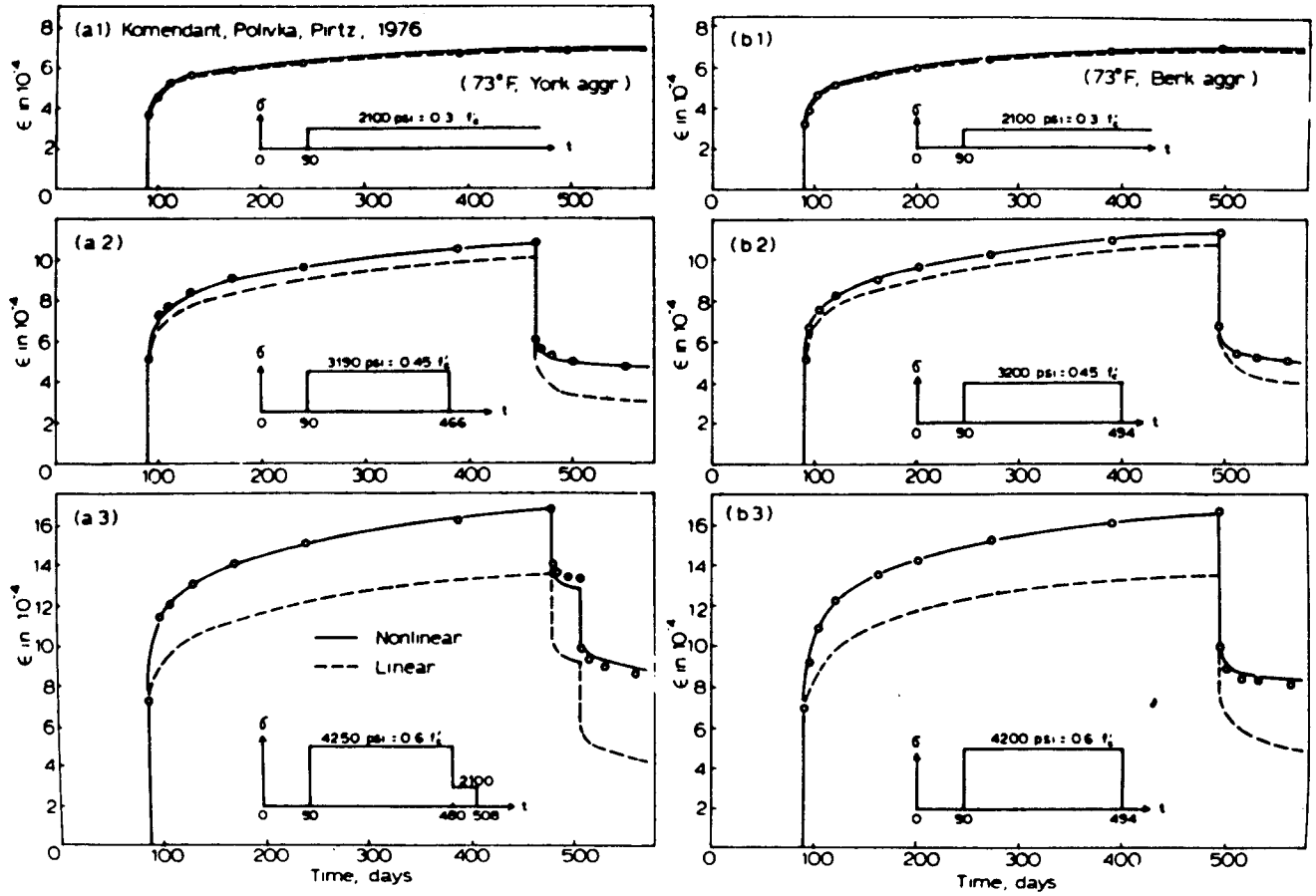

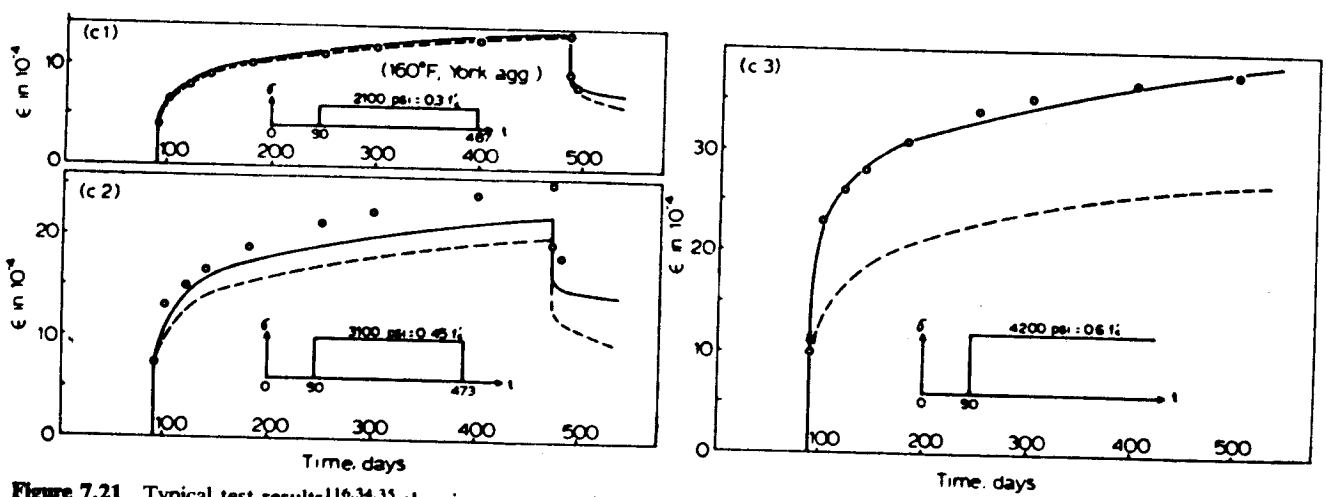

Figure 7.21 Typical test results[116,34,35] showing creep non-linearity at high stress (solid lines, predictions of non-linear theory; dashed lines, predictions of linear theory)

for $t \geq t'$) under the assumption $r = p + sv$, Equation (7.87) reduces to the form

$$\gamma(t) = \left[\sigma \frac{F}{(t')^m} \frac{r}{p} B(t, t')\right]^{1/r} \tag{7.90}$$

in which

$$B(t, t') = \int_{t'}^{t} \frac{d\tau}{\tau^k (\tau - t')^u} \tag{7.91}$$

For $t - t' \ll t'$, the following asymptotic expression holds:

$$\gamma(t) = \sigma \left(\frac{Fr}{(1-u)p} \frac{(t-t')^{1-u}}{(t')^{m+k}}\right)^{1/r} \tag{7.92}$$

Equation (7.87) has the following noteworthy features.

(1) For $p = r = 1$ with $v = k = 0$, it reduces to the linear integral-type creep law (superposition principle) based on the double power law and, with $v = 0$ and $k > 0$, it reduces to the one based on the triple power law[26] which has been verified as a slight refinement of the well-substantiated double power law.

(2) If any one of the conditions $p = 1, r = 1, v = 0$ is violated, this creep law ceases to be linear and, therefore, the principle of superposition does not apply. In particular, the stiffening non-linearity is obtained for $p > 1$.

(3) However, if at the same time

$$r = p + sv \tag{9.93}$$

this non-linear creep law exhibits proportionality in the sense that if $\gamma(t)$ corresponds to history $\sigma(t)$ then $k\gamma(t)$ corresponds to history $k\sigma(t)$. The fact that a non-linear creep law can be obtained without violating proportionality seems useful for modeling experimentally observed properties,[158,141] at working stress levels.

(4) It is also necessary that

$$u + sv < 1 \quad \text{and} \quad u + v < 1 \tag{7.94}$$

for the creep kernel to be weakly singular and, consequently, integrable. The latter of these conditions must be added with regard to the second and the subsequent steps of a multistep loading history, and prevails when $0 < s < 1$.

(5) As observed in Equation (7.90) for a single-step load history with the proportionality condition (Equation (7.93)) for $k = 0$, Equation (7.87) still leads to the well-verified double power creep law and, for $k > 0$, to the triple power law.[26] Therefore, using the previously obtained results on these power laws, it is possible to estimate some parameters involved in the present model.

(6) A further important property is that not only the term $(t-\tau)^{-u}$, which is present in the previous completely linear integral expressions for the creep rate, but also the term $[\kappa(t)^s - \kappa(\tau)^s]^{-v}$ yields an infinite creep rate $\dot{\gamma}$ (singularity) right after any sudden change in stress σ. If this term were omitted (i.e. $v = 0$ with $s > 0$), the strength of the singularity of $\dot{\gamma}$ would be given solely by $(t-\tau)^{-u}$, i.e. independent of γ, and would not contribute to expressing the non-linearity.

(7) With $s = 1$, the strength of the singularity at each stress jump is the same. Analysis of available test data,[158,141] suggests, however, that $s > 1$. This has an interesting consequence for a two-step stress history, i.e. $\sigma = 0$ for $t < t'$, $\sigma = \sigma_1 = \text{constant}$ (>0) for $t' < t < t''$ and $\sigma = \sigma_2 = \text{constant}$ $(>\sigma_1)$ for $t > t''$. If we let $\sigma_1 \to 0$ at constant σ_2, the history approaches a one-step history with a jump of σ_2 at t'', but the singularity strength $(u+v)$ in the limit is not the same as that for a one-step history (i.e. $u + sv$) if $s \neq 1$.

(8) The fact that the integral in Equation (7.87) expresses the creep rate $\dot{\gamma}$ rather than the total creep strain γ is appropriate for modelling the non-linear creep properties at high stress as mentioned before (Equation (7.84)).

(9) Asymptotic approximations as well as numerical integration of the creep law have further revealed that at low stress levels the creep law generally gives qualitatively correct deviations from the (linear) superposition principle. For a two-step increasing load the response is after the second step lower than the prediction of the superposition principle. For creep recovery after a period of creep at constant stress, the recovery response is and remains higher than the recovery curve predicted from the superposition principle. In both cases, the deviation vanishes as the duration of the first load step tends to zero. These properties represent the essential non-linear features of concrete creep at low stress levels.

(10) Function $\kappa(t)$ is needed for the case of unloading. This function, which is analogous to the well-known intrinsic time, assures the positiveness of $Q(t, \tau)$. Without excluding the case of creep recovery it is impossible to use $\kappa(t) = \gamma(t)$ because $Q(t, \tau)$ would be negative or undefined for unloading.

From the foregoing discussion, it appears that Equation (7.87) is qualitatively capable of capturing all the significant traits of the non-linear creep behaviour of concrete at working stress levels. It is also encouraging that the proposed creep law is compatible with a realistic picture of the creep mechanism.

We imagine that creep in concrete consists of a vast number of small particle migrations within the cement paste microstructure. Any sudden change of stress, $\Delta\sigma$, is assumed to activate a number of potential migration sites, the number of which, N_s, is very large. This points to an infinite strain rate right after any stress jump, which in turn suggests the existence of a

singularity in the kernel, resulting from the term $[\kappa(t)^s - \kappa(\tau)^s]^{-v}$. The subsequent growth of this term reflects the gradual exhaustion of potential particle migration sites, thus causing a reduction in creep rate. The exhaustion rate must decrease as the creep strain already caused by stress jump $\Delta\sigma$ increases, i.e. it must decrease as $[\kappa(t)^s - \kappa(\tau)^s]$ and $(t-\tau)$ grow, as reflected in Equations (7.87) and (7.88).

The creep rate must also decrease due to the continuing hydration of the cement paste while it carries the load. The hydration results in formation of further bonds in the microstructure, which reduces the number of potential migration sites. This reduction depends strictly on time and proceeds at a gradually decreasing time rate, as modeled by the term $\tau^{-m}(t-\tau)^{-u}$ in Equations (7.87) and (7.88).

7.5.4 Cyclic creep

Another important non-linear phenomenon arises for cyclic (or pulsating) loads with many repetitions. According to the principle of superposition, the creep due to cyclic stress should be approximately the same as the creep due to a constant stress equal to the average of the cyclic stress. In reality, a much higher creep is observed, the excess creep being larger for a larger amplitude of the cyclic component.[184,100,134,84,15,174]

The time-average compliance function for cyclic creep at constant stress amplitude Δ and constant mean stress may be reasonably well described by an extension of double power law in which $(t-t')^n$ is replaced by the expression $[(t-t')^n + 2.2\phi_\sigma \Delta^2 N^n]$ where N is the number of uniaxial stress cycles of amplitude Δ, ϕ_σ is a function of σ, equal to 1.0 when $\sigma = 0.3f'_c$. The cyclic loading does not seem to affect the drying creep component. For details, see Bažant and Panula[43] (Part VI).

7.5.5 Multiaxial generalization and operator form

Regarding the multiaxial aspects of non-linear creep, almost no experimental information is available. The multiaxial non-linear behaviour is reasonably explored experimentally only for short-time (rapid, 'instantaneous') loading, and the high-stress non-linearity of creep must approach this behaviour in the limit. This limiting condition is presently just about the only solid information on which generalizations of non-linear creep models to three dimensions can be based.

Based on this scant information, both the endochronic theory and the plastic fracturing theory for non-linear triaxial behaviour have been extended to describe non-linear triaxial creep.[29,39] These models are probably reasonably good for short load durations and large deformations near those for the usual short-time (rapid) tests, but they are entirely hypothetical as far as long load durations are concerned. The adaptation phenomena have not been included in these models. However, an inductive generalization of Equations (7.85) and (7.86), in which σ was replaced by certain stress invariants, has been given for the foregoing theory of adaptation (Section 7.5.2).

7.5.6 Cracking and tensile non-linear behaviour

The most typical deleterious effect of creep and shrinkage in structures is cracking, both invisible microcracking and, at a later stage, continuous visible cracks. Thus, the calculation of creep and shrinkage effects is complete only if a realistic model of cracking, as well as tensile non-linearity due to microcracking and fracture propagation, is considered.[202]

7.6 MOISTURE AND THERMAL EFFECTS

7.6.1 Effect of pore humidity and temperature on aging

The moisture effects are much more involved and much less understood than the effects analysed so far, despite considerable research efforts.

The previously indicated expressions for the effect of humidity (Section 7.2.6), as given in current code recommendations and practical creep prediction models, describe only the mean behaviour of the cross section and do not represent constitutive properties and constitutive relations of the material. Thus, they are usable in structural analysis only when the cross section is of single-element width (as is often used for plates and shells); it makes no sense to subdivide the cross section into more than one element.

To determine the distributions of pore humidity and water content within the cross section at various times, it is necessary to solve the moisture diffusion problem. This necessitates a constitutive equation which involves the pore humidity or water content but not the environmental humidity. The latter is inadmissible for use in a constitutive equation and is properly used only as a boundary condition.

One important effect of a decrease in pore humidity h (relative vapour pressure p/p_{sat}) is a deceleration and eventual arrest of the hydration process. This may be modelled by extending the previous definition of the equivalent hydration period, t_e (or maturity):

$$t_e = \int \beta_T \beta_h \, dt \tag{7.95}$$

where

$$\beta_h \simeq [1 + 6(1-h)^4]^{-1} \tag{7.96}$$

Here β_T is given by Equation (7.59); β_h is an empirical function. Compared

to $h = 1.0$, Equation (7.95) gives a reduction of aging rate to 9% at $h = 0.7$ and to 1% at $h = 0.5$.

Still more realistically, taking into account Equation (7.85) one should write $t_e = \int \beta_T \beta_h \beta_\sigma \, dt$.

7.6.2 Shrinkage as a constitutive property

Let us now consider shrinkage, ε_S, which is understood as a material property rather than a specimen property, and represents the free (unrestrained) shrinkage at a point of a continuum. As proposed by Carlson[67] and Pickett,[148] the shrinkage is properly modelled as a function of pore water content w (g of water per cm^3 of concrete), which is in turn a function of pore humidity h. Therefore,

$$\varepsilon_S = \varepsilon_S^0 f_S(h) \tag{7.97}$$

Here ε_S^0 is the maximum shrinkage (for $h = 0$), which is larger, perhaps much larger, than ε_{sh_∞} in Equation (7.9) because the value ε_{sh_∞} is reduced by microcracking of the specimen while ε_S^0 is not, by definition. The function $f_S(h)$ is emprical; approximately perhaps $f_S(h) = 1 - h^2$ but this needs to be checked more closely.

Note that, in contrast to Equation (7.9) for the mean cross-section shrinkage $\bar{\varepsilon}_S$, the shrinkage as a material property exhibits no dependence on the duration of drying $t - t_0$ and the age at the start of drying t_0. These times affect $\bar{\varepsilon}_S$ only indirectly, through the solution of the diffusion problem which is approximated by Equation (7.9).

There exists, however, some time-dependence in shrinkage, albeit different from that in Equation (7.9). Since the mechanism of shrinkage at least to some extent consists in deformation (compression) of solid particles and solid microstructural framework under the forces caused by changes in solid surface tension, capillary tension, and disjoining pressure in hindered adsorbed water layers, the deformation must depend on the stiffness of the microstructure. This, in turn, depends on the degree of hydration, and thus on the equivalent hydration period t_e. Hence, a more accurate expression for shrinkage should be

$$\varepsilon_S = \varepsilon_S^0 f_S(h) g_S(t_e) \tag{7.98}$$

where the function g_S may approximately be taken as $g_S(t_e) \simeq E_{28}/E(t_e)$, i.e. the inverse ratio of the increase in elastic modulus due to age (hydration).

Another time dependence may exist in shrinkage due to the delay needed to establish thermodynamic equilibrium of water between macropores and micropores. Part of the shrinkage, probably a large part, is due to a change in the disjoining pressure, and since the microdiffusion of water between micropores and macropores through which the thermodynamic equilibrium is established requires some time, the disjoing pressure must respond to humidity h in the macropores with a certain delay. This would mean that for determining the delayed part of $\varepsilon_S(t)$ at time t, one would have to substitute the value of h at an earlier time $t - \Delta$, Δ being the characteristic lag. Alternatively, the delay may be obtained through a formulation exemplified in Equations (7.99)–(7.101) in the sequel.

7.6.3 Creep at drying as a constitutive property

The effect of pore humidity on creep is not completely understood at present, chiefly because of the difficulty of determining creep properties from tests on drying specimens which are in a highly non-uniform moisture state during the test and probably undergo significant microcracking.

One effect of pore humidity is however clear; if the pore humidity is constant, then the lower the pore humidity, the smaller the creep.[189,191–194,160] At fully dried state ($h \simeq 0$) the creep rate is only about 10% of that at fully saturated state ($h = 1$). This effect may be described by replacing τ_μ in the preceding rate-type equations with τ_μ/ϕ_h where ϕ_h is a function of h, roughly given as $\phi_h \simeq 0.1 + 0.9h^2$.

Another effect is that of a change in humidity. This effect remains rather clouded. Whereas after drying (after h attains a constant value) creep is less at lower humidity, during the drying process the creep is higher than at a sealed state (Hansen,[90] Glucklich and Ishai,[87] Keeton,[111] Kesler *et al.*[113] Kesler and Kung,[112] L'Hermite,[121] L'Hermite and Mamillan,[122] Mamillan,[127] L'Hermite *et al.*,[123] Mamillan and Lelan,[28] Mullen and Dolch,[140] etc.). This phenomenon apparently persists even for some time after the pore humidity has come down and reached equilibrium throughout the specimen. What is uncertain is how much of the creep increase observed in drying specimens (Pickett effect) is due to the non-uniform stress state of the specimen and the inherent microcracking (or tensile non-linearity), and how much of it is due to constitutive properties, e.g. a possible effect of the rate of pore humidity $\dot{h}$ upon the creep rate coefficient $1/\tau_\mu$.

A model which describes both of the aforementioned effects has been developed[16,25,24,52] applying thermodynamics of multiphase systems and of adsorption to obtain a rate-type constitutive model. The effect of $\dot{h}$, if it exists, must be due to a thermodynamic imbalance between macropores and micropores, created by pore humidity changes, and to the resulting local diffusion between these two kinds of pores. In the process of drying (as well as wetting) of a concrete specimen one may distinguish two diffusion processes. One is the macroscopic diffusion in which the water molecules migrate through the pore passages of least resistance, involving the largest (capillary) pores and bypassing most of the micropores (gel pores and

interlayer spaces). This diffusion process controls the humidity in the macropores, h, and is essentially independent of the applied load and deformation. The other diffusion process is the local process of migration of water molecules on the microscale between the macropores and the micropores. This process is driven by a thermodynamic imbalance between these two kinds of pores; more precisely, an imbalance (difference) between the values, μ_w, μ_d, of the specific Gibbs' free energy μ in these pores. The values μ_w and μ_d depend on the water content of pores (as well as temperature) and, for the micropores but not the macropores, also on the stress in the solid gel that is transmitted through water (hindered adsorbed water or interlayer water) in the micropores and is caused by the applied load. The two separate diffusion processes are certain to exist, but at present it is just a hypothesis that the microscopic diffusion of water indeed affects to a significant extent the mobility in the solid microstructure, thereby influencing creep.

The foregoing hypothesis has been applied to the Maxwell chain model in which each partial stress σ_μ ($\mu = 1, 2, \ldots, N$) is separated into two parts, σ^s_μ and σ^w_μ, imagined to represent the stresses in solids and in micropore water. The uniaxial version of the constitutive equation then is:[25,52]

$$\dot{\sigma}^s_\mu + \phi_{ss_\mu}\sigma^s_\mu = E^s_\mu(\dot{\varepsilon} - \dot{\varepsilon}^0_{sh} - \alpha^s_\mu \dot{T}) \tag{7.99}$$

$$\dot{\sigma}^w_\mu + \phi_{ww_\mu}[\sigma^w_\mu - f_\mu(h, T)] = E^w_\mu(\dot{\varepsilon} - \dot{\varepsilon}^0_{sh} - \alpha^w_\mu \dot{T}) \tag{7.100}$$

$$\sigma = \sum_{\mu=1}^{N} (\sigma^s_\mu + \sigma^w_\mu) \tag{7.101}$$

Here $E^s_\mu(t)$ and $E^w_\mu(t)$ are separate spring moduli for solids and water; ε^0_{sh} is the part of shrinkage strain that is instantaneous with a change of humidity h (relative vapour pressure) in the capillary pores; α^s_μ, α^w_μ are coefficients of thermal dilation that are instantaneous with temperature change; ϕ_{ss_μ}, ϕ_{ww_μ} are the rate coefficients which replace the role of $1/\eta_\mu$ in Equation (7.56) and reflect the rate of diffusion (or migration) of solids and water (hindered adsorbed water and interlayer water) between the loaded and load-free areas of cement gel microstructure; and $f_\mu(h, T)$ are values of σ^w_μ for which the water in loaded areas (micropores) is in thermodynamic equilibrium with water in the adjacent capillary pores. Coefficient ϕ_{ss_μ} is assumed to increase as $[\sigma^w_\mu - f_\mu(h, T)]^2$ increases; this models the drying creep effect[25,52] and since it expresses the acceleration of creep when thermodynamic equilibrium does not exist between the water in loaded areas and the water in load-free areas. Material functions $f_\mu(h, T)$, ϕ_{ss_μ}, ϕ_{ww_μ}, E^s_μ, and E^w_μ, which give a good agreement with test data on creep and shrinkage for specimens of various sizes at various regimes of time-variable environmental humidity have been found.[52]

A step-by-step algorithm (of the exponential type) has been developed for Equations (7.99)–(7.101), and their triaxial version was applied to analyse

by finite elements the stresses in drying cylinders[52] and in drying floors.[106] Cracking or tensile non-linearity of concrete was considered in these analyses. This rather sophisticated model led to a good agreement with most of the existing test data on creep under various moisture conditions, exceeding by far the results obtained with other constitutive models.

The present test data are however limited in scope, and could perhaps be fitted equally well by different models. At present one cannot even exclude the possibility—an attractive one because of its simplicity—that the pore humidity rate $\dot{h}$ has no significant effect in the constitutive equation *per se* and all of the creep increase due to drying is the consequence of internal stresses and microcracking.[195] More tests and theoretical analyses are urgently needed to check this hypothesis.

Due to random fluctuations of environmental humidity, creep and shrinkage in drying structures should be analysed probabilistically and some steps in this direction have already been taken.[205,203]

7.6.4 Calculation of pore humidity

From the preceding exposition we see that calculation of pore humidity as a function of space and time is a necessary part of an analysis of stress distributions in the presence of drying. A satisfactory model already exists for this purpose.

In the early investigations, drying of concrete was considered as a linear diffusion problem, but serious discrepancies were found. It is now reasonably well documented by measurements that the diffusion equation that governs moisture diffusion in concrete at normal temperatures is highly non-linear, due to a strong dependence of permeability c and diffusivity on pore humidity h. The governing differential equation may be written as:[37]

$$\frac{\partial h}{\partial t} = k \operatorname{div} \mathbf{J} + \frac{\partial h_s(t_e)}{\partial t} + k\frac{\mathrm{d}T}{\mathrm{d}t} \qquad \mathbf{J} = -c \operatorname{grad} h \tag{7.102}$$

where $\mathbf{J}$ is water flux; $k = \partial h/\partial w$ at constant temperature T and constant age (= slope of desorption isotherm or sorption isotherm); w is the specific pore water content; $\kappa = \partial h/\partial T$ at constant h and constant t_e; and $\partial h_s/\partial t$ is the rate of self-desiccation, i.e. of the drop of h due to aging (hydration) at constant w and constant T. The function $h_s(t_e)$ is empirical and represents a gradual decrease of h from the initial value 1.00 to about 0.96 to 0.98 after long conservation (without external drying). For desorption at room temperature, coefficient k may be approximately taken as constant, in which case it may be combined with c, yielding $C = kc$ = diffusivity.

The graph of C (or c) versus h decreases to about 1/20 as h drops from 0.90 to 0.60 (Figure 7.22). This is doubtless due to the fact that the rate of moisture transfer is at room temperature controlled by migration of water

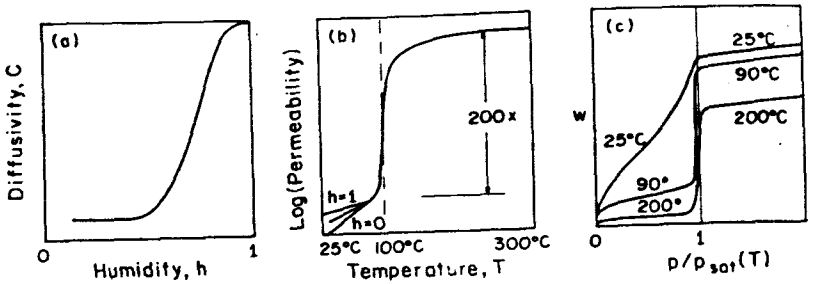

Figure 7.22 Dependence of drying diffusivity C of concrete on pore humidity, of permeability on temperature, and sorption isotherms

molecules in adsorbed layers, the rate of migration getting slower as the thickness of the adsorption layers decreases. A suitable empirical expression is[37] (Figure 7.22):

$$C = kc = C_1(T, t_e)\{0.05 + 0.95[1 + 3(1-h)^4]^{-1}\} \tag{7.103}$$

where C_1 is the diffusivity at $h = 1$, for which an approximate semi-empirical expression based on activation energy is also available:[25]

$$C_1(T, t_e) = C_0\left[0.3 + \left(\frac{13}{t_e}\right)^{1/2}\right]\frac{T}{T_0}\exp\left(\frac{Q}{RT_0} - \frac{Q}{RT}\right) \tag{7.104}$$

where $Q/R \simeq 4700$ K and T is absolute temperature.

The boundary conditions for $t > t_0$ are: for sealed surface, normal flux $\mathbf{J}_n = 0$; and for perfect moisture transfer, $h = p_{en}/p_{sat}(T)$ where p_{en} is the environmental vapour pressure and $p_{sat}(T)$ is the saturation pressure for temperature T in concrete at its surface.

From the foregoing equations we can determine the size dependence of the drying process. We consider constant temperature, and also neglect the term $\partial h_s/\partial t$ in Equation (7.102) since it is relatively small. We may further neglect the age dependence of slope k and permeability c. Then Equation (7.102) becomes

$$\frac{\partial h}{\partial t} = k(h)\frac{\partial}{\partial x_i}\left(c(h)\frac{\partial h}{\partial x_i}\right) \tag{7.105}$$

where x_i are Cartesian coordinates ($i = 1, 2, 3$). We now introduce the non-dimensional spatial coordinates $\xi_i = x_i/D$, where D is a characteristic dimension of the body, e.g. the effective thickness. We restrict attention to geometrically similar bodies, whose all dimensions are fully characterized by D, and we introduce the non-dimensional time

$$\theta = (t - t_0)/\tau_s \quad \text{with } \tau_s = D^2/C_1 \tag{7.106}$$

where t_0 is the age at the start of drying. Then $\partial/\partial t = C_1 D^{-2}\,\partial/\partial\theta$. Also $\partial/\partial x_i = D^{-1}\,\partial/\partial\xi_i$. Thus, Equation (7.105) yields:

$$\frac{\partial h}{\partial \theta} = \frac{k(h)}{k_i}\frac{\partial}{\partial \xi_i}\left(\frac{c(h)}{c_1}\frac{\partial h}{\partial \xi_i}\right) \tag{7.107}$$

This diffusion equation is to be solved always for the same region of ξ_i. The initial condition consists of prescribed values of h. Assuming that the boundary conditions also consist either of prescribed time-constant values of h or of a sealed boundary (normal flux $\mathbf{J}_n = 0$), the corresponding initial and boundary conditions in terms of variables ξ_i and θ are the same for any D. Thus, the solution in terms of ξ_i and θ is independent of D as well as of k, and of c_1 (or of C_1), and depends only on the coefficients of Equation (7.105), i.e. on the functions $k(h)/k_1$ and $c(h)/c_1$ representing the relative variation of slope k and of permeability c. These functions are the same for any D. So, the time to reach the same stage of drying (e.g. the shrinkage half-time) is proportional to t/τ_S, i.e. to D^2/C_1. This property, which we used in setting up Equation (7.12) for τ_s, is generally known for a linear diffusion equation (constant k and c) and here we show that it is also true for the non-linear diffusion equation, provided that the self-desiccation and the age dependence of permeability and of the slope of the sorption diagram are neglected.

When the pore humidity falls below 0.9, the hydration process is nearly arrested. Thus, neglect of the age dependence is well justified for drying at low ambient humidity, such as 0.5, while it is a poor assumption for a high ambient humidity such as 0.9; but this case is of little practical interest. The neglect of aging causes a more severe error for thicker bodies (larger D) since pore humidity lingers above 0.9 for a longer time period. Thus, the deviations from a D^2 dependence of shrinkage half-time τ_s are stronger for thicker bodies. On the other hand, in thin bodies another phenomenon may spoil the D^2 dependence significantly; it is the cracking (and microcracking) produced by drying, which is more severe for a faster drying because the stresses produced by drying have less time to get relaxed by creep. At present little is known, however, how much the cracking affects permeability.[202] It certainly greatly affects shrinkage and all deformations.

A finite element model for the foregoing diffusion equation (Equation (7.89)) may be developed using the Galerkin procedure, as is well known; see Bažant and Thonguthai[48,49,32] and Figure 7.23.

7.6.5 Coupled moisture and heat transfer

Migration of moisture in concrete is produced not only by gradient of moisture concentration w (pore water content) but also by gradient of temperature. It seems that this effect, called thermal moisture transfer, is

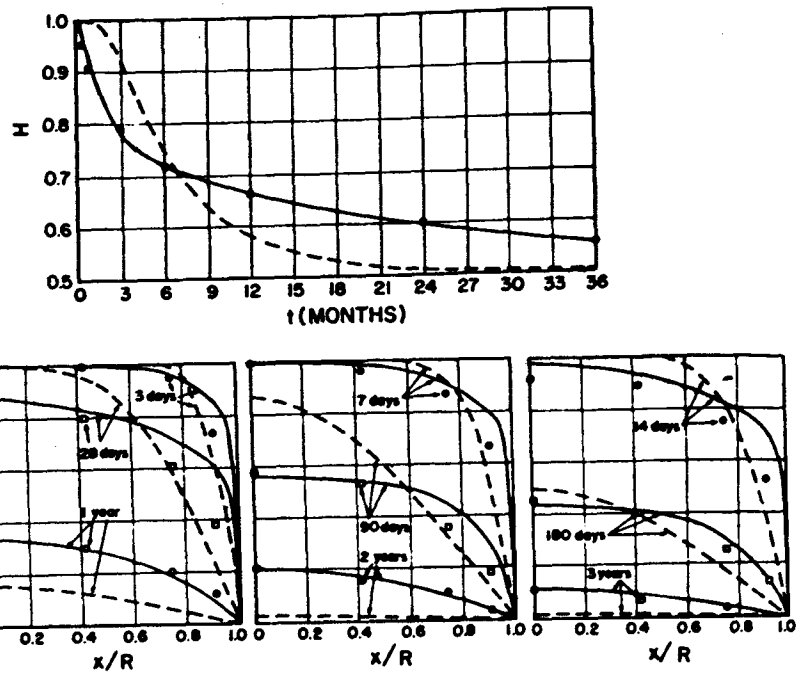

Figure 7.23 Typical measurements of pore humidity in solid cylinders exposed to drying environment. Test data from Hanson[95]. Solid lines, predictions of nonlinear diffusion theory; dashed lines, predictions of linear diffusion theory[37]

adequately modelled by considering that the driving force of the diffusion flux is not grad h or grad w but grad p where p is the vapour pressure in the pores.

Central to the model are realistic formulations for the moisture diffusivity (or permeability) and for the equation of state of the pore water (sorption isotherms). Both of these properties are rather involved. As already mentioned, the diffusivity at room temperature is found to decrease about twenty times as the pore humidity h decreases from 95% to 60%. Above 100 °C the diffusivity becomes independent of h (i.e. of pore pressure p), but another effect is observed (Figure 7.22): The permeability increases about 200 times as we increase the temperature from 90 °C to 120 °C. It seems that this effect may be explained by the enlargement of narrow necks on the flow passages in cement paste, and a transition to a flow that is controlled by viscosity of steam rather than migration of water molecules along adsorption layers which controls the diffusion at room temperature. These phenomena are illustrated in Figure 7.22.

In defining the equation of state, one must take into account the fact that the volume of pores decreases due to dehydration as concrete is heated beyond 100 °C, and that the pressure forces pore water into the microstructure, thereby enlarging the pore volume available to liquid water or vapour.

If these phenomena are taken into account, then the well-known thermodynamic properties of water can be used to calculate pore pressures and moisture transfer and obtain agreement with the scant available measurements. A finite element program, based on Galerkin approach, has been developed for this purpose.[48,49,32]

Due to the sharp rise of permeability, specimens heated over 100 °C lose moisture very rapidly. At room temperature one can almost never expect to deal with fully dried concrete specimens, but at high temperatures the dried condition is typical, except for massive walls as in reactor vessels.

Experimental information on creep and shrinkage under controlled moisture conditions is almost non-existent for high temperatures. Data exist nearly exclusively for uniaxial creep and shrinkage of specimens from which the evaporable water was driven out due to heating, and which probably suffered great non-uniform stresses and microcracking during the heating. Because above 100 °C the escape of water cannot be prevented without significant pressure on all specimen surfaces, triaxial tests are required if the moisture content should be controlled. In fact, uniaxial creep without moisture loss is a meaningless phenomenon above 100 °C, impossible to simulate experimentally.

7.7 DETAILS OF SOME MODELS

7.7.1 ACI model

The ultimate creep coefficient from Equation (7.13) is specified as follows:[5,61,58,59]

$$C_u = 2.35 K_t^c K_H^c K_T^c K_S^c K_F^c K_A^c \tag{7.108}$$

where K_t^c, K_H^c, K_T^c, K_S^c, K_F^c, and K_A^c are called creep correction factors. These factors equal 1.0 (i.e. $C_u = 2.35$) for the following standard conditions: 4 in. or less slump, 40% environmental relative humidity, minimum thickness of member 6 in. or less, loading age 7 days for moist cured concrete and 1–3 days for steam-cured concrete. For other than the standard conditions, one has

$$\begin{aligned}
K_t^c &= \begin{cases} 1.25 t'^{-0.118} & \text{for moist cured concrete} \\ 1.13 t'^{-0.095} & \text{for steam cured concrete} \end{cases} \\
K_H^c &= 1.27 - 0.0067 h_c \qquad h_c \geq 40\% \\
K_T^c &= \begin{cases} 1.14 - 0.023 T_m & \text{for } \leq 1 \text{ year loading} \\ 1.10 - 0.017 T_m & \text{for ultimate value} \end{cases} \\
K_S^c &= 0.82 + 0.067 S_c \qquad K_F^c = 0.88 + 0.0024 F_a \\
K_A^c &= \begin{cases} 1.00 & \text{for } A_c \leq 6\% \\ 0.46 + 0.090 A_c & \text{for } A_c > 6\% \end{cases}
\end{aligned} \tag{7.109}$$

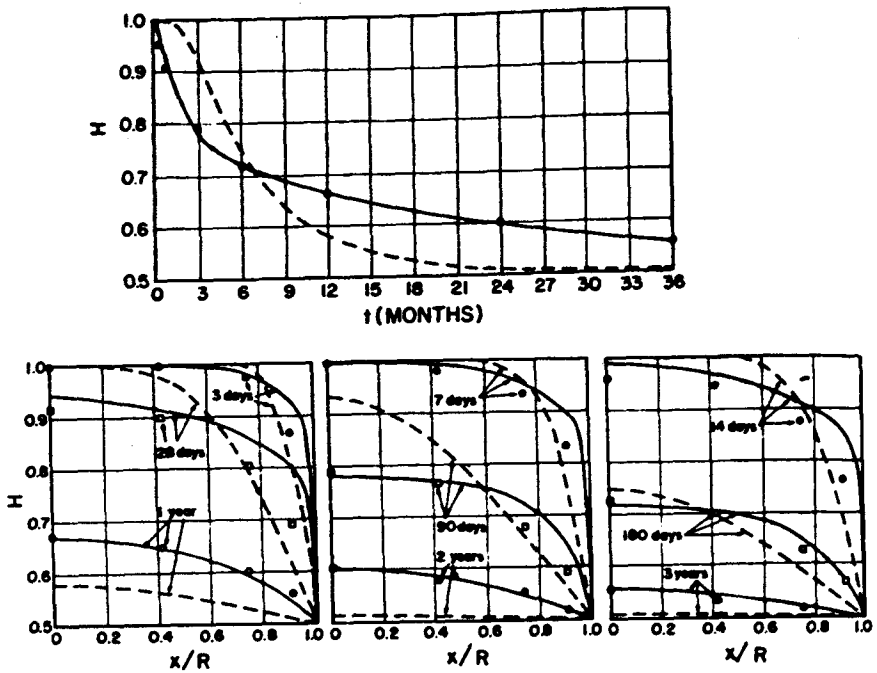

Figure 7.23 Typical measurements of pore humidity in solid cylinders exposed to drying environment. Test data from Hanson[95]. Solid lines, predictions of nonlinear diffusion theory; dashed lines, predictions of linear diffusion theory[37]

adequately modelled by considering that the driving force of the diffusion flux is not grad h or grad w but grad p where p is the vapour pressure in the pores.

Central to the model are realistic formulations for the moisture diffusivity (or permeability) and for the equation of state of the pore water (sorption isotherms). Both of these properties are rather involved. As already mentioned, the diffusivity at room temperature is found to decrease about twenty times as the pore humidity h decreases from 95% to 60%. Above 100 °C the diffusivity becomes independent of h (i.e. of pore pressure p), but another effect is observed (Figure 7.22): The permeability increases about 200 times as we increase the temperature from 90 °C to 120 °C. It seems that this effect may be explained by the enlargement of narrow necks on the flow passages in cement paste, and a transition to a flow that is controlled by viscosity of steam rather than migration of water molecules along adsorption layers which controls the diffusion at room temperature. These phenomena are illustrated in Figure 7.22.

In defining the equation of state, one must take into account the fact that the volume of pores decreases due to dehydration as concrete is heated beyond 100 °C, and that the pressure forces pore water into the microstructure, thereby enlarging the pore volume available to liquid water or vapour.

If these phenomena are taken into account, then the well-known thermodynamic properties of water can be used to calculate pore pressures and moisture transfer and obtain agreement with the scant available measurements. A finite element program, based on Galerkin approach, has been developed for this purpose.[48,49,32]

Due to the sharp rise of permeability, specimens heated over 100 °C lose moisture very rapidly. At room temperature one can almost never expect to deal with fully dried concrete specimens, but at high temperatures the dried condition is typical, except for massive walls as in reactor vessels.

Experimental information on creep and shrinkage under controlled moisture conditions is almost non-existent for high temperatures. Data exist nearly exclusively for uniaxial creep and shrinkage of specimens from which the evaporable water was driven out due to heating, and which probably suffered great non-uniform stresses and microcracking during the heating. Because above 100 °C the escape of water cannot be prevented without significant pressure on all specimen surfaces, triaxial tests are required if the moisture content should be controlled. In fact, uniaxial creep without moisture loss is a meaningless phenomenon above 100 °C, impossible to simulate experimentally.

7.7 DETAILS OF SOME MODELS

7.7.1 ACI model

The ultimate creep coefficient from Equation (7.13) is specified as follows:[5,61,58,59]

$$C_u = 2.35 K_t^c K_H^c K_T^c K_S^c K_F^c K_A^c \tag{7.108}$$

where K_t^c, K_H^c, K_T^c, K_S^c, K_F^c, and K_A^c are called creep correction factors. These factors equal 1.0 (i.e. $C_u = 2.35$) for the following standard conditions: 4 in. or less slump, 40% environmental relative humidity, minimum thickness of member 6 in. or less, loading age 7 days for moist cured concrete and 1–3 days for steam-cured concrete. For other than the standard conditions, one has

$$\begin{aligned}
K_t^c &= \begin{cases} 1.25 t'^{-0.118} & \text{for moist cured concrete} \\ 1.13 t'^{-0.095} & \text{for steam cured concrete} \end{cases} \\
K_H^c &= 1.27 - 0.0067 h_c \qquad h_c \geq 40\% \\
K_T^c &= \begin{cases} 1.14 - 0.023 T_m & \text{for } \leq 1 \text{ year loading} \\ 1.10 - 0.017 T_m & \text{for ultimate value} \end{cases} \\
K_S^c &= 0.82 + 0.067 S_c \qquad K_F^c = 0.88 + 0.0024 F_a \\
K_A^c &= \begin{cases} 1.00 & \text{for } A_c \leq 6\% \\ 0.46 + 0.090 A_c & \text{for } A_c > 6\% \end{cases}
\end{aligned} \tag{7.109}$$

where t' is the loading age in days, h_e is the environmental relative humidity in percent, T_m is the minimum thickness in inches, S_c is the slump in inches, F_a is the per cent of fine aggregate by weight, and A_c is the air content in per cent of volume of concrete. The initial deformation is defined by

$$E(t') = 33\sqrt{[\rho^3 f'_c(t')]} \qquad f'_c(t') = f'_{c28}\frac{t'}{4+0.85t'} \tag{7.110}$$

where ρ is the unit weight of concrete (normal-weight concretes only). The model is considered applicable only for ages at loading $t' \geq 7$ days.

The ultimate shrinkage coefficient ε^s_u is specified as follows:

$$\varepsilon^s_u = \begin{cases} 0.000800 K^s_H K^s_T K^s_S K^s_B K^s_F K^s_A & \text{for moist cured concrete,} \\ 0.000730 K^s_H K^s_T K^s_S K^s_B K^s_F K^s_A & \text{for steam cured concrete} \end{cases} \tag{7.111}$$

where K^s_H, K^s_T, K^s_S, K^s_B, K^s_F, and K^s_A are shrinkage correction factors. They equal 1.0 for the following standard conditions: 4 in. or less slump, 40% environmental relative humidity, and the minimum thickness of member 6 in. or less. For other than standard conditions the following shrinkage correction factors are used:

$$K^s_H = \begin{cases} 1.40 - 0.010 h_e & 40\% \leq h_e \leq 80\% \\ 3.00 - 0.030 h_e & 80\% \leq h_e \leq 100\% \end{cases}$$

$$K^s_T = \begin{cases} 1.23 - 0.038 T_m & \text{for } \leq 1 \text{ year loading} \\ 1.17 - 0.029 T_m & \text{for ultimate value} \end{cases}$$

$$K^s_S = 0.89 + 0.041 S_c \qquad K^s_B = 0.75 + 0.034 B_s \tag{7.112}$$

$$K^s_F = \begin{cases} 0.30 + 0.0140 F_a & \text{for } F_a \leq 50\% \\ 0.90 + 0.0020 F_a & \text{for } F_a \geq 50\% \end{cases}$$

$$K^s_A = 0.95 + 0.0080 A_c$$

where B_s is the number of 94-lb sacks of cement per cubic yard of concrete. For f_c and t_0, the following values are recommended: $f_c = 35$ days; $t_0 = 7$ days for moist cured concrete; and $f_c = 55$ days; $t_0 = 1$ to 3 days for steam-cured concrete.

As $T_m \to 0$ the factor K^c_T should approach 0.6 because an infinitely thick specimen is equivalent to concrete at pore humidity nearly 100%. Since Equation (7.109) for K^c_T does not satisfy this condition, the ACI Model cannot be applicable for very thick specimens.

7.7.2 CEB-FIP model

The functions and coefficients in Equations (7.14) and (7.15)[68,162] are specified as

$$\varepsilon_{s_0} = \varepsilon_{s_1}\varepsilon_{s_2} \qquad \phi_d = 0.4 \qquad \phi_f = \phi_{f_1}\phi_{f_2}$$

$$F_i(t') = \frac{1}{E_c(t')} + \frac{\beta_s(t')}{E_{c28}} \qquad \beta_s(t') = 0.8\left(1 - \frac{f'_c(t')}{f'_{c_\infty}}\right) \tag{7.113}$$

$$E_c(t') = 1.25 E_{c_\infty}(t') \qquad E_{c_\infty}(t') = 9500[f'_{c_\infty}(t')]^{1/3} \qquad E_{c28} = 9500 f'^{1/3}_c \tag{7.114}$$

Here strain ε_{s_1} is defined by Table 0.1, column 4, of CEB-FIP 'Model Code for Concrete Structures'[68] as a function of humidity h_e; ε_{s_2} is defined by a graph in Figure e.5 as a function of the effective thickness defined as $H_0 = \lambda(2A_c/U)$, A_c/U is the ratio of cross-sectional area to the exposed surface; λ is a function of h_e defined by Table e.1; $\beta_s(t')$ is a function of age t defined by six graphs in Figure e.6 for various values of effective thickness H_0. Furthermore, age t is corrected for temperature in Section e.5 of CEB-FIP, 'Model Code for Concrete Structures',[68] but the acceleration of creep due to temperature rise is not considered. Quantities f'_{c_∞}, E_{c_∞}, and E_c must all be given in MPa. The strength f'_c is given by a graph in Figure e.1 of CEB-FIP Model Code[68] as a function of t'; ϕ_{f_1} is given in Table e.1 of CEB-FIP Model Code[68] as a function of humidity h_e; ϕ_{f_2} is given by a graph in Figure e.2 of CEB-FIP Model Code[68] as a function of effective thickness H_0; β_d is defined by a graph in Figure e.3 of CEB-FIP Model Code[68] as a function of stress duration $t - t'$, β_f is given by six graphs in Figure e.4 for various effective thicknesses H_0 (Table 2.3 of CEB-FIP Model Code[68]) as a function of age t (corrected for temperature).

Note that in contrast to ACI and BP Models, the CEB-FIP Model is not defined completely by formulae. Graphs consisting of sixteen curves are used to define the functions.

7.7.3 BP model

The complete definition of this model[42-44] is as follows.

The shrinkage is described by:

$$\varepsilon_{sh}(\hat{t}, t_0) = \varepsilon_{sh_\infty} k_h S(\tilde{t}) \qquad \hat{t} = t - t_0$$

$$S(\hat{t}) = \left(\frac{\hat{t}}{\tau_{sh} + \hat{t}}\right)^{1/2} \qquad \tau_{sh} = 600\left(\frac{k_s}{150} D\right)^2 \frac{10}{C_1(t_0)} \qquad D = 2\frac{v}{s} \tag{7.115}$$

For

$$h \leq 0.98\text{: } k_h = 1 - h^3; \quad \text{for } h = 1.00\text{: } k_h = -0.2$$

$$C_1(t) = C_7 k'_T[0.05 + \sqrt{(6.3/t)}] \qquad \varepsilon_{sh_\infty} = \varepsilon_{s_\infty} \frac{E(7+600)}{E(t_0+\tau_{sh})} \tag{7.115}$$

$$k'_T = \frac{T}{T_0} \exp\left(\frac{5000}{T_0} - \frac{5000}{T}\right)$$

in which D is an effective thickness of cross section (in mm), v/s is the volume-to-surface ratio, $E(t') = 1/J(t'+0.1, t')$ is the conventional elastic modulus, $T_0 = 23\,^\circ\text{C}$ = reference temperature, $C_1(t)$ is drying diffusivity at age t (in mm^2/day), C_7 is a given or assumed value C_1 at age 7 days, k_S is the shape factor (= 1.0 for an infiite slab, 1.15 for an infinite cylinder, 1.25 for an infinite square prism, 1.30 for a sphere and 1.55 for a cube). Equations (9)–(10) of Bažant and Panula[43] give the coefficients ε_{s_∞} and C_7 as functions of strength f'_c, water/cement ratio w/c, cement content c, aggregate/cement ratio a/c, and sand/cement ratio s/c. If, however, at least one measured value of shrinkage on a small specimen is available, either ε_{s_∞} or C_7 may better be evaluated from this value, which improves the accuracy of prediction.

To take moisture effects into account, the BP Model distinguishes three long-time components of the creep function:

$$J(t, t') = \frac{1}{E_0} + C_0(t, t') + \bar{C}_d(t, t', t_0) - C_p(t, t', t_0) \tag{7.116}$$

in which $C_0(t, t')$ gives the basic creep, i.e. the creep in the absence of moisture exchange; $\bar{C}_d(t, t', t_0)$ gives the increases of creep due to simultaneous moisture exchange, in particular drying that proceeds simultaneously with creep; and $C_p(t, t', t_0)$ gives the decrease of creep due to pre-drying; this decrease occurs long after the drying process reaches the final, stable state. Time t_0 is the age at the time the exposure to a drying environment begins. Term $C_p(t, t', t_0)$ is negligible and may be omitted except when the cross section of concrete is very thin ($\leq$10 cm) or the temperature is elevated. E_0 represents the asymptotic modulus which gives the asymptotic value of the deformation extrapolated to extremely short load durations (less than a microsecond, beyond the range of interest).

The basic creep is given by the double power law:

$$C_0(t, t') = \frac{\phi_T}{E_0}(t_e'^{-m} + \alpha)(t - t')^{n_T} \tag{7.117}$$

in which $t'_e = \int \beta_T(t')\,dt'$, $\phi_T = \phi_1 C_T$, $n_T = n\beta_T$. Here C_T and β_T introduce the effect of temperature T and may be taken as 1.0 when $T = T_0 \simeq 23\,^\circ\text{C}$ = reference temperature; then $t'_e = t'$, $\phi_T = \phi_1$, $n_T = n$. Coefficients ϕ_1, n, m, and α characterize the basic creep at reference temperature from

load durations of $t - t' = 10^{-7}$ day (dynamic range) through the short-time static load range (about 0.1 day) until at least 30 years. These coefficients as well as E_0 may be evaluated from Equations (15)–(19) of Bažant and Panula[43] as functions of standard cylinder strength f'_c, water/cement ratio w/c, aggregate/cement ratio a/c, aggregate/gravel ratio s/g, unit mass of concrete ρ, and the type of cement. Coefficients β_T, C_T, and n_T are defined by Equations (36)–(39) from Bažant and Panula[43] as functions of temperature T, of age t'_T at which this temperature begins, and of w/c, a/c, and the cement type.

The creep increase during drying and the creep decrease after drying are given in the BP Model as:

$$\bar{C}_d(t, t', t_0) = \frac{\phi'_d}{E_0} t_e'^{-m/2} k'_h \varepsilon_{sh_\infty} S_d(t, t')$$
$$C_p(t, t', t_0) = \varepsilon_p k''_h S_p(t, t_0) C_0(t, t') \tag{7.118}$$

where

$$\phi'_d = \left(1 + \frac{\Delta\tau'}{10}\right)^{-1/2} \phi_d \qquad k'_h = 1 - h^{1.5} \qquad k''_h = 1 - h^2$$

$$S_d(t, t') = \left(1 + \frac{10\tau_{sh}(k'_T)^{1/4}}{t - t'}\right)^{-n'} \qquad S_p(t, t_0) = \left(1 + \frac{100}{\Delta\tau}\right)^{-n}$$

$$\Delta\tau' = \int_{t_0}^{t'} \frac{(\cdots_T)^{5/4}}{\tau_{sh}} dt \qquad \Delta\tau = \int_{t_0}^{t} \frac{dt}{\tau_{sh}} \tag{7.119}$$

$$n' = \frac{c_d^n}{K_T^2} \qquad k_T = 0.42 + 17.6\left[1 + \left(\frac{100}{\hat{T}}\right)^4\right]^{-1}$$

$$K_T = 1 + 0.4\left[1 + \left(\frac{93.5}{\hat{T}}\right)^4\right]^{-1}$$

Here h is the relative humidity of the environment. In the integrals, τ_{sh} must be evaluated for the given temperature as a function of time. When $T = T_0$, we have $k'_T = K_T = 1.0$. The material parameters C_p; C_d, and ϕ_d are functions of n, ε_{s_∞}, f'_c and of mix ratios s/a, g/s, and w/c as indicated by Equations (30)–(32) from Bažant and Panula.[43]

A relatively simple refinement allows one to obtain cyclic creep, i.e. creep when a cyclic load is superimposed on a static load.[43]

The composition effects in shrinkage are given by:

$$C_7 = \frac{c}{8}\frac{w}{c} - 12; \quad \text{for } C_7 < 7 \text{ set } C_7 = 7, \text{ for } C_7 > 21 \text{ set } C_7 = 21$$

$$\varepsilon_{s_\infty} = (1.21 - 0.88y)10^{-3} \qquad y = (390z^{-4} + 1)^{-1} \tag{7.120}$$

$$z = \left[1.25\left(\frac{a}{c}\right)^{1/2} + \frac{1}{2}\left(\frac{g}{s}\right)^2\right]\left(\frac{1 + s/c}{w/c}\right)^{1/3} (f'_c)^{1/2} - 12 \quad \text{if } z \geq 0\text{; else } z = 0$$

in which f'_c is the 28-day cylindrical strength in ksi ($= 1000$ psi $= 6.89$ MN/m^2); w, c, a = contents (masses) of water, cement and aggregate, kg/m^3 of concrete; $a = g + s$ where g, s are the masses of gravel and sand.

The composition effects in basic creep at reference temperature are:

$$\phi_1 = \frac{10^{3n}}{2(28^{-m}+\alpha)} \qquad \alpha = \frac{0.025}{w/c} \qquad m = 0.28 + f_c'^{-2}$$

$$n = \begin{cases} 0.12 + 0.07(1 + 5130x^{-6})^{-1} & \text{for } x > 4 \\ 0.12 & \text{for } x \leq 4 \end{cases} \tag{7.121}$$

$$x = [2.1(a/c)(s/c)^{-1.4} + 0.1(f'_c)^{1.5}(w/c)^{1/3}(a/g)^{2.2}]a_1$$

$$a_1 = \begin{cases} 1 & \text{for cement types I and II} \\ 0.93 & \text{for type III} \\ 1.05 & \text{for type IV} \end{cases}$$

When a measured value E of conventional elastic modulus is known, one substitutes $1/E = J(t' + 0.1, t')$ into Equation (7.116) for $T = T_0$ and solves for E_0. The same is done when any value of $J(t, t')$ is known. When there is no drying and E pertains to age 28 days, one simply has $E_0 = 1.5E$. When no measured value is known, one may use:

$$\frac{1}{E_0} = 0.09 + \frac{1}{1.7z_1^2} \qquad z_1 = 0.00005\rho^2 f'_c \tag{7.122}$$

The coefficients for the temperature effect in basic creep are:

$$\beta_T = \exp\left(\frac{4000}{T_0} - \frac{4000}{T}\right) \qquad C_T = c_T \tau_T c_0 \qquad c_0 = \frac{1}{8}\cdot\left(\frac{w}{c}\right)^2\left(\frac{a}{c}\right)a_1$$

$$c_T = \frac{19.4}{1 + (100/\hat{T})^{3.5}} - 1 \qquad \tau_T = \frac{1}{1 + 60(t'_T)^{-0.69}} + 0.78 \tag{7.123}$$

$$n_T = B_T n \qquad B_T = \frac{0.25}{1 + (74/\hat{T})^7} + 1 \qquad \hat{T} = T - 253.2.$$

Here f' and E must be in ksi, T in degrees Kelvin, $\hat{T}$ in degrees Celsius. The composition effects for drying creep are estimated as follows:

$$c_p = 0.83 \quad c_d = 2.8 - 7.5n$$

$$\text{For } r > 0\text{: } \phi_d = 0.008 + 0.027u \qquad u = \frac{1}{1 + 0.7r^{-1.4}}$$

$$r = 56000\left(\frac{s}{a}f'_c\right)^{0.3}\left(\frac{g}{s}\right)^{1.3}\left(\frac{w/c}{\varepsilon_{s_\infty}}\right)^{1.5} - 0.85; \tag{7.124}$$

$$\text{for } r \leq 0\text{: } \phi_d = 0.008.$$

A simplified version of the BP Model can be found in Bažant and Panula.[45]

7.7.4 Material characterization for a general purpose program

Different characterizations of creep and shrinkage may be appropriate in various situations. For the input of material properties, the following scheme, used in one recent finite element program[46] and listed in full in Ref. 199, may be provided for the input of material properties.

The data input subroutine, MATPAR,[199] has the following options:

(1) $J(t, t')$ is specified as an array of values. No drying.
(2) $\bar{J}(t, t')$ and $\varepsilon_s(t, t_0)$ are specified as an array. Drying.
(3) $J(t, t')$ is given by double power law, for which all parameters are given, no drying.
(4) Same as (3) but all double power law parameters except $E_{c_{28}}$ are generated from the given strength and composition parameters.
(5) Same as (4) except that $E_{c_{28}}$ is also predicted from the strength and composition parameters.
(6) $J(t, t')$ is defined by the double power law plus drying term $C_d(t, t')$, and shrinkage is given by a formula. All parameters are given.
(7) Same as (6) but all parameters except $E_{c_{28}}$ and ε_{sh_∞} are predicted from the strength and composition.
(8) Same as (6) but all parameters except $E_{c_{28}}$ are predicted from the strength and composition.
(9) Same as (6) but all parameters are predicted from the strength and composition.
(10) The double power law parameters E_0 and ϕ_1 are determined by the best fit of the given array of values $J(t, t')$ which may be of limited range; m, n, α are given. No drying. Coefficient of variation for the deviations from given $J(t, t')$ is computed and printed.
(11) Same as (10) but m, n, α are predicted from given strength and composition.
(12) Same as (10) but drying is included.
(13) Same as (11) but drying is included.

The subroutine for evaluating the compliance function, COMPLF, has the following options:[199]

(1) $J(t, t')$ is evaluated by interpolation or extrapolation from a given array of values.
(2) $J(t, t')$ is evaluated from a formula without the drying term.
(3) $J(t, t')$ is evaluated from a formula with the drying term.

Subroutine for Dirichlet series expansion,[199] DIREX

The coefficients $\hat{E}_\mu(t')$ of Dirichlet series expansion of $J(t, t')$ or $R(t, t')$ at various discrete times are automatically generated from $J(t, t')$. Then, as a check, the values of $J(t, t')$ are calculated from the Dirichlet series expansion of $J(t, t')$ or $R(t, t')$, and the coefficient of variation of their deviations from the originally given $J(t, t')$ is computed and printed.

In case that Dirichlet series expansion of $R(t, t')$ is used, this subroutine[199] consists of subroutine RELAX that computes the discrete values of $R(t, t')$ from $J(t, t')$, subroutine MAXW that computes the discrete values of the moduli $E_\mu(t')$ of the Maxwell chain, and subroutine CRCURV that computes for a check the discrete values of the creep curves back from the discrete values of $E_\mu(t')$ and evaluates the coefficient of variation of deviations.

The subroutine for shrinkage function, SHRF, has the options:

(1) $\bar{\varepsilon}_S(t, t_0)$ is evaluated by interpolation or extrapolation from given array of values.
(2) $\bar{\varepsilon}_S(t, t_0)$ is evaluated from a formula.

Subroutine for Dirichlet series coefficients or Maxwell chain moduli $E_\mu(t')$

These coefficients at any time are evaluated by interpolation from the values of E_μ at certain discrete times.

7.7.5 Proof of age-adjusted effective modulus method[23]

Assume that the strain in excess of the shrinkage strain $\varepsilon^0(t)$ varies linearly with $J(t, t_0)$. This means that it also varies linearly with $\phi(t, t_0)$, i.e.

$$\varepsilon(t)-\varepsilon^0(t)=\varepsilon_0+c\phi(t, t_0) \quad (\text{for } t>t_0) \tag{7.125}$$

and $\varepsilon(t)-\varepsilon^0(t)=0$ for $t<t_0$. Substituting $\phi(t, t_0)=E(t_0)J(t, t_0)-1$, and noting that, by definition, $J(t, t_0)=\mathbf{E}^{-1}H(t-t_0)$ where $\mathbf{E}^{-1}$ = creep operator such that Equation (7.16) has the form $\varepsilon(t)=\mathbf{E}^{-1}\sigma(t)+\varepsilon^0(t)$, and $H(t-t_0)$ = Heaviside step function (= 1 for $t>t_0$, 0 for $t<t_0$), Equation (7.125) may be rewritten as

$$\varepsilon(t)-\varepsilon^0(t)=(\varepsilon_0-c)H(t-t_0)+cE(t_0)\mathbf{E}^{-1}H(t-t_0) \tag{7.126}$$

Observing that

$$\mathbf{E}H(t-t_0)=R(t, t_0), \qquad \mathbf{E}\mathbf{E}^{-1}H(t-t_0)=H(t-t_0) \tag{7.127}$$

where $\mathbf{E}$ = relaxation operator such that Equation (7.19) has the form $\sigma(t)=\mathbf{E}[\varepsilon(t)-\varepsilon^0(t)]$, we may apply operator $\mathbf{E}$ to both sides of Equation (7.126). This yields

$$\sigma(t)=(\varepsilon_0-c)R(t, t_0)+cE(t_0) \tag{7.128}$$

We conclude that if the strain varies linearly with $J(t, t_0)$ or $\phi(t, t_0)$, then the stress varies linearly with $R(t, t_0)$.

Denote now

$$\Delta\sigma(t)=\sigma(t)-\sigma(t_0), \qquad \Delta\varepsilon(t)=\varepsilon(t)-\varepsilon(t_0), \qquad \Delta\varepsilon^0(t)=\varepsilon^0(t)-\varepsilon^0(t_0) \tag{7.129}$$

Substituting this and the relations

$$\varepsilon_0=\frac{\sigma(t_0)}{E(t_0)}+\varepsilon^0(t_0), \qquad c=\frac{\Delta\varepsilon(t)-\Delta\varepsilon^0(t)}{\phi(t, t_0)} \tag{7.130}$$

into Equation (7.128), we obtain

$$\sigma(t_0)+\Delta\sigma(t)=\left[\frac{\sigma(t_0)}{E(t_0)}+\varepsilon^0(t_0)\right]R(t, t_0)+[E(t_0)-R(t, t_0)]\frac{\Delta\varepsilon(t)-\Delta\varepsilon^0(t)}{\phi(t, t_0)} \tag{7.131}$$

or

$$\Delta\sigma=\frac{E(t_0)-R(t, t_0)}{\phi(t, t_0)}(\Delta\varepsilon-\Delta\varepsilon^0-\Delta\varepsilon'') \quad \text{with } \Delta\varepsilon''=\frac{\sigma(t_0)}{E(t_0)}\phi(t, t_0) \tag{7.132}$$

This is identical to Equations (7.28)–(7.29), which completes the proof.[23]

7.7.6 Sign of $\partial^2 J/\partial t\,\partial t'$ for Maxwell chain

The fact that for Maxwell chain model the sign of this mixed derivative is not restricted to be positive (Section 7.5.1) was proven by Bažant and Kim.[33] A shorter proof may be given as follows. We consider a strain history $\varepsilon(t)$ that starts with a jump at t' and is smooth afterwards. Equation (7.19) may then be written as

$$R(t, t')\varepsilon(t')+\int_{t'+}^{t} R(t, \tau)\frac{d\varepsilon(\tau)}{d\tau}d\tau=\sigma(t) \tag{7.133}$$

In particular we consider that $\varepsilon(t)=J(t, t')$, in which case $\sigma=1$ for $t>t'$. Equation (7.133) then becomes

$$\frac{R(t, t')}{E(t')}+\int_{t'+}^{t} R(t, \tau)\frac{\partial J(\tau, t')}{\partial\tau}d\tau=1 \tag{7.134}$$

where $E(t')=R(t', t')$. Now we substitute Equation (7.40) for $R(t, t')$ according to the Maxwell chain model, and we get

$$\frac{1}{E(t')}\sum_{\mu} E_{\mu}(t') \exp\left[y_{\mu}(t')-y_{\mu}(t)\right]+\int_{t'+}^{t} \sum_{\mu} E_{\mu}(\tau) \times \exp\left[y_{\mu}(\tau)-y_{\mu}(t)\right]\frac{\partial J(\tau, t')}{\partial \tau}\,d\tau = 1 \quad (7.135)$$

where $E(t')=\sum_{\mu} E_{\mu}(t')$. Differentiating this first with respect to t we get rid of the integral, and differentiating again with respect to t' we obtain

$$\frac{\partial^2 J(t, t')}{\partial t\, \partial t'}=\frac{1}{\sum_{\mu} E_{\mu}(t)}\sum_{\mu} \dot{y}_{\mu}(t) \exp\left[-y_{\mu}(t)\right]\frac{d}{dt'}\left(\frac{E_{\mu}(t')}{\sum_{\mu} E_{\mu}(t')} \exp\left[y_{\mu}(t')\right]\right) \quad (7.136)$$

Here $E_{\mu}(t')$ and $y_{\mu}(t')$ are increasing functions, but because of the increasing sum $\sum_{\mu} E_{\mu}(t')$ in the denominator, there is no reason for this expression to be always non-negative.

7.8 SUMMARY AND CONCLUSIONS

The greatest uncertainty in the analysis of creep and shrinkage effects in concrete structures stems from material characterization, both the numerical values of material parameters defining creep and shrinkage and the form of the constitutive relations. The determination of creep at constant stress is described first and various practical prediction models are given. For the case of exposed concrete subjected to drying, the existing models do not specify material properties but the mean compliance function and the mean shrinkage of the entire drying cross section. Such material characteristics allow determining the mean forces and deformations in the cross sections of beams, frames, plates or shells but not the stresses and strains at various points of the cross section.

As for the constitutive relations applicable at arbitrarily variable stress, only the linear theory based on the principle of superposition is well developed. Various forms of the integral-type constitutive relations, based on the compliance function, the impulse memory function, the relaxation function, and their multiaxial forms are outlined. Subsequently, step-by-step-algorithms based on approximating the history integral by a finite sum are presented. Finally, a simple method called the age-adjusted effective modulus method, which allows an easy approximate determination of creep and shrinkage effects by means of a single elastic finite element analysis, is indicated.

For the analysis of large structural systems it is necessary to avoid history integrals and use an equivalent rate-type formulation. Such a formulation is generally obtained by expanding the compliance function or the relaxation function into a series of real exponentials, called a Dirichlet series. This representation is equivalent to assuming an age-dependent Kelvin or Maxwell chain model. The rate-type formulation also allows a simple extension to variable temperature, in which the activation energy concept is used to model both the acceleration of creep rate due to heating and the acceleration of aging (hydration) which offsets the increase in creep rate. Special step-by-step algorithms, called exponential algorithms, are required to allow an unrestricted increase of the time step as the rate of change of stresses and strains declines with the passage of time.

Most of the discrepancies between measurements and linear theory applications can be traced back to various non-linear effects. First, the phenomenon of aging in the context of linear constitutive relations leads to certain violations of thermodynamic restrictions relative to the dissipation of energy in the chemical hydration process. It seems that such violations cannot be avoided without passing to a non-linear theory. The main non-linear phenomena in creep are the flow, which consists in an increase of creep well beyond proportionality as the stress approaches the strength limit, and the adaptation or stiffening non-linearity, which describes the stiffening of the material due to previous sustained compression. A proper model for cracking and tensile non-linear behaviour is also an important ingredient of a finite element program if realistic results should be obtained.

The most complicated aspect of concrete creep is the moisture effect. The pore humidity as well as temperature affect the rate of aging (hydration). Shrinkage, when considered as a constitutive (material) property rather than a cross-section mean property, is not a function of time but a function of pore humidity or specific water content. Regarding the constitutive relations for creep at the presence of drying, it is not clear at present whether the acceleration of creep observed at drying is due mainly to microcracking and tensile non-linear behaviour, or whether some intrinsic mechanism on the microscale, such as, for example, the diffusion of moisture (water) between gel micropores and capillary macropores, causes a significant increase of creep rate. Calculation of creep and shrinkage effects requires, of course, numerical determination of pore humidity distributions at various times. For this purpose a non-linear diffusion model, which agrees with experiments relatively well, is available. When both water content and temperature vary in time and space, a coupled moisture and heat transfer must be considered.

Overall, it may be concluded that the theory of creep and shrinkage has seen a tremendous progress during the last decade. However, a number of important questions are still open and much further research, which is likely to lead to many revisions in the foregoing presentation, will have to be carried out.

ACKNOWLEDGEMENT

Financial support by the US National Science Foundation provided through Grant No. CME-8009050 to Northwestern University is gratefully acknowledged.

REFERENCES

1. Aleksandrovskii, S. V. (1966). *Analysis of Plain and Reinforced Concrete Structures for Temperature and Moisture Effects with Account of Creep*, (in Russian), Stroyizdat, Moscow, 443 pp.
2. Aleksandrovskii, S. V., and Kolensnikov, N. S. (1971), 'Non-linear creep of concrete at step-wise varying stress' (in Russian), *Beton i Zhelezobeton*, **16,** 24–7.
3. Aleksandrovskii, S. V., and Popkova, O. M. (1970), 'Nonlinear creep strains of concrete at complex load histories' (in Russian), *Beton i Zhelezobeton*, **16,** 27–32.
4. Ali, J., and Kesler, C. E. (1963), 'Creep in concrete with and without exchange of moisture with the environment', *Univ. Illinois, Urbana, Dept Theor. Appl. Mech., Rep. No.* 641.
5. American Concrete Institute Comm. 209, Subcomm. II (1971), 'Prediction of creep, shrinkage and temperature effects in concrete structures', in *Designing for Effects of Creep, Shrinkage and Temperature, Am. Concr. Inst. Spec. Publ.* No. 27.
6. Anderson, C. A. (1980), 'Numerical creep analysis of structures', *Los Alamos Scientific Laboratory Rep.* LA-UR-80-2585, 1980, also in Z. P. Bažant and F. H. Wittman (Eds) *Creep and Shrinkage in Concrete Structures*, Wiley, London, pp. 259–303.
7. Argyris, J. H., Pister, K. S., Szimmat, J., and Willam, K. J. (1977), 'Unified concepts of constitutive modelling and numerical solution methods for concrete creep problems', *Comput. Meth. Appl. Mech. Eng.*, **10,** 199–246.
8. Argyris, J. H., Vaz, L. E., and Willam, K. J. (1978), 'Improved solution methods for inelastic rate problems', *Comput. Meth. Appl. Mech. Eng.*, **16,** 231–277.
9. Arthanari, S., and Yu, C. W. (1967), 'Creep of concrete under uniaxial and biaxial stresses at elevated temperatures', *Mag. Concr. Res.*, **19,** 149–56.
10. Arutyunian, N. Kh. (1952), *Some Problems in the Theory of Creep* (in Russian), Techteorizdat, Moscow; Engl. Transl. Pergamon Press (1966).
11. Bažant, Z. P., (1962), *Theory of Creep and Shrinkage of Concrete in Nonhomogeneous Structures and Cross Sections* (in Czech), Stavebnícky Časopis SAV **10,** pp. 552–76.
12. Bažant, Z. P. (1964), 'Die Berechnung des Kriechens und Schwindens Nichtomogener Betonkonstruktionen', *Proc. 7th Congr., Int. Assoc. for Bridge and Struct. Eng., Rio de Janeiro*, pp. 887–96.
13. Bažant, Z. P. (1966a), *Creep of Concrete in Structural Analysis* (in Czech), State Publishers of Technical Literature SNTL, Prague.
14. Bažant, Z. P. (1966b), 'Phenomenological theories for creep of concrete based on rheological models', *Acta Technica ČSAV, Prague*, **11,** 82–109.
15. Bažant, Z. P. (1968), 'Langzeitige Durchbiegungen von Spannbetonbrücken infolge des Schwingkriechens unter Verkehrslasten', *Beton und Stahlbetonbau* **63,** 282–5.

16. Bažant, Z. P. (1970a), 'Constitutive equation for concrete creep and shrinkage based on thermodynamics of multiphase systems', *Materials and Structures* (RILEM, Paris), **3,** 3–36; see also Rep. 68/1, Dept Civ. Eng., University of Toronto (1968).
17. Bažant, Z. P. (1970b), 'Delayed thermal dilatations of cement paste and concrete due to mass transport', *Nucl Eng. Des.*, **14,** 308–18.
18. Bažant, Z. P. (1970c), 'Numerical analysis of creep of an indeterminate composite beam', *J. Appl. Mech., ASME*, **37,** 1161–4.
19. Bažant, Z. P. (1971a), 'Numerical analysis of creep of reinforced plates', *Acta Technica Hung.*, **70,** 415–8.
20. Bažant, Z. P. (1971b), 'Numerical solution of non-linear creep problems with application to plates', *Int. J. Solids Struct.*, **7,** 83–97.
21. Bažant, Z. P. (1971c), 'Numerically stable algorithm with increasing time steps for integral-type aging creep', *Proc. 1st Int. Conf. on Structural Mechanics in Reactor Technology, West Berlin*, Vol. 3, Paper H2/3.
22. Bažant, Z. P. (1972a), 'Numerical determination of long-range stress history from strain history in concrete', *Materials and Structures* RILEM, Paris, **5,** 135–41.
23. Bažant, Z. P. (1972b), 'Prediction of concrete creep effects using age-adjusted effective modulus method', *Am. Concr. Inst. J.*, **19,** 212–7.
24. Bažant, Z. P. (1972c), 'Thermodynamics of interacting continua with surfaces and créep analysis of concrete structures', *Nucl. Eng. Des.*, **20,** 477–505; see also *Cem. Concr. Res.*, **2,** 1–16.
25. Bažant, Z. P. (1975), 'Theory of creep and shrinkage in concrete structures: a précis of recent developments', *Mech. Today*, **2,** 1–93.
26. Bažant, Z. P. (1977), 'Viscoelasticity of porous solidifying material—concrete', *J. Eng. Mech. Div. ASCE*, **102,** 1049–67.
27. Bažant, Z. P. (1979), 'Thermodynamics of solidifying or melting viscoelastic material', *J. Eng. Mech. Div. ASCE*, **105,** 933–52.
28. Bažant, Z. P., and Asghari, A. (1974), 'Computation of age-dependent relaxation spectra', *Cem. Concr. Res.*, **4,** 567–79; see also 'Computation of Kelvin-chain retardation spectra', *Cem. Concr. Res.*, **4,** 797–806.
29. Bažant, Z. P., and Asghari, A. A. (1977), 'Constitutive law for non-linear creep of concrete', *J. Eng. Mech. Div. ASCE*, **103,** No. EM1, Proc. Paper 12729, 113–24.
30. Bažant, Z. P., Carreira, D. J., and Walser, A. (1975), 'Creep and shrinkage in reactor containment shells', *J. Struct. Div. ASCE*, **202** No. ST10, Proc. Paper 11632, 2117–31.
31. Bažant, Z. P., and Chern, J. C. (1982), 'Comment on the use of Ross' hyperbola and recent comparisons of various practical creep prediction models', *Cem. Concr. Res.*, **12,** 527–532.
32. Bažant, Z. P., Chern, J. C., and Thonguthai, W. (1981), 'Finite element program for moisture and heat transfer in heated concrete', *Nucl. Eng. Des.*, **68,** 61–70.
33. Bažant, Z. P., and Kim, S. S. (1978), 'Can the creep curves for different ages at loading diverge?', *Cem. Concr. Res.*, **8,** No. 5, 601–12.
34. Bažant, Z. P., and Kim, S. S. (1979a), 'Approximate relaxation function for concrete', *J. Struct. Div. ASCE*, **105,** ST12, 2695–705.
35. Bažant, Z. P., and Kim, S. S. (1979b), 'Nonlinear creep of concrete—adaptation and flow', *J. Eng. Mech. Div.*, **105,** EM3, 419–46.
36. Bažant, Z. P., Kim. S. S., and Meiri, S. (1979), 'Triaxial moisture-controlled

creep tests of hardened cement paste at high temperature', *Materials and Structures* (RILEM, Paris), **12,** 447–56.
37. Bažant, Z. P., and Najjar, L. J. (1972), 'Nonlinear water diffusion in nonsaturated concrete', *Materials and Structures*, (RILEM, Paris) **5,** 3–20.
38. Bažant, Z. P., and Najjar, L. J. (1973), 'Comparison of approximate linear methods for concrete creep', *J. Struct. Div. ASCE*, **99,** 1851–74.
39. Bažant, Z. P., and Oh, B. (1980), 'Strain-rate effect in rapid nonlinear triaxial deformation of concrete', *Struct. Eng. Rep. No.* 80–8/640s, *Northwestern University, Evanston, Ill.*; also *J. Eng. Mech. Div. ASCE*, **108,** Nov. 1982.
40. Bažant, Z. P., and Osman, E. (1975), 'On the choice of creep function for standard recommendations on practical analysis of structures', *Cem. Concr. Res.*, **5,** 631–41; 1976, **6,** 149–57; 1977, **7,** 111–30; 1978, **8,** 129–30.
41. Bažant, Z. P., and Osman, E. (1976), 'Double power law for basic creep of concrete', *Materials and Structures*, (RILEM, Paris) **9,** No. 49, 3–11.
42. Bažant, Z. P., Osman, E., and Thonguthai, W. (1976), 'Practical formulation of shrinkage and creep of concrete', *Materials and Structures*, (RILEM, Paris) **9,** No. 54, 395–406.
43. Bažant, Z. P., and Panula, L. (1978a), 'Practical prediction of creep and shrinkage of concrete', *Materials and Structures*, (RILEM, Paris), Parts I and II, No. 69, 1978, 415–34; Parts V and VI, **12,** No. 72, 1979.
44. Bažant, Z. P., and Panula, L. (1978b), 'New model for practical prediction of creep and shrinkage', Presented at *A. Pauw Symp. on Creep, ACI Convention, Houston, October* 1978, to be published as ACI Special Publication, 1982.
45. Bažant, Z. P., and Panula, L. (1980), 'Creep and shrinkage chracterization for analyzing prestressed concrete structures, *Prestr. Concr. Inst. J.*, **25,** No. 3, 86–122.
46. Bažant, Z. P., Rossow, E. C., and Horrigmoe, G. (1981), 'Finite element program for creep analysis of concrete structures', *Proc. 6th Int. Conf. on Structural Mechanics in Reactor Technology, Paris*, Paper H2/1.
47. Bažant, Z. P., and Thonguthai, W. (1976), 'Optimization check of certain recent practical formulations for concrete creep', *Materials and Structures*, (RILEM, Paris), **9,** 91–6.
48. Bažant, Z. P., and Thonguthai, W. (1978), 'Pore pressure and drying of concrete at high temperature', *J. Eng. Mech. Div. ASCE*, **104,** EM5, 1059–79.
49. Bažant, Z. P. and Thonguthai, W. (1979), 'Pore pressure in heated concrete walls: theoretical prediction', *Mag. Concr. Res.*, **32,** No. 107, 67–76.
50. Bažant, Z. P., and Tsubaki, T. (1980), 'Weakly singular integral for creep rate of concrete', *Mech. Res. Commun.*, **7,** 335–40.
51. Bažant, Z. P., and Wu, S. T. (1973), 'Dirichlet series creep function for aging concrete', *J. Eng. Mech. Div. ASCE*, **99,** No. EM2, Proc. Paper 9645.
52. Bažant, Z. P., and Wu, S. T. (1974a), 'Creep and shrinkage law for concrete at variable humidity', *J. Eng. Mech. Div. ASCE*, **100,** EM6, 1183–209.
53. Bažant, Z. P., and Wu, S. T. (1974b), 'Rate-type creep law of aging concrete based on Maxwell chain', *Materials and Structures*, (RILEM, Paris), **7,** 45–60.
54. Bažant, Z. P., and Wu, S. T. (1974c), 'Thermoviscoelasticity of aging concrete', *J. Eng. Mech. Div. ASCE*, **100,** 575–97; also (1973), *ASCE Preprint* 2110.
55. Berwanger, C. (1971), 'The modulus of concrete and the coefficient of thermal expansion below normal temperatures', *Am. Concr. Inst. Spec. Publ. No.* 25, *Temperature and Concrete, Detroit*, pp. 191–234.
56. Biot, M. A. (1955), 'Variational principles of irreversible thermodynamics with application to viscoelasticity', *Phys. Rev.*, **97,** 1463–69.

57. Boltzmann, Z. (1876), 'Zur Theorie der Elastischen Nachwirkung', *Sitzber. Akad. Wiss., Wiener Bericht* 70, *Wiss. Abh.* **1** (1874), 275–306; see also *Pogg. Ann. Phys.*, **7,** 624.
58. Branson, D. E., Meyers, B. L., and Kripanarayanan, K. M. (1970a), 'Time-dependent deformation of non-composite and composite prestressed concrete structures', *Highway Res. Rec. No.* 324, pp. 15–33.
59. Branson, D. E., Meyers, B. L., and Kripanarayanan, K. M. (1970b), 'Loss of prestress, camber, and deflection of noncomposite and composite structures using different weight concretes', *Final Rep. No.* 70–6 *Iowa Highway Commision, Aug.* 1970, pp. 1–229. Also, condensed papers presented at the *49th Annual Meeting, Highway Research Board, Washington, DC, Jan. 1970*, pp. 1–42, and at the *Sixth Congress, Fédération Internationale de la Précontrainte, Prague*, pp. 1–28.
60. Branson, D. E., and Christianson, M. L. (1971), 'Time-dependent concrete properties related to design strength and elastic properties, creep and shrinkage', *Am. Concr. Inst. Spec. Publ.* SP-27, *Designing for Creep, Shrinkage and Temperature, Detroit*, pp. 257–77.
61. Branson, D. E. (1977), *Deformations of Concrete Structures*, McGraw-Hill, New York.
62. Bresler, B., and Selna, L. (1964), 'Analysis of time-dependent behavior of reinforced concrete structures', *ACI Symp. on Creep of Concrete, ACI Spec. Publ.* SP-9.
63. Brettle, H. J., (1958), 'Increase in concrete modulus of elasticity due to prestress and its effect on beam deflections', *Constructional Rev. (Sydney)*, **31,** 32–5.
64. Browne, R. D. (1967), 'Properties of concrete in reactor vessels', *Proc. Conf. on Prestressed Concrete Reactor Pressure Vessels, Inst. Civ. Eng., London*, Paper 13, pp. 11–13.
65. Browne, R. D., and Blundell, R. (1969), 'The influence of loading age and temperature on the long term creep behavior of concrete in a sealed, moisture stable state', *Materials and Structures*, (RILEM, Paris) **2,** 133–44.
66. Browne, R. D., and Bamforth, P. P. (1975), 'The long term creep of the Wylfa P. V. concrete for loading ages up to $12\frac{1}{2}$ years, *Proc. 3rd Int. Conf. on Structural Mechanics in Reactor Technology, London*, Paper H1/8.
67. Carlson, R. W. (1937), 'Drying shrinkage of large concrete members', *J. Am. Concr. Inst.*, **33,** 327–36.
68. CEB-FIP (1978), *Model Code for Concrete Structures*, Comité Euro-International du Béton, Paris, Vol. 2, Appendix e.
69. Cederberg, H. and Davis, M. (1969), 'Computation of creep effects in prestressed concrete pressure vessels using dynamic relaxation', *Nucl. Eng. Des.*, **9,** 439–48.
70. Chiorino, M. A., and Levi, R. (1967), 'Influence de l'élasticité différée sur le régime des contraintes des constructions en béton', *Cah. Rech. No.* 24, Institut Technique du Bâtiment et des Travaux Publics, Eyrolles, Paris, France (see also Giornale del Genio Civile, 1967; and Academia Nazionale dei Lincei, Fasc. 5, Seri. 8, **28,** May, 1965).
71. Çinlar, E., Bažant, Z. P., and Osman, E. (1977), 'Stochastic process for extrapolating concrete creep', *J. Eng. Mech. Div., ASCE*, **103,** No. EM6, Proc. Paper 13447, 1069–88.
72. Copeland, L. E., Kantro, D. L. and Verbeck, G. (1960), *Chemistry of Hydration of Portland Cement, Natl. Bur. Stand. Monogr.* 43, *4th Int. Symp. on the Chemistry of Cement, Washington, DC*, pp. 429–65.

73. Cost, T. M., (1964), 'Approximate Laplace transform inversions in viscoelastic stress analysis', *AIAA J.* **2,** 2157–66.
74. Cottrell, A. H. (1965), *The Mechanical Properties of Matter*, Wiley, New York.
75. Cruz, C. R. (1967), 'Elastic properties of concrete at high temperatures', *J. Portland Cem. Assoc. Res. Dev. Lab.*, **9,** 37–45.
76. Davies, R. D., (1957), 'Some experiments on the applicability of the principle of superposition to the strain of concrete subjected to changes of stress, with particular reference to prestressed concrete', *Mag. Concr. Res.*, **9,** 161–72.
77. Dischinger, F. (1937), 'Untersuchungen über die Knicksicherheit; die Elastische Verformung und das Kriechen des Betons bei Bogenbrücken', *Der Bauingenieur*, **18,** 487–520, 539–52, 595–621.
78. Dischinger, F., (1939), 'Elastische und plastische Verformungen bei Eisenbetontragwerke', *Der Bauingenieur*, **20,** 53–63, 286–94, 426–37, 563–72.
79. England, G. L., and Illston, J. M. (1965), 'Methods of computing stress in concrete from a history of measured strain', *Civ. Eng. Publ. Works Rev.*, 513–7, 692–4, 845–7.
80. Faber, H. (1927–28), 'Plastic yield, shrinkage and other problems of concrete and their effect on design', *Minutes Proc. Inst. Civ. Eng.*, **225,** London, England, pp. 27–76; disc. pp. 75–130.
81. Fahmi, H. M., Polivka, M., and Bresler, B. (1972), 'Effect of sustained and cyclic elevated temperature on creep of concrete', *Cem. Concr. Res.*, **2,** 591–606.
82. Ferry, J. D., (1970), *Viscoelastic Properties of Polymers*, 2nd Edn, Wiley, New York.
83. Freudenthal, A. M., and Roll, F. (1958), 'Creep and creep recovery of concrete under high compressive stress', *J. Am. Concr. Inst.*, **54,** 1111–42.
84. Gaede, K. (1962), 'Versuche über die Festigkeit und die Verformungen von Beton bei Druck-Schwellbeanspruchung', *Deutscher Ausschuss für Stahlbeton, Schriftenr. Heft* 144.
85. Glanville, W. H., (1930), 'Studies in reinforced concrete III—creep or flow of concrete under load', *Building Res. Tech. Paper No.* 12, *Dept. Sci. Ind. Res., London*; also (1933), *Struct. Eng.*, **II,** 54.
86. Glasston, S., Laidler, K. J., and Eyring, H. (1941), *The Theory of Rate Processes*, McGraw-Hill, New York.
87. Glucklich, J., and Ishai, O. (1962), 'Creep mechanism in cement mortar', *J. Am. Concr. Inst.*, **59,** 923–48.
88. Hannant, D. J. (1967), 'Strain behavior of concrete up to 95 °C under compressive stresses', *Proc. Conf. on Prestressed Concrete Pressure Vessels*, Group C, Paper 17, Institution of Civil Engineers, London, pp. 57–71.
89. Hannant, D. (1968), 'The mechanism of creep of concrete', *Mater. Struct.*, (RILEM, Paris) **1,** 403–10.
90. Hansen, T. C. (1960), 'Creep and stress relaxation in concrete', *Proc., Swed. Cem. Concr. Res. Inst.* (CBI), *Royal Inst. Tech., Stockholm*, No. 31.
91. Hansen, T. C. (1964), 'Estimating stress relaxation from creep data', *Mater. Res. Stand.* (*ASTM*), **4,** 12–14.
92. Hansen, T. C., and Mattock, A. H. (1966), 'Influence of size and shape of member on the shrinkage and creep of concrete', *J. Am. Concr. Inst.*, **63,** 267–90.
93. Harboe, E. M., *et al.* (1958), 'A comparison of the instantaneous and the sustained modulus of elasticity of concrete', *Concr. Lab. Rep. No.* C-854, Division of Engineering Laboratories, US Department of the Interior, Bureau of Reclamation, Denver, Colo.

94. Hanson, J. A. (1953), 'A 10-year study of creep properties of concrete', *Concr. Lab. Rep. No.* Sp-38, US Department of the Interior, Bureau of Reclamation, Denver, Colorado.
95. Hanson, J. A. (1968), 'Effects of curing and drying environments on splitting tensile strength', *J. Am. Concr. Inst.*, **65,** 535–43 (also *PCA Bull.* D141).
96. Hardy, G. M., and Riesz, M. (1915), *The General Theory of Dirichlet Series, Cambridge Tracts in Mathematics and Mathematical Physics, No.* 18, Cambridge Univ. Press, Cambridge.
97. Hatt, W. K. (1907), 'Notes on the effect of time element in loading reinforced concrete beams', *Proc. ASTM*, **7,** 421–33.
98. Hellesland, J., and Green, R. (1972), 'A stress and time-dependent strength law for concrete', *Cem. Concr. Res.*, **2,** 261–75.
99. Hickey, K. B. (1967), 'Creep, strength, and elasticity of concrete at elevated temperatures', *Rep. No.* C-1257, *Concr. Struct. Branch*, Division of Research, United States Department of the Interior, Bureau of Reclamation, Denver, Colorado.
100. Hirst, G. A., and Neville, A. M. (1977), 'Activation energy of creep of concrete under short-term static and cyclic stresses', *Mag. Concr. Res.*, **29,** No. 98, 13–18.
101. Honk, I. E., Orville, E. B., and Houghton, D. L. (1969), 'Studies of autogeneous volume change in concrete for Dworshak Dam', *J. Am. Concr. Inst.*, **66,** 560–8.
102. Huet, C. (1980), 'Adaptation of Bazant's algorithm to the analysis of aging viscoelastic composite structures', *Materials and Structures*, (RILEM, Paris), **13,** No. 75, 91–98, (in French).
103. Illston, J. M., and Jordaan, I. J. (1972), 'Creep prediction for concrete under multiaxial stress', *J. Am. Concr. Inst.*, **69,** 158–64.
104. Illston, J. M., and Sanders, P. D. (1973), 'The effect of temperature upon the creep of mortar under torsional loading', *Mag. Concr. Res.*, **25,** No. 84, 136–66.
105. Ishai, O. (1964), 'Elastic and inelastic behavior of cement mortar in torsion', *Am. Concr. Inst. Spec. Publ.* SP-9, *Symp. on Creep, Detroit*, pp. 65–94, 115–28.
106. Jonasson, J. E. (1978), 'Analysis of creep and shrinkage in concrete and its application to concrete top layers', *Cem. Concr. Res.*, **8,** 397–518.
107. Kabir, A. F. (1976), 'Nonlinear analysis of reinforced concrete panels, slabs and shells for time-dependent effects', *PhD Dissertation*, Division of Structural Engineering and Structural Mechanics, University of California, Berkeley, *Rep. No.* UC-SESM 76–6.
108. Kabir, A. F., and Scordelis, A. C. (1979), 'Analysis of RC shells for time dependent effects', *IASS Bull.* **XXI,** No. 69.
109. Kang, Y. J. (1977), 'Nonlinear geometric, material and time-dependent analysis of reinforced and prestressed concrete frames', *PhD Dissertation*, Division of Structural Engineering and Structural Mechanics, University of California, Berkeley, *Rep. No.* UC-SESM 77–1.
110. Kang, Y. J., and Scordelis, A. C. (1980), 'Nonlinear analysis of prestressed concrete frames', *J. Struct. Div. ASCE*, **106,** No. 1.
111. Keeton, J. R. (1965), 'Study of creep in concrete', *Tech. Reps.* R333-I, R333-II, R333-III, *US Naval Civil Engineering Laboratory, Port Hueneme, California.*
112. Kesler, C. E., and Kung, S. H. (1964), 'A study of free and restrained shrinkage of mortar', *T. & A.M. Rep. No.* 647, *Department of Theoretical and Applied Mechanics, University of Illinois, Urbana, Illinois.*

113. Kesler, C. E., Wallo, E. M., Yuan, R. L., and Lott, J. L. (1965), 'Prediction of creep in structural concrete from short-time tests', *6th Prog. Rep., Department of Theoretical and Applied Mechanics, University of Illinois, Urbana, Illinois.*
114. Kimishima, H., and Kitahara, H. (1964), 'Creep and creep recovery of mass concrete', *Tech. Rep.* C-64001, *Central Research Institute of Electric Power Industry, Tokyo, Japan.*
115. Klug, P., and Wittmann, T. (1970), 'The correlation between creep deformation and stress relaxation in concrete', *Materials and Structures* (RILEM, Paris) **3,** 75–80.
116. Komendant, G. J., Polivka, M., and Pirtz, D. (1976), 'Study of concrete properties for prestressed concrete reactor vessels', *Final Rep. Part* II, 'Creep and strength characteristics of concrete at elevated temperatures', *Rep. No.* UCSESM76-3, *Structures and Materials Research, Department of Civil Engineering, Report to General Atomic Company, San Diego, California, Berkeley, California.*
117. Lambotte, H., and Mommens, A. (1976), 'L'évolution du fluage du béton en fonction de sa composition, du taux de contrainte et de l'age', *Groupe de travail* GT 22, *Centre national de recherches scientifiques et techniques pour' l'industrie cimentière, Bruxelles.*
118. Lanczos, C. (1964), *Applied Analysis,* Prentice-Hall, Englewood Cliffs, pp. 272–80.
119. LeCamus, B. (1947), 'Recherches expérimentales sur la déformation du béton et du béton armé, Part II', *Annales Inst. Techn. du Bâtiment et des Travaux Publics, Paris.*
120. Levi, F., and Pizzetti, G. (1951), *Fluage, Plasticité, Précontrainte,* Dunod, Paris.
121. L'Hermite, R. (1970), *Volume Changes of Concrete, US Natl Bur. Stand. Monogr.* 43, *4th Int. Symp. on Chemistry of Cements, Washington,* Vol. 3, pp. 659–94.
122. L'Hermite, R., and Mamillan, M. (1968), 'Retrait et fluage des bétons', *Annales, Inst. Techn. du Bâtiment et des Travaus Publics (Suppl.),* **21,** 1334 (No. 249); and (1969), 'Nouveaux résultats et récentes études sur le fluage du béton', *Materials and Structures,* **2,** 35–41; and Mamillan, M., and Bouineau, A. (1970), 'Influence de la dimension des éprouvettes sur le retrait', *Ann. Inst. Tech. Bat. Trav. Publics (Suppl.),* **23,** 5–6 (No. 270).
123. L'Hermite, R., Mamillan, M., and Lefèvre, C. (1965), 'Nouveaux résultats de recherches sur la déformation et la rupture du béton', *Annales de l'Institut Technique du Bâtiment et des Travaux Publics* **18,** pp. 325–360; see also (1968), *Int. Conf. on the Structure of Concrete,* Cement and Concrete Assoc., pp. 423–33.
124. McDonald, J. E. (1972), 'An experimental study of multiaxial creep in concrete', *Amr. Concr. Inst. Spec. Publ. No.* 34, *Concrete for Nuclear Reactors,* Detroit, pp. 732–68.
125. McHenry, D. (1943), 'A new aspect of creep in concrete and its application to design', *Proc. ASTM,* **43,** 1069–86.
126. McMillan, F. R. (1916), 'Method of designing reinforced concrete slabs', discussion by A. C. Janni, *Trans. ASCE,* **80,** 1738.
127. Mamillan, M. (1969), 'Evolution du fluage et des propriétés de béton', *Ann. Inst. Tech. Bat. Trav. Publics* **21,** 1033; and (1960), **13,** 1017–52.
128. Mamillan, M., and Lelan, M. (1970), 'Le Fluage de béton', *Ann. Inst. Tech. Bât. Trav. Publics (Suppl.)* **23,** 7–13, (No. 270), and (1968), **21,** 847–50 (No. 246).

129. Mandel, J. (1958), 'Sur les corps viscoélastiques linéaire dont les propriétés dépendent de l'age', *C.R. Séances Acad. Sci.,* **247,** 175–8.
130. Maréchal, J. C. (1969), 'Fluage du béton en fonction de la température', *Materials and Structures* (RILEM, Paris) **2,** 111–15; see also (1970), *Mater. Struct.,* **3,** 395–406.
131. Máréchal, J. C. (1970a), 'Contribution a l'étude des propriétés thermiques et mécaniques du béton en fonction de la température', *Annales de l'Institut Technique du Bâtiment et des Travaux Publics,* **23,** No. 274, 123–145.
132. Maréchal, J. C. (1970b), 'Fluage du béton en fonction de la température', *Ann. Inst. Tech. Bât. Trav. Publics,* **23,** No. 266, 13–24.
133. Maslov, G. N. (1940), 'Thermal stress states in concrete masses, with consideration of concrete creep', (in Russian), *Izvestia Nauchno-Issledovatel'skogo Instituta Gidrotekhniki, Gosenergoizdat,* **28,** 175–88.
134. Mehmel, A., and Kern, E. (1962), 'Elastische und Plastische Stauchungen von Beton infolge Druckschwell-und Standbelastung', *Dtsch. Ausschuss Stahlbeton Schriftenr. Heft* 153.
135. Meyer, H. G. (1969), 'On the influence of water content and of drying conditions on lateral creep of plain concrete', *Mater. Struct.* (RILEM, Paris) **2,** 125–31.
136. Meyers, B. L., and Slate, F. O. (1970), 'Creep and creep recovery of plain concrete as influenced by moisture conditions and associated variables', *Mag. Concr. Res.,* **22,** 37–8.
137. Mörsch, E. (1947), *Statik der Gewölbe und Rahmen,* Teil, A., Wittwer, Stuttgart.
138. Mukaddam, M. (1974), 'Creep analysis of concrete at elevated temperatures', *ACI J.,* **71,** No. 2.
139. Mukaddam, M. A., and Bresler, B. (1972), 'Behavior of concrete under variable temperature and loading', *Am. Concr. Inst. Spec. Publ. No.* 34, *Concrete for Nuclear Reactors,* Detroit, pp. 771–97.
140. Mullen, W. G., and Dolch, W. L. (1966), 'Creep of Portland cement paste', *Proc. ASTM,* **64,** 1146–70.
141. Mullick, A. K. (1972), 'Effect of stress-history on the microstructure and creep properties of maturing concrete', Ph.D. Thesis, *University of Calgary,* Alberta, Canada.
142. Nasser, K. W., and Neville, A. M. (1965), 'Creep of concrete at elevated temperatures', *J. Am. Concr. Inst.,* **62,** 1567–79.
143. Nasser, J. W., and Neville, A. M. (1967), 'Creep of old concrete at normal and elevated temperatures', *J. Am. Concr. Inst.,* **64,** 97–103.
144. Neville, A. M. (1973), *Properties of Concrete,* 2nd Edn., Wiley, New York.
145. Neville, A. M., and Dilger, W. (1970), *Creep of Concrete, Plain, Reinforced, Prestressed,* North-Holland, Amsterdam.
146. Nielsen, L. F. (1970), 'Kriechen und relaxation des betons', *Beton-und Stahlbetonbau,* **65,** 272–5.
147. Nielsen, L. F. (1977), 'On the applicability of modified Dischinger equations', *Cem. Concr. Res.,* **7,** 149; (discussion, **8,** 117).
148. Pickett, G. (1946), 'The effect of change in moisture content on the creep of concrete under a sustained load', *J. Am. Concr. Inst.,* **36,** 333–5; see also 'Shrinkage stresses in concrete', *J. Am. Concr. Inst.,* **42,** 165–204, 361–400.
149. Pirtz, D. (1968), 'Creep characteristics of mass concrete for Dworshak Dam', *Rep. No.* 65–2, *Structural Enginerring Laboratory, University of California, Berkeley.*

150. Pister, K. S., Argyris, J. H., and Willam, K. J. (1976), 'Creep and shrinkage of aging concrete, *ACI Symp. on Concrete and Concrete Structures*, 24–29 Oct. 1976, *Mexico City*, ACI SP55–1.
151. Powers, T. C. (1965), 'Mechanism of shrinkage and reversible creep of hardened cement paste', *Proc. Int. Conf. on the Sstructure of Concrete, London*, Cem. Concr. Assoc., London, pp. 319–44.
152. Powers, T. C. (1966), 'Some observations on the interpretation of creep data', *RILEM Bull.* (Paris) No. 33, 381–91.
153. Powers, T. C. and Brownyard, T. C. (1946), 'Studies of the physical properties of hardened Portland cement paste', *J. Am. Concr. Inst.* **42,** 101–32, 249–366, 469–504; **43** (1947) 549–602, 669–712, 854–80, 933–92.
154. Rashid, Y. R. (1972), 'Nonlinear analysis of two-dimensional problems in concrete creep', *J. Appl. Mech.*, **39,** 475–82.
155. Rice, J. (1971), 'Inelastic constitutive relations for solids: an internal variable theory and its application to metal plasticity', *J. Mech. Phys. Solids*, **19,** 433–55.
156. Roll, F. (1964), 'Long-time creep-recovery of highly stressed concrete cylinders', *Am. Concr. Inst. Spec. Publ.* SP-9, *Symp. on Creep, Detroit*, pp. 115–28.
157. Roscoe, R. (1950), 'Mechanical models for the representation of viscoelastic properties', *Br. J. Appl. Phys.*, **1,** 171–3.
158. Ross, A. D. (1958), 'Creep of concrete under variable stress', *J. Am. Concr. Inst.*, **54,** 739–58.
159. Rostasy, F. S., Teichen, K. Th., and Engleke, H. (1972), 'Beitrag zur Klärung der Zusammenhanges von Kriechen und Relaxation bei Normal-beton', *Amtliche Forschungs-und Materialprufüngsanstalt für das Bauwesen, Otto-Graf-Institut, Universität, Stuttgart, Strassenbau und Strassenverkehrstechnik, Heft* 139.
160. Ruetz, W. (1968), 'A hypothesis for the creep of hardened cement paste and the influence of simultaneous shrinkage', *Proc. Int. Conf. on the Structure of Concrete, London, 1965*, Cem. Concr. Assoc., London, pp. 365–87; see also (1966), *Deutscher Ausschuss für Stahlbeton, Schriftenr. Heft* 183.
161. Rüsch, H., *et al.* (1968), 'Festigkeit und Verformung von unbewehrten Beton unter konstanter Dauerlast', *Deutscher Ausschuss für Stahlbeton, Schriftenr. Heft* 198; see also (1968), *J. Am. Concr. Inst.* **57,** 1–58.
162. Rüsch, H., Jungwirth, D., and Hilsdorf, H. (1973), 'Kritische Sichtung der Verfahren zur Berücksightigung der Einfüsse von Kriechen", *Beton-und Stahlbetonbau*, **68,** 49–60, 76–86, 152–8; (discussion, **69,** (1974), 150–1).
163. Sackman, J. L. (1963), 'Creep in concrete and concrete structures', *Proc. Princeton Univ. Conf. on Solid Mech.*, pp. 15–48.
164. Saugy, B., Zimmermann, Th., and Hussain, J. (1976), 'Three-dimensional rupture analysis of prestressed concrete pressure vessel including creep effects', *Nucl. Eng. Des.*, **28,** 97–102.
165. Schade, D., and Haas, W. (1975), 'Elektronische Berechnung der Auswirkungen von Kriechen und Schwinden bei abschnittsweise *hergestellten verbundtragwerken, Deutscher Ausschuss Stahlbeton, Schriftenr. Heft* 244.
166. Schapery, R. A. (1962), 'Approximate methods of transform inversion for viscoelastic stress analysis', *Proc. 4th US Natl. Congr. on Appl. Mech., Berkeley, Calif.*, Vol. 2, ASME, pp. 1075–85.
167. Seki, S., and Kawasumi, M. (1972), 'Creep of concrete at elevated temperature', *Am. Concr. Inst. Spec. Publ.* SP-34, *Symp. on Concrete for Nuclear Reactors*, Vol. 1, pp. 591–638.

168. Selna, L. G. (1967), 'Time-dependent behavior of reinforced concrete structures', *UC-SESM Rep. No.* 67–19, *University of California, Berkeley.*
169. Selna, L. G. (1969), 'A concrete creep, shrinkage and cracking law for frame structures', *J. Am. Concr. Inst.*, **66,** 847–8; with *Suppl. No.* 66–76.
170. Shank, J. R. (1935), 'The plastic flow of concrete, *Ohio State Univ. Eng. Exp. Stn., Bull. No.* 91.
171. Smith, P. D., Cook, W. A., and Anderson, C. A. (1977), 'Finite element analysis of prestressed concrete reactor vessels', *Proc. 4th Int. Conf. on Structural Mechanics in Reactor Technology, San Francisco, Ca.*
172. Smith, P. D., and Anderson, C. A. (1978), 'NONSAP-C: a nonlinear stress analysis program for concrete containments under static, dynamic, and long-term loadings', *Los Alamos Sci. Lab. Rep.* LA-7496-MS.
173. Straub, H. (1930), 'Plastic flow in concrete arches', *Proc. ASCE*, **56,** 49–114.
174. Suter, G. T., and Mickelborough, N. C. (1975), 'Creep of concrete under cyclically varying dynamic loads', *Cem. Concr. Res.*, **5,** No. 6, 565–76.
175. Taylor, R. L., Pister, K. S., and Goudreau, G. L. (1970), 'Thermomechanical analysis of viscoelastic solids', *Int. J. Num. Meth. Eng.*, **2,** 45–60.
176. Trost, H. (1967). 'Auswirkungen des Superpositionsprinzips auf Kriech- und Relaxationsprobleme bei Beton und Spannbeton', *Beton-und Stahlbetonbau*, **61,** 230–8; see also (1970) **65,** 155–79.
177. Troxell, G. E., Raphael, J. M., and Davis, R. W. (1958), 'Long-time creep and shrinkage tests of plain and reinforced concrete', *Proc. ASTM*, **58,** 1101–20.
178. VanGreunen, J. (1979), 'Nonlinear geometric, material and time dependent analysis of reinforced and prestressed concrete slabs and panels', *PhD Dissertation*, Division of Structural Engineering and Structural Mechanics, University of California, Berkeley, *Rep. No.* UC-SESM 79–3.
179. Van Zyl, S. F. (1978), 'Analysis of curved segmentally erected prestressed concrete box girder bridges', *PhD Dissertation*, Division of Structural Engineering and Structural Mechanics, University of California, Berkeley, *Rep. No.* UC-SESM 78–2.
180. Van Zyl, S. F., and Scordelis, A. C. (1979), 'Analysis of curved prestresssed segmental bridges', *J. Struct. Div. ASCE*, **105,** No. 11.
181. Volterra, V. (1913), *Leçons sur les Fonctions de Ligne*, Gauthier-Villars, Paris; and (1959), *Theory of Functionals and of Integral and Integro-differential Equations*, Dover, New York.
182. Wagner, O. (1958), 'Das Kriechen unbewehrten Betons', *Deutscher Ausschuss für Stahlbeton, Schriftenr. Heft* 13.
183. Weil, G. (1959), 'Influence des dimensions et des tensions sur le retrait et le fluage de béton', *RILEM Bull.*, No. 3, 4–14.
184. Whaley, C. P., and Neville, A. M. (1973), 'Non-elastic deformation of concrete under cyclic compression', *Mag. Concr. Res.*, **25,** No. 84, 145–54.
185. Whitney, G. S. (1932), 'Plain and reinforced concrete arches', *J. Am. Concr. Inst.*, **28,** No. 7, 479–519; Disc., **29,** 87–100.
186. Willam, K. J. (1978), 'Numerical solution of inelastic rate processes', *Comput. Struct.* **8,** 511–31.
187. Williams, M. L. (1964), 'The structural analysis of viscoelastic materials', *AIAA J.*, **2,** 785–808.
188. Williamson, R. B. (1972), 'Solidification of Portland cement', in B. Chalmers *et al.* (Eds), *Progress in Materials Science*, Vol. 15, No. 3, Pergamon Press, New York, London.

189. Wittmann, F. (1966), 'Kriechen bei Gleichzeitigem Schwinden des Zementsteins', *Rheol. Acta*, **5**, 198–204.
190. Wittmann, F. (1968), 'Surface tension, shrinkage and strength of hardened cement paste', *Materials and Structures* (RILEM, Paris) **1**, 547–52.
191. Wittmann, F. (1970), 'Einfluss des Feuchtigkeitsgelhaltes auf das Kriechen des Zementsteines', *Rheol. Acta*, **9**, 282–7.
192. Wittmann, F. (1971a), 'Kriechverformung des Betons unter Statischer und unter Dynamischer Belastung', *Rheol. Acta*, **20**, 422–8.
193. Wittman, F. H. (1971b), 'Vergleich einiger Kriechfunktionen mit Versuchsergebnissen', *Cem. Concr. Res.*, **1**, 679–90.
194. Wittmann, F. (1974), 'Bestimmung Physikalischer Eigenschaften des Zementsteins', *Deutscher Ausschuss für Stahlbeton, Schriftenr. Heft* 232.
195. Wittmann, F. H., and Roelfstra, P. (1980), 'Total deformation of loaded drying concrete', *Cem. Concr. Res.*, **10**, 601–10.
196. York, G. P., Kennedy, T. W., and Perry, E. S. (1970) 'Experimental investigation of creep in concrete subjected to multiaxial compressive stresses and elevated temperatures', *Res. Rep.* 2864–2, *University of Texas, Austin*; see also (1971), *Am. Concr. Inst. Spec. Publ. No.* 34, 641–700.
197. Zienkiewicz, O. C., Watson, M., and King, I. P. (1968), 'A numerical method of viscoelastic stress analysis', *Int. J. Mech. Sci.*, **10**, 807–27.
198. Zienkiewicz, O. C., and Watson, M. (1966), 'Some creep effects in stress analysis with particular reference to concrete pressure vessels', *Nucl. Eng. Des.*, No. 4.
199. Bažant, Z. P. (1982), 'Input of creep and shrinkage characteristics for a structural analysis program', *Materials and Structures* (RILEM; Paris), Vol. 15.
200. Bažant, Z. P., Ashgari, A. A., and Schmidt, J. (1976), 'Experimental study of creep of hardened cement paste at variable water content', *Materials and structures* (RILEM, Paris) **9**, 279–290.
201. Bažant, Z. P., and Ong. J. S. (1981), 'Creep in continuous beams built span-by-span', *Report No.* 81–12/665c, Center for Concrete and Geomaterials, Northwestern University, Evanston, IL. (submitted to ASCE Struct. Div. J.)
202. Bažant, Z. P., and Raftshol, W. J. (1982), 'Effect of cracking in drying and shrinkage specimens', *Cement and Concrete Research*, **12**, 209–226.
203. Madsen, H. O., and Bažant, Z. P. (1982) 'Uncertainty analysis of creep and shrinkage effects in concrete structures', *Report No. 82–2/665u*, Center for Concrete and Geomaterials, Northwestern University, Evanston, IL.
204. Bažant, Z. P., and Zebich, S. (1982), 'Statistical regression analysis of creep prediction models', *Report No. 82–4/665s*, Center for Concrete and Geomaterials, Northwestern University, Evanston, IL.
205. Tsubaki, T., and Bazant. Z. P. (1982), 'Random shrinkage stresses in aging viscoelastic vessel, *J. Engng. Mech. Div., ASCE* **108**, EM3, June, 527–45.
206. Bažant, Z. P., Tsubaki, T., and Celep, Z., 'Singular History Integral for Creep Rate of Concrete, *J. Engng. Mech. Div., ASCE*, in press.
207. Anderson, C. A., Smith, P. D., and Carruthers, L. M., "NONSAP-C: A Nonlinear Strain Analysis Program for Concrete Containments under Static, Dynamic and Long-Term Loadings, Report NUREG/CR0416, LA-7496-MS, Rev. 1, R7 & R8, Los Alamos National Laboratory, New Mexico, Jan. 1982 (available from NTIS, Springfield, Va.).